2018

Elucidation of ERK1/2 Signaling Pathways Leading to Mitochondrial Biogenesis

Justin Brandon Collier
Medical University of South Carolina

Elucidation of ERK1/2 Signaling Pathways Leading to Mitochondrial Biogenesis

By

Justin Brandon Collier

A dissertation submitted to the faculty of the Medical University of South Carolina in partial fulfillment of the requirements for the degree of Doctor of Philosophy in the College of Graduate Studies.

Department of Drug Discovery and Biomedical Sciences

2018

Approved by:

Chairman, Advisory Committee

_____
Craig C. Beeson

_____
Rick G. Schnellmann

_____
James Chou

_____
Sherine Chan

_____
Scott T. Eblen

_____
Michael D. Wyatt

Dedication

This dissertation is dedicated to my wife and son who have provided unwavering support, love, and encouragement throughout each step of my educational journey. Both of whom were stronger than I was while dealing with the final months of my PhD work and subsequent move. If you ever read this (not sure you will), I would like you to know that I could not have done it without you. To my loving mom and dad who always believed in me - thank you for everything.

Acknowledgments

I would like to thank Dr. Rick G. Schnellmann for his guidance and mentoring throughout my graduate career. I also wish to acknowledge my committee members: Dr. Craig Beeson, Dr. James Chou, Dr. Sherine Chan, Dr. Scott Eblen, and Dr. Michael Wyatt for their advice, support, and communication even while across country.

Table of Contents

List of Figures

Chapter 1

Chapter 2

List of Abbreviations

AIN	Acute interstitial nephritis
AKI	Acute kidney injury
AKIN	Acute Kidney Injury Network
AMP	Adenosine monophosphate
ANOVA	One-way analysis of variance
ARF	Acute renal failure
ATP	Adenosine triphosphate
ATPSβ	Adenosine triphosphate synthase subunit beta
BUN	Blood urea nitrogen
cGMP	Cyclic guanosine monophosphate
Chk1	Checkpoint kinase 1
CKD	Chronic kidney disease
CLP	Cecal ligation and puncture
COX1	Cytochrome c oxidase I
Drp1	Dynamin-related protein 1
EGF	Epidermal growth factor
EGFR	Epidermal growth factor receptor
ERK	Extracellular single-regulated kinase
ErL	Erlotinib
ESRD	End-stage renal disease
ETC	Electron transport chain
FCCP	carbonylcyanide-p-trifluoromethoxyphenylhydrazone
FOXO3a/1	Forkhead box protein O3/O1
GFR	Glomerular filtration rate

GPCR	G-protein coupled receptors
Grb2	Growth factor receptor-bound protein 2
GSK	Trametinib
H2O2	Hydrogen peroxide
HIF	Hypoxia-inducible factor
HU	Hydroxyurea
IMM	Inner mitochondrial membrane
IP	Intraperitoneal
IR	Ischemia-reperfusion
JNK	Jun N-terminal kinase
KDIGO	Kidney disease improving global outcomes
KIM1	Kidney injury molecule-1
LPS	Lipopolysaccharide
MAPK	Mitogen-activated protein kinase
MB	Mitochondrial biogenesis
MEK	Mitogen-activated protein kinase kinase
Mfn	Mitofusin
MMP	Mitochondrial membrane potential
MMPs	Matrix metalloproteinases
mtDNA	Mitochondrial DNA
NAD(H)	Nicotinamide adenine dinucleotide
NAM	Nicotinamide
NDUFS1	NADH Dehydrogenase (Ubiquinone) Fe-S Protein 1
NGAL	Neutrophil gelatinase-associated lipocalin
NMN	Nicotinamide mononucleotide
NRF1	Nuclear respiratory factor-1

OCR	Oxygen consumption rate
Opa1	Optic atrophy protein 1
PDGF	Platelet-derived growth factor
PGC-1α	Peroxisome proliferator-activated receptor coactivator-1 alpha
RIFLE	Risk, Injury, Failure, Loss, and End-stage renal disease
ROS	Reactive oxygen species
RPTC	Renal proximal tubule epithelial cells
RRT	Renal replacement therapy
RTK	Receptor tyrosine kinases
SCr	Serum creatinine
SOD2	Mitochondrial superoxide dismutase 2
SOS	Son of sevenless
STAT3	Signal transducer and activator of transcription 3
TBHP	tert-butyl hydroperoxide
TFAM	Mitochondrial transcription factor A
TK	Transgenic kidney
TLR4	Toll-like receptor 4
TNF-α	Tumor necrosis factor alpha

ABSTRACT

JUSTIN BRANDON COLLIER. Elucidation of ERK1/2 Signaling Pathways Leading to Mitochondrial Biogenesis. (Under the direction of RICK G. SCHNELLMANN)

Acute kidney injury (AKI) is a rapid loss of normal kidney function and is accompanied by a dysregulation of cellular and mitochondrial metabolism, which can be observed before organ dysfunction. A hallmark of AKI is the early and persistent disruption of mitochondrial homeostasis. Mitochondrial biogenesis (MB), the process by which new mitochondria are generated, has been shown to prevent injury and increase the rate of recovery of ischemia-reperfusion injury (IRI)-induced renal dysfunction. However, the molecular mechanisms mediating MB and dysfunction following IRI remain unclear.

We elucidated that extracellular signal-regulated kinase 1/2 (ERK1/2) regulates two key mitochondrial and cellular metabolism pathways following AKI. The first is the rapid downregulation of MB through decreased peroxisome proliferator-activated receptor gamma coactivator-1α (PGC-1α) expression, the master regulator of MB. The second is nicotinamide adenine dinucleotide (NAD) loss after IRI, particularly the oxidized form, NAD^+.

Trametinib, an FDA approved drug, prevents ERK1/2 activation by inhibiting mitogen-activated protein kinase kinase 1/2 (MEK1/2). ERK1/2 inhibition prior to IRI prevents the downregulation of PGC-1α gene expression. In addition, trametinib prevented PGC-1α acetylation, which deactivates PGC-1α, after IRI. This was verified by determining that trametinib inhibited the loss of downstream PGC-1α and MB targets after IRI, including both nuclear- and mitochondrial-encoded genes.

NAD^+ is a vital coenzyme in cellular metabolism, redox signaling, and contributes to overall cellular health. NAD^+ is depleted during injury, and restoration or prevention of this depletion averts worsening injury and often promotes recovery. Inhibition of ERK1/2 activation attenuated NAD^+ loss and was mediated through increased nicotinamide phosphoribosyltransferase (NAMPT), the rate-limiting enzyme of the NAD^+ biosynthetic salvage pathway. Inhibition of renal ERK1/2 activation decreased miR34a, a known regulator of NAMPT, and led to an increase in NAMPT protein.

In conclusion, inhibiting ERK1/2 activation restored PGC-1α protein levels, attenuated the loss of downstream MB targets, increased NAMPT protein, and restored NAD^+ after IRI. These cellular alterations ultimately led to restored kidney function following IRI-induced AKI. These studies may help support the identification of potential therapeutic targets for the treatment of AKI.

CHAPTER ONE:

Review of renal anatomy and physiology, acute kidney injury, mitochondrial biology and biogenesis, and extracellular signal-regulated kinase 1/2 signaling

RENAL ANATOMY AND PHYSIOLOGY

Overview

Normally there are two kidneys working simultaneously in the human body filtering blood to maintain fluid homeostasis by removing waste products and extra fluid. The kidney maintains the proper balance of fluid volume, electrolytes (sodium, potassium), minerals (calcium, phosphorous), and blood pH. By maintaining proper fluid homeostasis all the other organs are able to function properly. In addition to fluid homeostasis, the kidneys also serve a critical role in eliminating harmful toxins, xenobiotics, and waste products (ex. ammonia and urea) that can build up in the circulatory system, and cause harmful side effects. Two other major contributions to a healthy functioning body are the control of blood pressure and the production of red blood cells. Blood pressure is controlled through both fluid homeostasis and through the secretion of the hormone renin and subsequent renin-angiotensin-aldosterone signaling pathways. The kidneys contribute to the creation of new red blood cells by releasing the hormone erythropoietin, which signals the bone marrow to produce more red blood cells, often as a way to increase oxygen supply to the rest of the body. The kidney anatomy can typically be divided into three regions (working from outermost to inner): the renal cortex, the renal medulla (consisting of the outer and inner medulla), and the renal pelvis. A diagram is provided below (Figure 1.1).

The Nephron

The kidney consists of around a million nephrons, which are considered the basic functional unit of the kidney. The nephrons filter, excrete, and reabsorb solutes and fluid to help maintain fluid and electrolyte balance through complex pressure and gradient pathways. Blood enters the nephron via the renal artery and into the section of the nephron called the glomerulus. The glomerulus is the first step in the filtration process and the filtrate then flows into the renal tubule. The renal tubule is comprised of the proximal tubule, ascending and descending limbs of the loop of Henle, the distal tubule, and the collecting duct. A diagram is provided below for further observation (Figure 1.2).

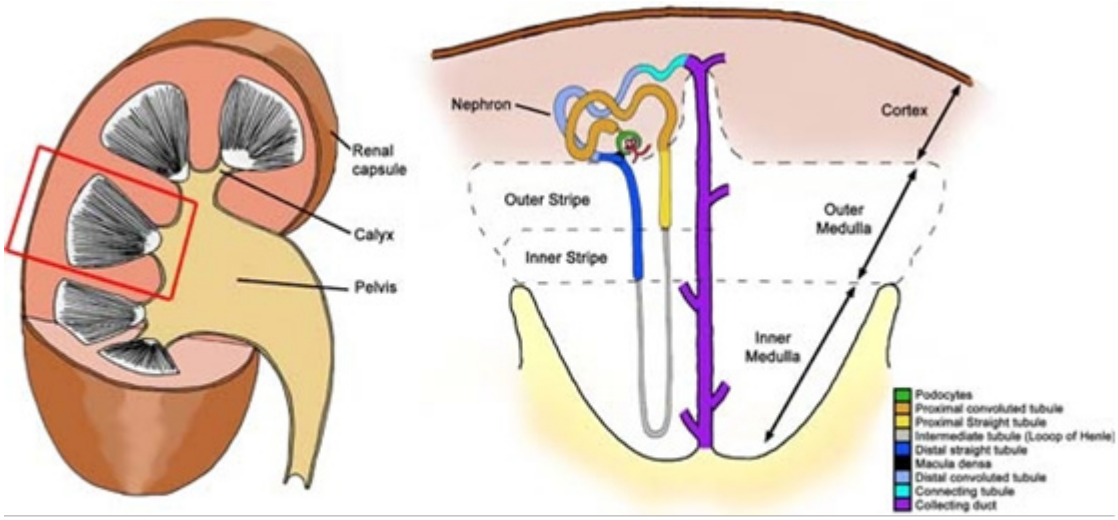

Figure 1.1: Kidney gross anatomy.

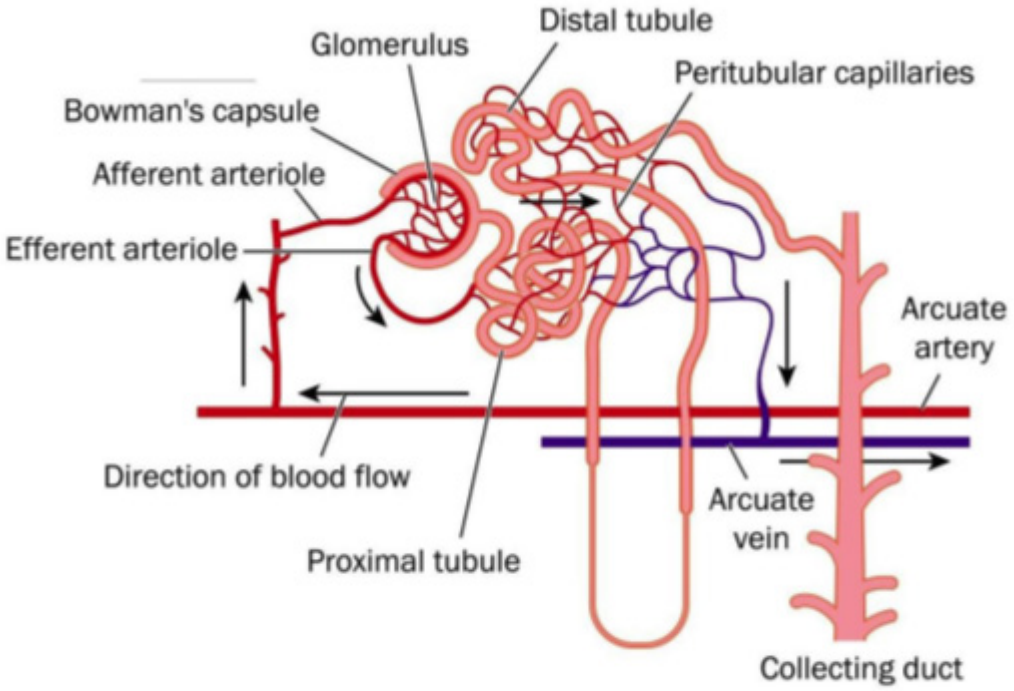

Figure 1.2: Kidney nephron structure and blood supply.

Renal Vasculature

Blood from the renal artery enters the glomerulus via the afferent arterioles and is filtered in the glomerular capillary bed. Blood that passes through the glomerulus without being filtered exits via the efferent arteriole and consists of larger molecules, such as various blood cells and higher molecular weight proteins. The efferent blood continues flowing to supply the renal cortex and the renal medulla and papilla, as well as allow for the return of water and solutes the tubule filters and reabsorbs. The renal cortex filters around 90% of the renal blood flow. This disparity in blood flow within the kidney is due to the cortex consisting of mainly proximal tubules which rely heavily on oxidative phosphorylation for energy production, which requires more oxygen availability and therefore more blood flow. The renal medulla and papilla utilize mainly glycolysis for energy production and requires less oxygen than the proximal tubules. The small capillaries eventually return to the renal venules to form segmental renal veins. The renal vein then takes blood away from the kidney that has now been filtered, reabsorbed, and deoxygenated.

The Glomerulus

The purpose of the glomerulus is to be the beginning step of the blood filtration process. The thin walls allow water and waste products to pass through the glomerulus and into the tubule where further filtration and concentration can occur. Glomerular filtration can be affected by changes in blood volume, blood pressure, and vascular tone to the afferent and efferent arterioles. The afferent arteriole blood flows into the glomerulus and into an area called Bowman's capsule. Blood is filtered through various layers of cells and membranes composed of capillary endothelium, glomerular basement membrane, and podocytes. Podocytes are a specific cell type that are found on the outside of capillaries inside the Bowman's capsule. Substances found in the blood generally are filtered depending on their size and charge. Smaller molecules can pass through and into the renal tubules, whereas proteins greater than ~60 kDa continue into the efferent arteriole. Smaller proteins that are highly anionic are potentially limited in their filtration, most likely due to the glomerular basement membrane also being anionic, causing a repulsion effect. The rate at which blood is filtered in the glomerulus and the fluid passes into the tubule is termed the glomerular filtration rate or GFR, and is used as a renal functional diagnostic test in hospitals and laboratory settings. A person with no kidney disease will typically have a GFR of greater than 60 mL/min, and a GFR under 60 mL/min is diagnosed with some form of kidney dysfunction, injury, or disease.

The Proximal Tubule

The glomerular filtrate passes through the Bowman's space and into the proximal tubule, where the filtrate is further filtered. The proximal tubule further reabsorbs both fluid and electrolytes, including a majority of the water that passes through the glomerulus. Electrolytes and ions are reabsorbed here by way of ion transporters, including sodium chloride, potassium, calcium, phosphate, and bicarbonate, where they enter back into the systemic blood supply. Glucose, carbohydrates, and various amino acids are also reabsorbed here through active and facilitated diffusion. As mentioned earlier, the proximal tubules have a high-energy demand and thus utilize oxidative phosphorylation for ATP production. The abundance of the various transporters and the activity of reabsorption places a high-energy burden (need for ATP) on the proximal tubules and oxygen demand; which highlights why the renal cortex receives 90% of the blood supply. The proximal tubule can be further divided into 3 sections: the S1, S2, and S3 segments. The S1 segment is where around 90% of the glucose is reabsorbed, and most of the bicarbonate, amino acids, and other carbohydrates. The S2 and S3 segment reabsorb the remaining glucose and has organic anion transporters involved in the secretion of various exogenous compounds, including antibiotics, NSAIDs, methotrexate, etc. The fluid passes into the Loop of Henle and ultimately into the bladder as urine. Morphologically, the three segments can be observed to possess different brush border characteristics.

Loop of Henle – Distal Tubule – Collecting Duct

The Loop of Henle is a U-shaped section of the nephron, and consists of the thin descending and ascending limbs and a thick ascending limb. In the descending limb additional water is reabsorbed, further concentrating the filtrate. As the fluid enters the ascending limb, sodium chloride is further reabsorbed by diffusion and as the fluid reaches higher segments of the ascending limb, sodium chloride and potassium can be actively transported out of the filtrate, if necessary. In a person with high sodium intake, these transporters will not be utilized to the extent of a person with very low sodium intake. The remaining sodium chloride is expelled in the urine. The distal convoluted tubule receives the fluid from the ascending limb and is a major area of pH regulation. The distal tubule maintains proper pH by absorbing and/or secreting bicarbonate and protons (H^+) into the filtrate. Sodium and potassium can be further influenced in the distal tubule and is where the thiazide diuretics mechanism of action is located. Thiazide diuretics inhibit the sodium chloride reabsorption in the distal tubule by inhibiting the sodium chloride symporter. The fluid passing through the distal tubule flows into the collecting duct that acts as a connecting region from the tubules to the minor calyx or renal pelvis. The collecting duct is the final area of electrolyte and water reabsorption. Normally the collecting duct reabsorbs around 5% of the sodium and 5% water, however during times of dehydration, and in the presence of antidiuretic hormones, the collecting duct may reabsorb much more water to prevent bodily harm due to dehydration. Both aldosterone and vasopressin have

effects on the collecting duct's reabsorption and filtration system. Aldosterone increases sodium and water reabsorption and increases potassium excretion. Vasopressin increases the amount of water reabsorbed without altering solute reabsorption by increasing aquaporin channels, ultimately creating urine that is more concentrated. Fluid remaining in the collecting duct will enter various regions of the kidney in succession: the minor calyx, major calyx, renal pelvis, ureter, and bladder. Once in the bladder, the urine can be expelled. A diagram is provided below that depicts the kidney gross anatomy and inner nephron together with the renal vasculature (Figure 1.3).

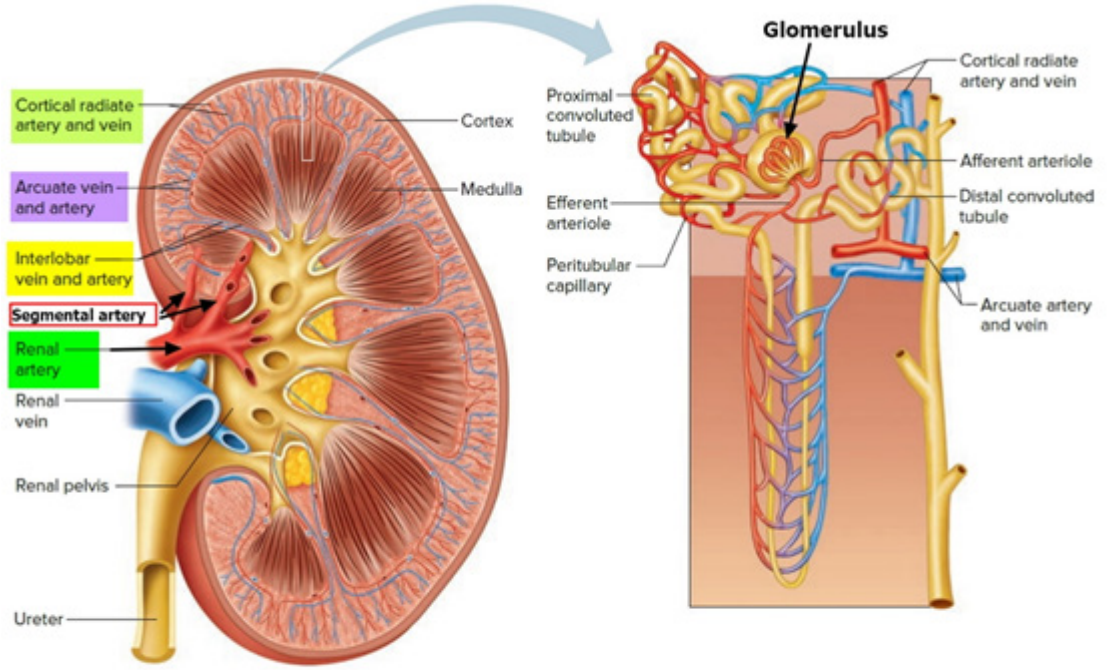

Figure 1.3: Renal vasculature in context with the kidney and the inner nephron.

ACUTE KIDNEY INJURY

Definition and Clinical Classification

Acute kidney injury (AKI) is defined as the rapid and abrupt loss of normal renal function (usually within less than 7 days). Decreased urine output, electrolyte and mineral imbalance, improper fluid balance, and an increase of waste products in the serum are all potential symptoms of AKI. Two of the most well-known waste products that become elevated are creatinine and urea. An older term for an abrupt loss of kidney function was acute renal failure (ARF). This term has been phased out in lieu of AKI, to more properly demonstrate the reality that less severe kidney injury (i.e. not reaching kidney failure status) can still have a detrimental impact on the patient's renal function and overall health. Clinically, a patient will be categorized as having AKI by their estimated glomerular filtration rate (GFR), which requires their serum creatinine (SCr) and urine output. The American Journal of Kidney Diseases and the National Kidney Foundation released 2018 AKI guidelines, titled, "Management of Acute Kidney Injury: Core Curriculum 2018." These guidelines utilized three distinct classification systems (Figure 1.4): 1) Kidney Disease: Improving Global Outcomes (KDIGO), 2) Acute Kidney Injury Network (AKIN), 3) Risk, Injury, Failure, Loss, and End-stage renal disease (RIFLE) [1].

The overall comparisons of the three different classifications can be found below in Figure 1.4, taken from the American Journal of Kidney Diseases and the National Kidney Foundation 2018 AKI guidelines (Figure 1.4). The RIFLE classification is the

lone system that contains five different categories versus three for the other classification systems. RIFLE associates varying degrees of kidney dysfunction to the five criteria levels:

1) Risk- defined as a ≥ 1.5-fold increase in SCr within 7 days and sustained for ≥ 24 hr in conjunction with urine output < 0.5 mL/kg/h for 6-12 hr
2) Injury- is a ≥ 2-fold increase in SCr and urine output < 0.5 mL/kg/h for ≥ 12 hr 3) Failure- is a SCr ≥ 3.0 mg/dL OR SCr increase to ≥ 4.0 mg/dL with an increase to 0.5 mg/dL OR initiation of renal replacement therapy (RRT), in combination with < 0.3 mL/kg/h for ≥ 24 hr or anuria for ≥ 12 hr
4) Loss- is the complete loss of kidney function for > 4 weeks
5) ESKD- is end-stage kidney disease defined as a sustained absence in renal function for > 3 months.

RIFLE classification is one of the first systems to identify an increase in AKI severity as an independent determinant for increased mortality [9]. RIFLE is also one of the better systems for predicting patient outcomes, especially for patients in intensive care [9-13]. A few limitations are identified for the RIFLE classification system. One limitation is that a baseline serum creatinine is needed, and this number is routinely not known. Another limitation is the RIFLE system uses serum creatinine and urine output as its lone diagnostic markers, which gives no indication of where the injury or

dysfunction is originating from; in contrast with some of the newer renal injury biomarkers [9, 14-17]. Regardless, the various classification systems and standardization for renal dysfunction have allowed for a plethora of controlled studies to help determine causative correlations with morbidity and mortality, as well as being a key diagnostic tool for patient prognosis and for therapeutic interventions.

Table 1. Comparison of Recent Consensus AKI Definitions

AKI Stage	Urine Output[a]	KDIGO	AKIN	RIFLE
1	<0.5 mL/kg/h for 6-12 h	Scr to 1.5-1.9 × baseline over 7 d or ≥0.3 mg/dL absolute increase over 48 h	Scr to 1.5-2 × baseline or ≥0.3 mg/dL absolute Scr increase within 48 h	*Risk*: Scr to ≥1.5 × increase within 7 d, sustained for ≥24 h
2	<0.5 mL/kg/h for ≥12 h	Scr to 2.0-2.9 × baseline	Scr to >2-3 × baseline	*Injury*: Scr to ≥2 × increase
3	<0.3 mL/kg/h for ≥24 h or anuria for ≥12 h	Scr to ≥3.0 × baseline, or Scr increase to ≥4.0 mg/dL or initiation of RRT	Scr to >3.0 × baseline, or Scr increase to ≥4.0 mg/dL (with increase of 0.5 mg/dL) or initiation of RRT	*Failure*: Scr to ≥3.0 × increase or Scr increase to ≥4.0 mg/dL (with increase of 0.5 mg/dL) or initiation of RRT
				Loss: Complete loss of kidney function for >4 wk
				ESKD: ESKD for >3 mo

Note: The first classification system, RIFLE, from the ADQI, incorporated 3 categories of injury and 2 outcomes that varied by severity. The outcomes (Loss, ESKD) were eliminated from the subsequent AKIN and KDIGO definitions. The AKIN definition incorporated smaller changes in Scr concentration, and the KDIGO definition added more definitive time frames to the definition. A key concept for the Scr-based definitions of AKI is the identification of baseline Scr concentration. Although the initial RIFLE criteria recommended the use of an Scr concentration that would equate to eGFR of 75 mL/min/1.73 m^2 by the MDRD Study equation (MDRD-75) if no baseline was available, this definition does not account for chronic kidney disease if present. It is essential to look for a prior baseline/reference Scr concentration, ideally from the 365 days before hospital admission from a clinical context in which there was not concern for AKI (eg, a stable clinic visit). This concept is discussed in detail in the KDIGO AKI clinical practice guideline.

Abbreviations: ADQI, Acute Dialysis Quality Initiative; AKI, acute kidney injury; AKIN, Acute Kidney Injury Network; eGFR, estimated glomerular filtration rate; ESKD, end-stage kidney disease; KDIGO, Kidney Disease: Improving Global Outcomes; MDRD, Modification in Diet in Renal Disease; RIFLE, risk, injury, failure, loss of kidney function, and end-stage kidney disease; RRT, renal replacement therapy; Scr, serum creatinine.

[a]All 3 definitions (KDIGO, AKIN, RIFLE) use common urine output criteria.

Figure 1.4: Comparison of Recent Consensus AKI Definitions. Table is from AJKD's Core Curriculum 2018 update on *Management of Acute Kidney Injury* [1].

AKI Epidemiology

Because AKI has been defined by various classification systems, and each could use different functional markers for the level of dysfunction, AKI incidence can vary significantly within reviews and renal studies. However, a thorough United States community-based study that followed nearly four million participants estimated the incidence of non-dialysis-requiring AKI to be approximately 384.1 per 100,000 person-years and the incidence of dialysis-requiring AKI was 24.4 per 100,000 person-years [18]. In the aforementioned study, males and the elderly experienced AKI at a higher rate than other populations [18]. Another study demonstrated that AKI incident rates could reach up to 65% in the critical hospitalized patients found in ICU settings [19]. Besides being an already common disorder in the hospital and ICU settings, studies suggest that AKI incidence may be increasing [20-22]. The reasons for this phenomenon range from better reporting, clearer guidelines and rules for diagnosing, to better overall healthcare for the elderly.

Morbidity and Mortality Associated with AKI

Mortality has been demonstrated to correlate with increased severity of AKI in hospitalized patient settings, such as cardiac surgery, major trauma, and critical illness [12, 23, 24]. In fact, approximately 24% of adults and 14% of children from mainly developed nations are associated with AKI mortality [2] (Figure 1.5). As one might expect as patients with higher level of care needed in a hospitalized setting, the mortality rate increases. Critically ill patients in the intensive care unit, requiring renal replacement therapy, have mortality rates around 55% [25, 26]. In a study following US military veterans, found that those with AKI had a long-term mortality rate two times larger compared to those vets without AKI [27]. As mentioned earlier under section AKI Epidemiology, reporting of AKI has increased, however, mortality from AKI is decreasing [10, 28]. Better diagnostics and supportive treatment care are the most likely reasons for this change in mortality [10, 28]. Morbidity associated with AKI is concomitant with patients who survive an initial acute injury, and these patients remain at high risk for poor outcomes and long-term mortality, as well as a significant financial burden [29]. Chronic kidney disease (CKD) and end-stage renal disease (ESRD) are more likely to occur in patients who have had AKI in the past; in fact, AKI is an independent risk factor for CKD and ESRD leading to increased mortality and poorer outcomes [30-32]. An estimated 34 million people are hospitalized per year, with an estimated financial burden of around 10 billion dollars in healthcare costs associated with the hospital stays within the United States [28].

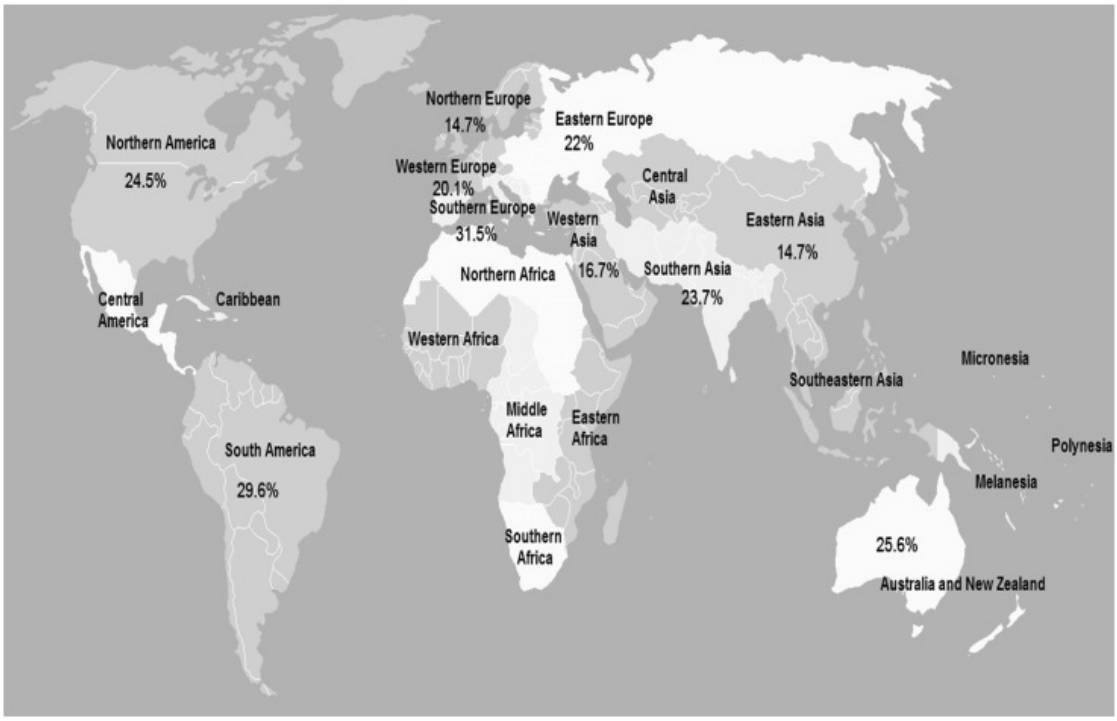

Figure 1.5: Pooled incidence rate of AKI by world zones. Studies used Kidney Disease Improving Global Outcomes (KDIGO) equivalent AKI definition. Adapted from [2]

Types of AKI

AKI can be classified into three distinct categories based on the origin of the injury causing the AKI. The three categories are 1) prerenal, 2) renal or intrinsic, 3) postrenal. AKI incidents due to prerenal alterations in blood volume or a reduction in blood flow into the kidney are estimated at around 70% for community-acquired AKI and 40% for hospital-acquired AKI [33, 34]. Some prerenal AKI causes are cardiac surgery, septic shock, blood loss (ex. hemorrhaging), and vascular disease, which all ultimately decreases the amount of blood reaching the kidney causing ischemic conditions and injury and organ dysfunction. As mentioned previously, the renal epithelial cells of the proximal tubule mainly utilize oxidative phosphorylation to meet their energy demands of various transport processes [7]. With an ischemic injury, the oxygen levels plummet, significantly affecting the proximal tubules cells. Intrinsic renal injury is when the injury originates inside the kidney, usually within the nephron [35]. Medications, drugs, toxins, and ischemia are causes of intrinsic renal injury. Postrenal AKI is an injury originating in the urinary tract but not inside the kidney, commonly caused by an obstruction in the bladder or urethra [35]. This obstruction causes pressure build-up and hydronephrosis [35].

Causes of AKI

AKI can be caused by various etiologies including septic shock, cardiac surgery or other major types of surgery, blood loss, vascular disease, urinary obstruction, and drug/toxicant exposure. In the critically ill and hospitalized patient, sepsis is the major cause of AKI and is responsible for nearly 50% of AKI cases [36]. Interestingly, the medications that patients receive in the hospital can cause AKI, such as aminoglycoside antibiotics, a plethora of chemotherapeutic agents, radiocontrast media, and certain pain medication (non-steroidal anti-inflammatory drugs-NSAIDs). Aminoglycosides, in particular, will accumulate in the proximal tubules cells of the kidney and cause phospholipid metabolism alterations leading to nephrotoxicity and decreased kidney function [37]. Aminoglycosides are very important life-saving antibiotics; however, their toxicity to the kidney can compound renal dysfunction, especially in ICU settings [38]. In a study following 61 patients in the ICU, 11.5% of patients developed aminoglycoside-associated nephrotoxicity [39]. One of the more well-known and studied chemotherapeutic agents, cisplatin, is associated with renal toxicity. Recent evidence suggests that a metabolite of cisplatin preferentially accumulates in the mitochondria and severely damages mitochondrial DNA [40, 41]. The renal proximal tubules have the highest density of mitochondria found in the kidney, which leads to cisplatin metabolite accumulation and mitochondrial DNA damage, and depletion of mitochondrial-encoded proteins [42]. Another common renal tubule agent is radiocontrast media [43]. Various imaging machines and techniques

need the patient to ingest or inject the media. This agent mainly affects patient population with preexisting renal impairment associated diseases; however, this population is also associated with needing radiocontrast media, causing increased AKI incidence [44, 45]. NSAIDs are a common over the counter pain medication that has been demonstrated to cause AKI, particularly in the elderly and people with poor renal function before starting on NSAIDs [46]. NSAIDs cause damage by reducing blood flow into the kidney by inhibiting prostaglandin production, and therefore affecting vasodilation and vasoconstriction of the renal vessels. NSAID use is also associated with acute interstitial nephritis (AIN), where inflammatory cells infiltrate the kidney and cause inflammatory related renal damage [46, 47].

Pathogenesis of Ischemia-Reperfusion Induced AKI

As mentioned previously, ischemia-reperfusion (IR) is a common AKI etiology. Certain drugs and toxicants, major surgery (cardiac surgery), as well as certain disease states including sepsis and vascular diseases are associated with reducing or stopping blood flow to the kidney causing ischemic damage [48-50]. The lack of oxygen and nutrients damages multiple cell types within the kidney and causes an inflammatory response. The epithelial, endothelial, and inflammatory cells respond to this ischemic environment and contribute to the AKI, [51]. Below is a chart outlining IR-induced AKI pathogenesis (Figure 1.6).

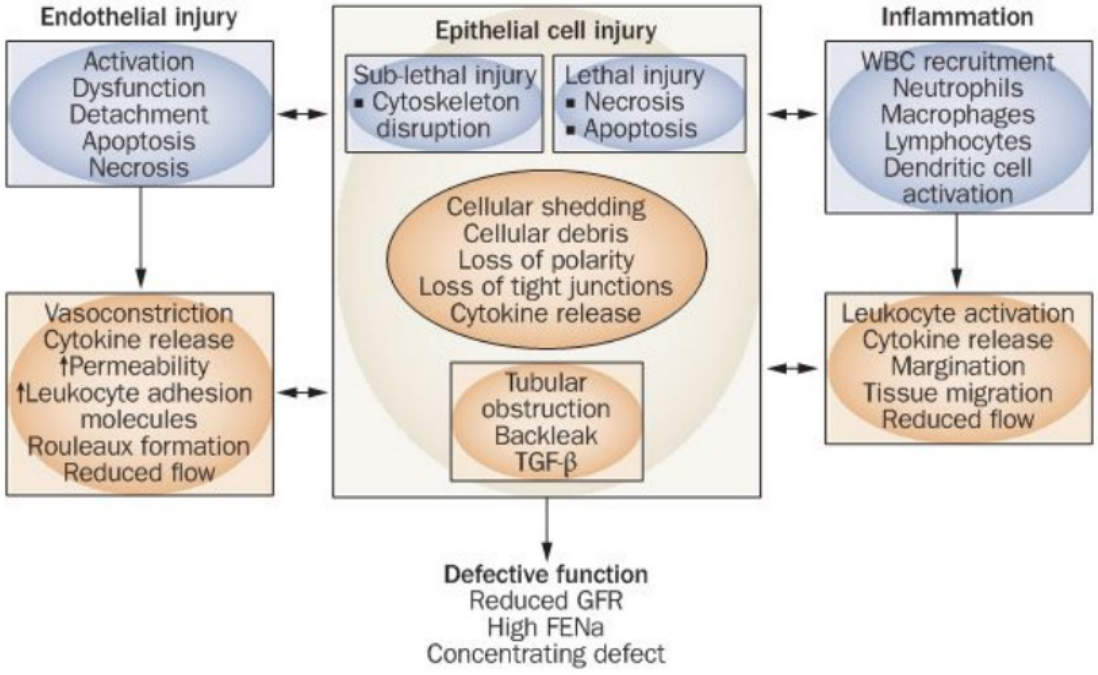

Figure 1.6: Pathogenesis of ischemic AKI. The major pathways of GFR impairment in ischemic acute tubular injury are caused by ATP depletion in vascular and tubular cells. Numerous interactions exist between endothelial cells, WBCs, and epithelial cells in the pathophysiology of ischemic AKI. These interactions are bidirectional between the cells involved, and result in specific functional and structural alterations. Inflammatory mediators released from proximal tubular cells influence endothelial cell processes (e.g. increase vasoconstriction and expression of cell adhesion molecules) that in turn influence the interactions between WBCs and endothelial cells, leading to reduced microvascular flow and continued hypoxia within the local environment. Additional functional changes occur, such as a marked reduction in production of erythropoietin and 25-hydroxylation of vitamin D. Electrolyte accumulation can rapidly lead to requirement of renal replacement therapy. Metabolic acidosis as a consequence of AKI must also be carefully monitored. Abbreviations: AKI, acute kidney injury; FENa, fractional excretion of sodium; GFR, glomerular filtration rate; TGF-β, transforming growth factor β; WBC, white blood cell [24].

The endothelial cells play a big role in renal damage due to IR injury. Endothelial cells are responsible for maintaining vascular permeability, proper blood flow, regulating vascular tone, as well as proper smooth muscle function [52, 53]. Even following IR-injury, the kidney continues to receive poor blood flow due to the damaged endothelium. Vasoconstriction is left unchecked due to increased cytokine production and release from endothelial-adhered leukocytes, such as IL-1β, TNF-α, and ET-1, and decreased nitric oxide production following IR-injury [52, 54-56]. Other inflammatory cells are easily passed through the damaged vasculature including neutrophils, lymphocytes, and macrophages. These inflammatory cells will release inflammatory mediators that can cause vasoconstriction, further restricting proper blood flow [57, 58]. Endothelial mitochondrial damage plays a role in endothelial-associated decreases in microvasculature density, and by protecting the mitochondria, the microvasculature becomes less injured [59, 60].

Renal epithelial cells, particularly the renal proximal tubule epithelial cells (RPTC), are very sensitive to IR AKI. RPTC absorb and secrete many different substances and these processes consume high levels of ATP, and therefore RPTC rely on oxidative phosphorylation for their energy production. ATP depletion is a common occurrence after IR injury and causes dysfunctional cellular process, and ultimately cell death [61, 62]. Loss of polarity, sodium-potassium ATPase transport activity, cytoskeletal alterations, and mitochondrial dysfunction are other key RPTC processes that become

dysfunctional after IR injury leading to poor renal outcomes [7, 63, 64]. Apoptotic and necrotic cell death are both observed following IR injury due to the aforementioned altered processes [61, 62]. Severely damaged RPTC will have disruptions in their adhesion complexes, making the RPTC unstable. If enough adhesion proteins are disrupted, the tubule epithelial cells will detach from the basolateral membrane and can form tubular casts in the tubular lumen, potentiating renal damage [7, 65]. New cells will migrate and take up the space where the previous RPTC was and replace the old dead epithelial cell. The exact source of these cells range from bone marrow stromal cells, renal specific stem cells, and surviving renal epithelial cells dedifferentiating [66-68]. Most recent evidence suggests that RPTC that become damaged but do not undergo necrosis or initiate apoptosis, may actually dedifferentiate, and migrate along the basement membrane and redifferentiate to restore lost epithelial cells [65, 69]. The differentiated epithelial cells will undergo gene and protein expression changes to express stem cell-related markers that help in the repair processes, and become a renal-specific cell that resembles a typical stem cell, [70-72]. Below is a diagram of normal repair in ischemic AKI, and two different possible routes of restoring lost tubular cells after injury (Figure 1.7 and Figure 1.8).

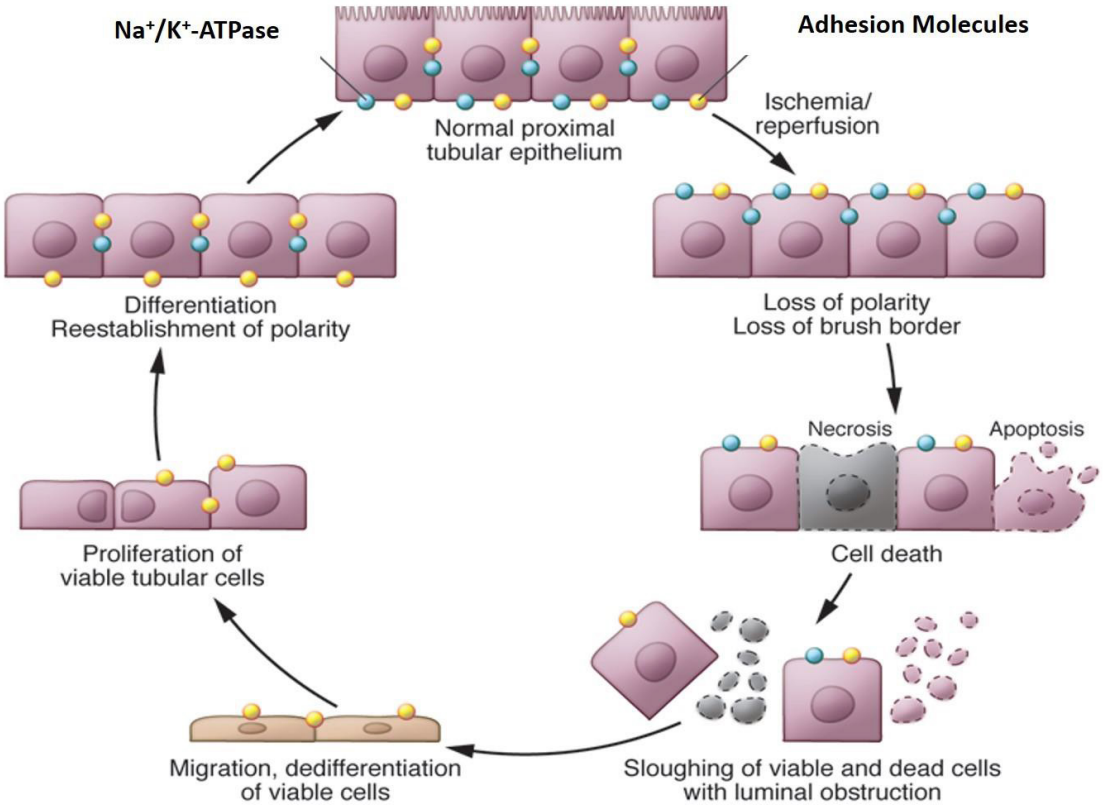

Figure 1.7: Normal Repair in Ischemic AKI. Following ischemic renal injury, renal epithelial cells lose their polarity and brush border with proteins translocated from the basolateral membrane to the apical membrane. In the case of severe ischemia, cell death occurs via necrosis and/or apoptosis. Necrotic debris and detached viable cells are released into the lumen, potentiating renal dysfunction. Viable cells undergo division to replace lost cells, and subsequent differentiation to restore nephron structure and function. Adapted from [7]

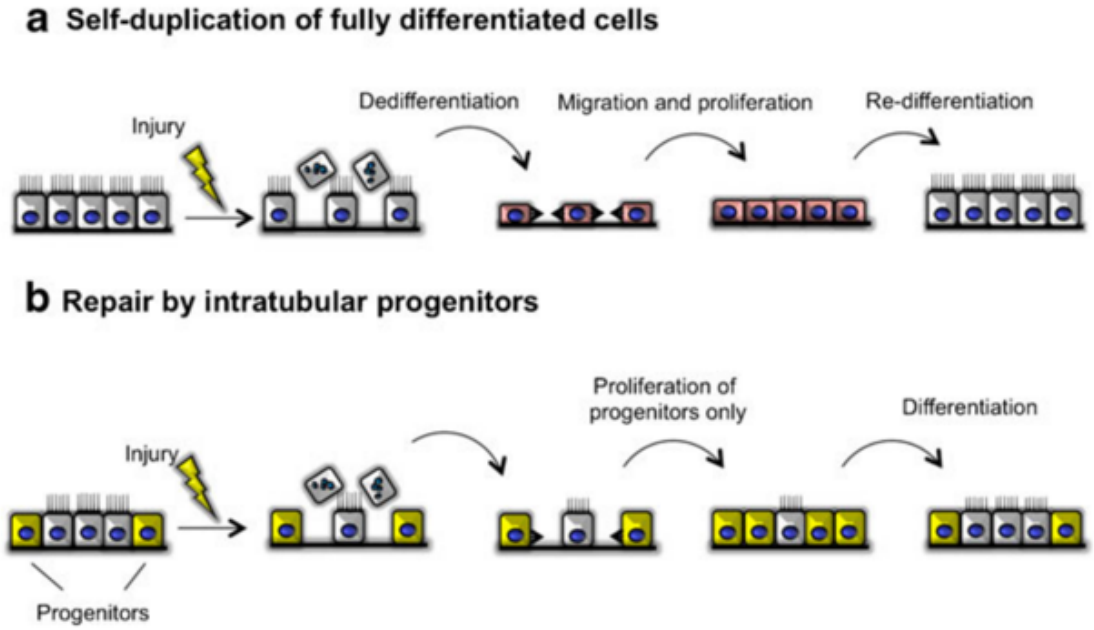

Figure 1.8: Comparison of Self-duplicating repair vs intratubular progenitor cells. The exact mechanism of repair of lost tubular cells and regeneration is not fully elucidated.

As mentioned previously, mitochondria play a substantial role in providing the ATP requirements for the various transport processes required to filter blood constantly in the renal proximal tubules. As the main organelle in the RPTC for energy production, any dysfunction to the mitochondria will have detrimental effects on the RPTC and impair the transport processes, leading to improper absorption and secretion [73-75]. Studies have demonstrated that mitochondria become damaged after IR injury before cellular injury and morphological changes can be observed, especially in the RPTC [76]. Likewise, recent research has strongly suggested that preventing mitochondrial damage from occurring after an insult and/or promoting repair of damaged mitochondria can prevent maximal injury resulting from the insult and increase the rate of renal recovery [75, 77].

Ischemia-Reperfusion Model of AKI

Rodents, particularly rats and mice, are commonly used for renal IR experiments to mimic human AKI. After a surgical midline excision, through both skin and muscle layers, while the animal is under anesthesia, the renal artery or pedicle is located. The renal artery is clamped either bilateral or unilateral for a specific amount of time, depending on the specific model of AKI. After ischemia, the clamps are removed and blood flow is observed to reperfuse the kidney, as a color change will occur (Figure 1.9). Experimental ischemia times can vary from one experimental study to the next while achieving the same final outcome changes (ex. BUN, SCr). This most likely stems from different core rodent body temperature maintained during surgery. Without maintaining a specific core body temperature, clamping/ischemia times must be greater than rodents with a maintained core body temperature [78-80]. In general, rats are less sensitive to IR injury and require longer ischemia times than mice, as bilateral clamping of rat renal pedicles typically needs 60 minutes to achieve the injury level of 18-30 minutes of clamping in mice [79]. Cell death, altered renal tubule blood flow, loss of RPTC adhesion and cellular integrity, and lumen cast formation are all observed, resulting from IR injury [81, 82].

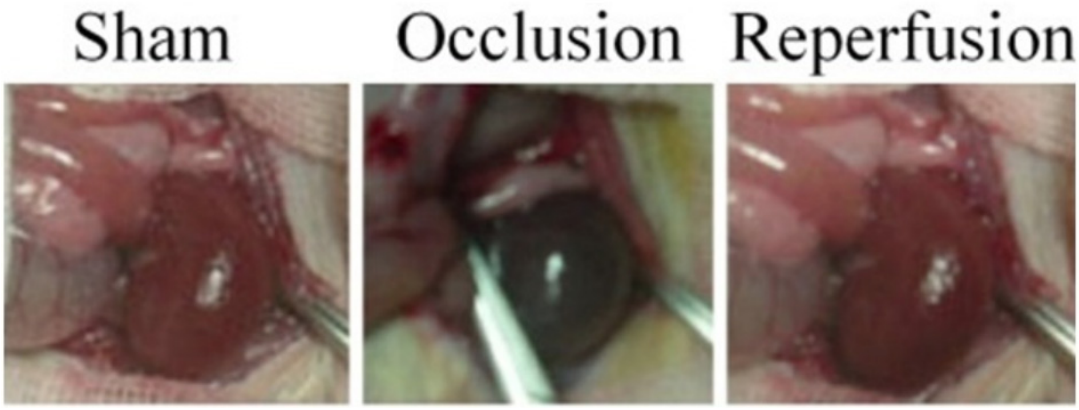

Figure 1.9: Representative images demonstrating induction of renal ischemia following by reperfusion. Adapted from [4].

Biomarkers of AKI

Novel AKI biomarkers have been researched heavily over the past decade. The earlier renal injury can be detected the earlier potential treatment options may be initiated for the patient, leading to better renal functional outcomes. Both urine and serum biomarkers could be easily tested in a hospital setting. Serum creatinine (SCr) and blood urea nitrogen (BUN) are two of the oldest and most common measurements for renal dysfunction in both a clinical and research setting [83]. However, both SCr and BUN have downfalls as a biomarker. The first is that increases in SCr and BUN may not be observed until days after an injury has occurred, yet, GFR is well-below normal [84]. This, in turn, could lead to an underestimated degree of injury, delayed treatment, and a failure to discontinue renal toxic medications. Second, SCr and BUN measurements can be altered by muscle mass, age, nutrition status, and medications [85]. An ideal biomarker would not change due to the above non-injury related factors. With the above limitations, there are now a multitude of new renal biomarkers being studied, with greater sensitivity and fewer alterations due to non-injury related changes in the patient. These biomarkers are being further studied to determine their practical use in a hospital setting [86] (Figure 1.10). The below paragraphs will focus on two specific biomarkers of kidney injury, neutrophil gelatinase-associated lipocalin (NGAL) and kidney injury molecule-1 (KIM-1), as these are two molecules we focused on in our research projects.

NGAL, also known as lipocalin-2, was originally found in neutrophils and has a molecular weight of 25-kDa [87]. NGAL is found in various epithelial cells within the kidney, trachea, lungs, stomach, and colon, and its function is to scavenge labile iron [88]. Labile iron is released from cellular organelles during an ischemic or septic injury, and can further cause oxidative stress after the ischemic injury has abated [89]. NGAL is highly upregulated following renal ischemia, and was found expressed in renal tubular cells in a mouse model of IR AKI [90, 91]. One of the first studies demonstrating the favorable biomarker profile of NGAL over SCr, was performed in 2005, where in pediatric patients who had subclinical AKI expressed high NGAL levels before SCr increased by 1-3 days [16]. An interesting finding was NGAL could be tested for in the blood and/or urine [16]. Renal ischemia studies have revealed NGAL expression levels increase in proportion to renal injury severity and duration, with NGAL levels increasing as early as 1 hr after IR injury and up to 3 days before any clinically relevant SCr changes [90, 92-94]. A potential limitation of NGAL as a clinically relevant biomarker of AKI, is if the patient has a bacterial infection or sepsis. Because neutrophils release NGAL after activation during a bacterial systemic infection, the NGAL assay measurements become difficult to interrupt and distinguish between infection and AKI [95, 96]. However, Canada and Europe has approved NGAL for clinical use for patients with suspected AKI [92, 97, 98].

KIM-1 is a conserved type-1 transmembrane glycoprotein that contains an immunoglobulin-like and glycosylated mucin domain [99]. KIM-1 protein is localized

to the renal proximal tubular cells, and is expressed at very low levels under non-injured conditions [99]. However, following an ischemic or septic injury KIM-1 expression rapidly increases significantly [100]. Unique to KIM-1, as a biomarker, is the specificity of demonstrating proximal tubule injury during AKI [99]. Following renal injury, the ectodomain of KIM-1 is cleaved and shed into the tubular filtrate within the lumen where it is excreted with the urine. Urine immunoassays were developed to test for KIM-1 ectodomain in high-risk patients for AKI, such as following cardiopulmonary bypass, cardiac catheterization, and ICU emergency surgery [101, 102]. KIM-1 recognizes phosphatidylserine and oxidized lipoprotein epitopes on the surface of apoptotic bodies that are found in the lumen following renal injury. Once recognized, KIM-1 helps clear the lumen debris by facilitating phagocytosis, which decreases an inflammatory response and helps prevent obstruction within the tubule [103, 104]. KIM-1 mRNA increases within 3 hr following renal IR injury and increased protein expression can be observed before changes in SCr and BUN [105, 106]. Because KIM-1 is found in the proximal tubules, the sensitivity for specifically denoting renal injury is higher than other biomarkers for AKI (Figure 1.10) [105]. However, a limitation of KIM-1 is that the receptor helps with repair processes, therefore finding increased KIM-1 in the urine may not help in identifying early AKI as the KIM-1 in the urine may be present due to the recovery phase. Recently, 32 urine biomarkers were studied following cardiac surgery for their

predictive value in determining AKI severity; the combination of IL-18 and KIM-1 had the best predictability towards severe AKI [107, 108].

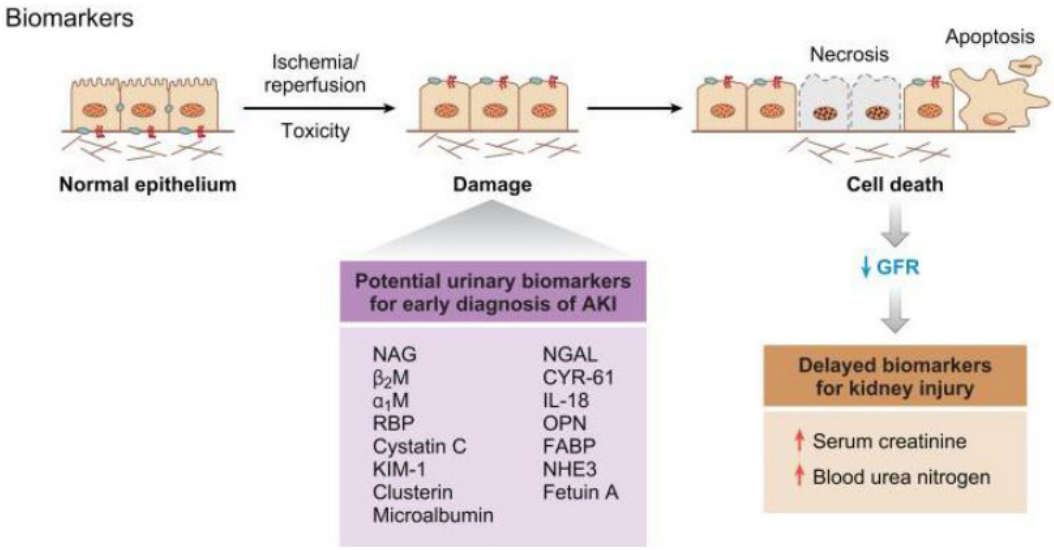

Figure 1.10: Biomarkers of AKI. Traditionally used markers, such as blood urea nitrogen (BUN) and creatinine (CR), are insensitive, nonspecific, and do not adequately differentiate between the different stages of AKI. A delay in diagnosis prevents timely patient management decisions, including administration of putative therapeutic agents. Urinary biomarkers of AKI will facilitate earlier diagnosis and specific preventative and therapeutic strategies, ultimately resulting in fewer complications and improved outcomes [3]

Pharmacological Treatment of AKI

Currently, there is no effective pharmacological treatment for AKI. Therapeutic strategies for managing AKI involve maintaining proper fluid volume status, controlling disease states associated with renal damage, discontinuing renal toxic medications, and renal replacement therapy. Pharmacological agents have been studied in the literature and include vasoactive drugs (dopamine, fenoldopam, theophylline), anti-inflammatory drugs (aspirin, dexamethasone), and antioxidants (N-acetylcysteine) [109-114]. Figure 1.11 shows recent novel therapeutic agents for the treatment of AKI (Figure 1.11) [115]. Developing a treatment option for AKI is difficult as there are multiple pathophysiological mechanism of injury occurring in parallel and in sequence [115]. Oxidative stress, disrupted cellular metabolism, mitochondrial bioenergetics dysfunction, inflammation, apoptosis, and necrosis occur simultaneously at the initiation of the injury and progression to AKI [116]. Because of the aforementioned multitude of altered cellular and mitochondrial process, future pharmacological drug trials will conceivably focus on a multi-targeted approach possibly with more than one active drug being tested. The logic behind this approach is to restore multiple known dysfunctional pathways after AKI, as single agent approaches have not succeeded.

Table 1. Novel therapeutic agents for acute kidney injury

Agent	Mechanism of action	Potential indication(s)
Renal blood flow modifiers		
Angiotensin	Constricts efferent arterioles to a greater degree than afferent arterioles Regulates release of aldosterone and vasopressin	Sepsis
Adenosine antagonists	Reduces GFR in response to hypoxia Constricts afferent arterioles → increase NaCl levels in proximal tubules	CIN IRI Cardiorenal syndrome
Antioxidants		
Alpha-lipoic acid	Reduced form eliminates free radicals Improves glomerular function Reduces renal inflammation	IRI CIN
Selenium	Cofactor that reduces free radicals	Cisplatin injury ECSL
MESNA	Scavenges for free radical oxygen species	CIN
Propofol	Converts free oxygen radicals into a phenoxyl form	IRI
Curcumin	Scavenges for free oxygen radicals Stimulates activity of antioxidant molecules such as superoxide dismutase, catalase, and glutathione peroxidase	IRI Diabetic nephropathy Lupus nephritis
Anti-inflammatory mediators		
Alkaline phosphatase	Dephosphorylates lipopolysaccharide Dephosphorylates ATP	Gram-negative sepsis
Dipeptidylpeptidase-4 Inhibitors	Extends half-life of glucagon-like peptide-1	Diabetic nephropathy Cisplatin injury
Sphingosine 1 phosphate (S1P) analogues	Mitigates endothelial damage Decreases recruitment of inflammatory mediators to the renal tubules	None to date
Genetic modifiers		
I5NP	Inhibits p53 gene	IRI

ATP, adenosine triphosphate; CIN, contrast induced nephropathy; ECSL, extracorporeal shockwave lithotripsy; GFR, glomerular filtration rate; IRI, ischemia reperfusion injury; MESNA, sodium 2-mercaptoethane sulfonate; NaCl, sodium chloride.

Figure 1.11: Novel therapeutic agents for acute kidney injury.
Adapted from [112]

MITOCHONDRIAL BIOLOGY

Mitochondrial Function

Mitochondria are subcellular organelles that generate the energy-rich molecule, ATP, through oxidative phosphorylation, which regulates cellular metabolism and homeostasis. Beyond ATP production, mitochondria are involved in a host of other pathways, including, calcium storage and signaling, fatty acid oxidation, ROS generation and signaling, citric acid cycle, regulating programmed cell death, initial steroid hormone synthesis, heme synthesis, and heat production.

Mitochondrial Structure

The mitochondria is a membrane-bound organelle consisting of two membrane layers made up of phospholipid bilayers, the outer mitochondrial membrane (OMM) and the inner mitochondrial membrane (IMM). The OMM is a selectively permeable membrane containing porins, channel proteins, for transporting various essential molecules into the mitochondria. Because the IMM is much larger than the OMM, the IMM is able to fit inside the OMM because it contains membrane folds called cristae, and is a much more selective membrane barrier than the OMM [117]. The nature of the mitochondrial structure consisting of the OMM and IMM helps form four different areas within the mitochondria. The first consists of the OMM and the transport channel proteins and some metabolic enzymes. The second, is the intermembrane space, the space between the OMM and IMM, which maintains a proton gradient for

the proper function of the electron transport chain (ETC). The third is the IMM, where the ETC components are located, including, Complex 1-IV and ATP synthase. The fourth is the mitochondrial matrix where many metabolic pathways occur, including the citric acid cycle and fatty acid oxidation. The mitochondrial matrix contains the mitochondrial DNA (mtDNA), which is circular double stranded DNA located in the mitochondria and separate from the nuclear DNA. The mitochondrial matrix also contains the enzymes and ribosomes for mtDNA transcription and mitochondrial-encoded protein translation [117, 118].

Mitochondrial DNA

The mitochondria contain the only other source of DNA within the cell besides the eukaryotic nucleus. mtDNA are maternally inherited DNA that are packaged inside the inner mitochondrial membrane, usually along the cristae, in nucleoids [119, 120]. These nucleoids consist of mtDNA and specific mtDNA proteins required for stability, replication, transcription, repair, and packaging [121]. mtDNA is circular double stranded DNA containing 37 genes that encodes 13 subunits of the mitochondrial oxidative phosphorylation system, 22 tRNAs, and 2 rRNAs. The other ~1500 mitochondrial proteins are transcribed from nuclear DNA [122]. The exact number of mtDNA molecules per cell varies wildly from hundreds to thousands based on tissue specific needs [123]. The kidney is the second highest mitochondrially dense organ

behind the heart, although the mitochondria within the proximal convoluted tubules are denser than the heart [124].

Mitochondrial Homeostasis

Because the mitochondria play such a critical role in most cells life cycle, the proper functioning of the mitochondria is essential for a healthy cell. Mitochondrial homeostasis is the termed used for quality control over generating new mitochondria (mitochondrial biogenesis) or programmed removal of damaged mitochondria (mitophagy), as well as mitochondrial dynamics (fission and fusion) [125, 126]. Mitochondrial dynamics alters the morphology and consists of the interplay between two distinctly different process, fission and fusion. Mitochondrial fission is the process of dividing mitochondria into smaller mitochondrion. Fission requires the cytosolic GTPase dynamin-related protein 1 (Drp1) and OMM located mitochondrial fission 1 protein (Fis1). Mitochondrial fusion is the joining of separate mitochondria to form branched and elongated mitochondrial networks. Fusion requires the OMM located mitofusins 1 and 2 (Mfn1 and Mfn2) and the IMM located optic atrophy 1 (OPA1). Fusion and fission occur constantly throughout the cells life cycle and this interplay can determine the energy status of the cell [127, 128]. Mitochondrial mitophagy is the way in which the cell is able to degrade damaged or dysfunctional mitochondrial by way of lysosomal digestion. Mitophagy is regulated through the OMM located PTEN-induced putative kinase 1 (PINK1) and the cytosolic E3 ubiquitin ligase Parkin [129]. Figure 1.12 depicts the mitochondrial life cycle. (Figure 1.12 [8]

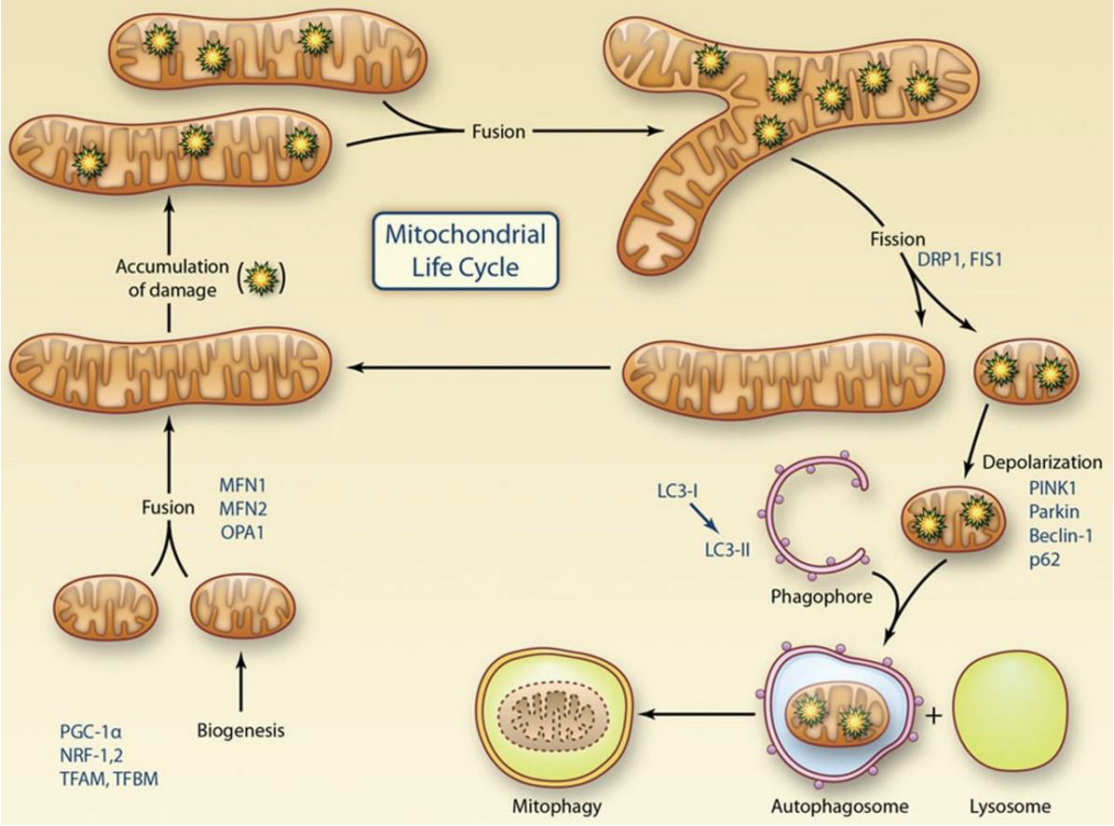

Figure 1.12: Mitochondrial Life Cycle. Mitochondrial homeostasis is a multifactorial process governed by MB, fission/fusion and mitophagy. PGC-1α activates nuclear respiratory factor 1 (Nrf1) and nuclear respiratory factor 2 (Nrf2) to coordinate the expression of nuclear genes required for MB. PGC-1α also activate mitochondrial transcription factor A (TFAM) and mitochondrial transcription factor B (TFBM), which regulate the transcription of genes encoded by mtDNA. Mitochondria undergo cycles of fusion, which is mediated by mitofusin (Mfn) 1, Mfn2 and optic atrophy protein (Opa1). Fission is mediated by dynamin-related protein 1 (Drp1) and fission 1 (Fis1). Fission also promotes the isolation of damaged mitochondria for selective mitochondrial degradation, a process called mitophagy. Mitophagy involves the mitochondrial depolarization, accumulation of putative kinase protein kinase 1 (Pink1) on the mitochondrial membrane, recruitment of Parkin, which targets the mitochondria to the autophagosome through the ubiquitination of mitochondrial proteins. Assembly of the phagosome involves beclin-1, p62 and conjugation of microtubule-associated protein 1 light chain 3 (LC3II). Adapted from [8].

Mitochondrial Biogenesis

Mitochondrial biogenesis (MB) is broadly defined as the cell's pathway to generate new functioning mitochondria. MB can increase preexisting mitochondrial mass and copy number and therefore, has the potential to increase energy production by way of ATP synthesis. MB occurs under physiological conditions, but can be highly induced due to various extracellular stressors, exercise, calorie insufficiency, and low body temperatures [130, 131]. The master regulator of MB is the nuclear transcriptional coactivator peroxisome proliferator-activated receptor coactivator-1 alpha (PGC-1α). The PGC-1 family of transcriptional co-activators also includes PGC-1β and PGC-1-related coactivator (PRC) that can also regulate MB. However, PGC-1α has been shown to be abundantly expressed in tissues with high-energy demands, such as the heart, skeletal muscle and the kidney. Increased PGC-1α or increased activity of PGC-1α increases MB specific nuclear- and mitochondrial-encoded proteins required for the generation of new mitochondria or increased mitochondrial mass [132, 133]. PGC-1α enhances the following transcription factors, PPARs (PPARα, PPARδ, PPARγ), estrogen related receptors (ERRα, ERRβ, and ERRγ), nuclear respiratory factors (NRF-1 and NRF-2), and FOXO3 (forkhead box protein O3) [134, 135]. PGC-1α, like its other PGC-1 family, contains an N-terminal activation domain consisting of leucine-rich LXXLL motif that mediates its activity with other nuclear transcription factors. As PGC-1α is a co-activator, it does not bind DNA but enhances the activity of other transcriptional factor and their associated-protein binding complexes.

NRF Transcriptional Regulation of Mitochondrial Biogenesis

NRF-1 and NRF-2 are nuclear transcription factors that upregulate specific nuclear-encoded mitochondrial genes, and are enhanced by PGC-1α. NRF-1 increases the expression of various mitochondrial-related genes, including mitochondrial ETC complex components (ETC complex subunits, cytochrome C), mtDNA transcription and translation (transcription factor A, TFAM), and mitochondrial protein transport and assembly (TOM20, COX17) [136, 137]. NRF-2 is also a transcriptional factor for other mitochondrial related targets, including mitochondrial respiration (subunit IV of cytochrome c oxidase), mitochondrial import proteins (Tom20, Tom70), and mtDNA transcription (TFAM) [136]. The importance of properly functioning mitochondrial regulation can be found in NRF-1 and NRF-2 knockout mice, as mice with both NRFs knocked out are lethal [138, 139].

Mitochondrial Biogenesis in Renal Injury

As mentioned previously, the renal proximal tubule epithelial cells require lots of oxygen to power oxidative phosphorylation, which supplies their high energy requirements for the various transport processes that are constantly active for filtering the blood. The mitochondrial density within RPTC is one of the highest of any organ cell type in the body; hence, any injury that causes mitochondria dysfunction will cause detrimental affects to the RPTC and ultimately kidney dysfunction. Acute oxidant injury has been shown to cause mitochondrial dysfunction in RPTC, by decreasing ATP levels and oxygen consumption rate in the mitochondria [140, 141]. Interestingly, overexpression of PGC-1α after oxidant injury in RPTC increased mitochondrial specific proteins, ATP levels, and mitochondrial oxygen consumption (Figure 1.13) [6]. In two experimental models of AKI, IR- and sepsis-induced, PGC-1α mRNA is rapidly downregulated within 3 hr of initiated injury. This rapid regulation of mitochondrial biogenesis after AKI, demonstrates the potential to target PGC-1α and MB as a target of pharmacological treatment [142, 143].

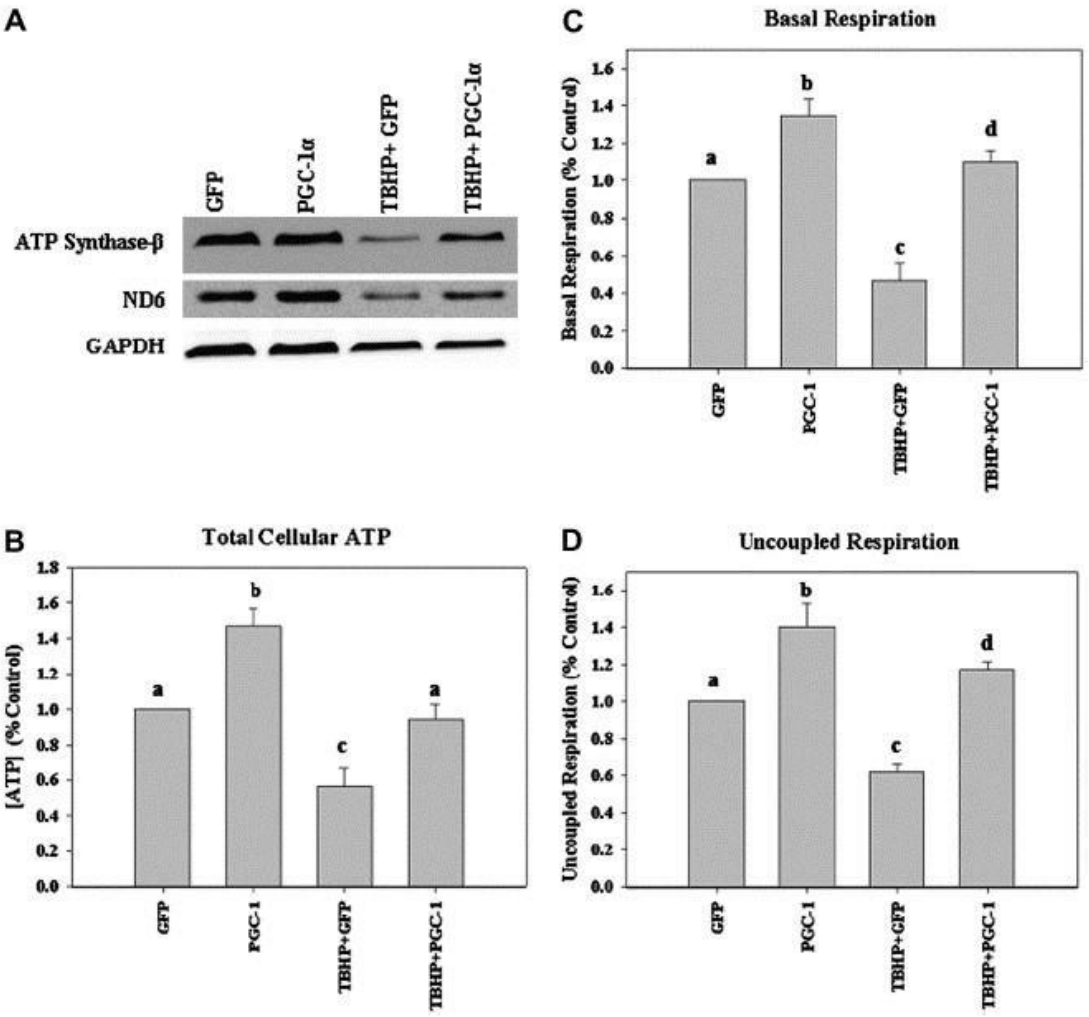

Figure 1.13: Overexpression of PGC-1α after oxidant injury restored mitochondrial protein expression (A) as well as total cellular ATP (B) and basal (C) and uncoupled (C) oxygen consumption in RPTC exposed to tertbutyl-hydroperoxide [6]. Different superscripts indicate statistically significant differences.

Pharmacological Activation of Mitochondrial Biogenesis

Because the mitochondria play such a big role in RPTC physiology and pathophysiology as mentioned above, the identification of a pharmacological agent that would activate MB would be a great therapeutic strategy for prevention of RPTC injury or increasing repair following AKI. For this reason, pharmacological agents that control PGC-1α have been a central focus in our lab, as well as many others. Using pharmacological agents to modulate upstream MB pathways such as AMP kinase, sirtuins, cyclic AMP and GMP, B2 receptor, and the 5-HT1F receptor has shown promise in activating MB [144-151]. Figure 1.14 showcases the multitude of pathways that regulate MB, mostly through the co-activator PGC-1α [152].

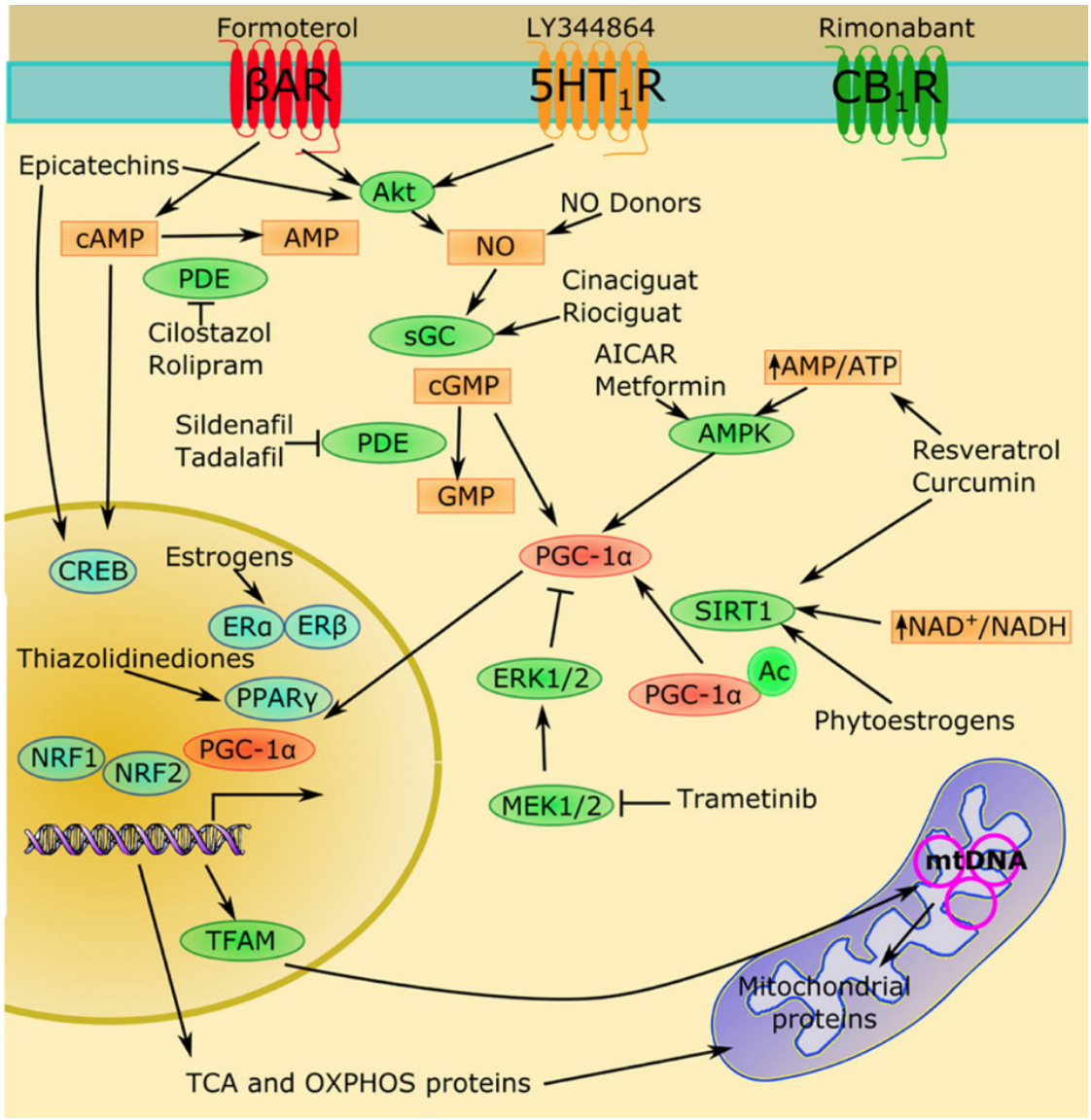

Figure 1.14: Pharmacological Activation of MB. MB is a complex process controlled by the transcriptional regulator, PGC-1α. PGC-1α expression and activity is regulated by a variety of pathways including receptor tyrosine kinases, G-protein coupled receptors (GPCR), naturetic peptide receptors, cyclic guanosine monophosphate (cGMP), ERK1/2, as well as SIRT1-mediated deacetylation.

Likewise, targeting negative regulators of MB would be of therapeutic benefit. Instead of increasing an activation pathway (as discussed above), an inhibition or blockade of physiological or pathological signaling that negatively regulates PGC-1α or other MB pathways would conceivably be of benefit before, during, or after AKI has occurred. Negative regulation of MB has been observed in multiple forms of AKI, including IR injury, sepsis, gentamycin toxicity, and folic acid nephropathy, where mitochondrial gene targets and proteins are downregulated rapidly after injury [126, 142, 143, 153-156]. Negative regulation of MB does not only occur in injured states, but has also been observed to occur in an age-associated manner [157, 158]. Multiple negative regulator pathways have been studied including the transcription factors, receptor-interacting protein 140 (RIP140), hypoxia-inducible factor 1-α (HIF-1α), and mitochondrial transcription termination factor 3 (MTERF3) [132]. The pro-inflammatory cytokine tumor necrosis factor alpha (TNF-α) has been demonstrated to downregulate MB through an eNOS dependent manner and cause mitochondrial dysfunction by decreasing mitochondrial proximity with sarcoplasmic reticulum. [159-161]. The mitogen-activated protein kinase (MAPK), ERK1/2 (extracellular signal-regulated kinases 1/2), when activated, has been shown to reduce mitochondrial basal respiration and ATP production, reduce uncoupled oxygen consumption, disrupt mitochondrial membrane potential, initiate iron-induced mitochondrial swelling, and decrease MB targets [142, 162-167]. The remainder of the dissertation will focus on

ERK1/2 signaling and inhibition of ERK1/2 activation following multiple models of AKI in mice, with a key focus on MB and disruption of mitochondrial homeostasis.

Intracellular Signaling

Intracellular signaling is an important and complex cellular pathway by which all different cell types respond to extracellular stimuli and events. The purpose of intracellular signaling is to allow the cell to respond and adjust to environmental factors and extracellular stimuli presented to the cellular surface. In this way the cell can upregulate or downregulate certain signaling pathways that would potentially be more beneficial for the cell in their current environment. These intracellular signaling events can occur rapidly, which allows the cell to respond in a timely manner to adapt and thrive. Examples of changes within the cell that could occur are alterations in gene transcription, protein expression, post-translational modifications, protein translocation, enzyme activity rates, and changes in cellular metabolism [168, 169].

Extracellular stimuli and/or environmental factors have the ability to stimulate various receptors on the cell surface causing activation of the receptors through ligand binding and/or non-binding (temperature) of the receptor. These receptors could be ion channel-linked (ex. 5-HT receptor), enzyme-linked (ex. receptor tyrosine kinase), and G-protein-coupled (ex. β2-adrenergic receptor). Once activated the receptors stimulate intracellular targets by way of recruitment and adapter proteins that are usually located near the cell surface from the cytosolic side along the membrane [170, 171]. Depending on the receptor type and activation, the adaptor proteins stimulate a signaling cascade where one activation leads to another activation in a stepwise

manner. One of the most well-known and studied intracellular signaling cascade is the mitogen-activated protein (MAP) kinase pathway. The classical MAP kinases are Jun N-terminal kinase (JNK), p38, and ERK. The ERK family is one of the best-characterized family of MAP kinases, specifically ERK1 and ERK2 [172].

Extracellular Signal-Regulated Kinase 1/2

ERK1/2 was found to become highly phosphorylated by addition of epidermal growth factor (EGF) and platelet-derived growth factor (PDGF) to developing chicken embryos [173]. At the time (1983), the authors did not know they were studying ERK1/2 just proteins of 40 and 42 kDa [173]. ERK1/2 becomes phosphorylated through growth factor stimulation because once bound to the receptor, a signaling cascade begins and preceding in a step-wise manner until phosphorylation of ERK1/2. Stimulation of receptor tyrosine kinases (RTKs) causes dimerization of the receptor, and allows autophosphorylation to occur [174]. The adapter protein growth factor receptor-bound protein 2 (Grb2) can now bind to the intracellular phosphorylated portion of the RTK, and recruits Son of Sevenless (Sos). This Grb2 and Sos complex allows for inactive Ras GTPases to locate to the activated RTK [175]. The three subfamily of Ras proteins that activate the ERK1/2 signaling cascade are H-Ras, K-Ras, and N-Ras. Inactive Ras is Ras bound with GDP. Upon association with Grb2 and Sos complex, Ras releases GDP and binds GTP, which promotes conformational changes to Ras. These changes create a better surface for protein-protein interactions,

which leads to activation of various effector proteins (Raf, phospholipase C) from the cell surface and downstream signaling throughout the cytosol, mitochondria, and nucleus [172].

The main effector, with respect to ERK1/2 signaling, is the Raf family of kinases. There is A-Raf, B-Raf, and C-Raf, which are serine/threonine kinases. Once Ras has become activated, Rafs phosphorylate and activate MEK1 and MEK2 (MEK1/2) [176, 177]. Raf kinase localization and activity are dependent on the multiple conformational changes and phosphorylations they can undergo [177, 178]. For C-Raf, phosphorylation at Ser338 and Tyr341 are needed for Raf kinase activity. B-Raf has a higher basal kinase activity than C-Raf because B-Raf contains a phosphomimetic at position 448, which mimics C-Raf phosphorylation at Tyr341. Raf kinases (and other MAP kinase kinases) phosphorylate MEK1 and MEK2 on Ser218 and Ser222, and both amino acids becoming phosphorylated are required for full activation [172, 179]. MEK1/2, once activated, can phosphorylate ERK1 and ERK2, which are the only known substrates of MEK1/2. Figure 1.15 shows the ERK1/2 signaling cascade [5].

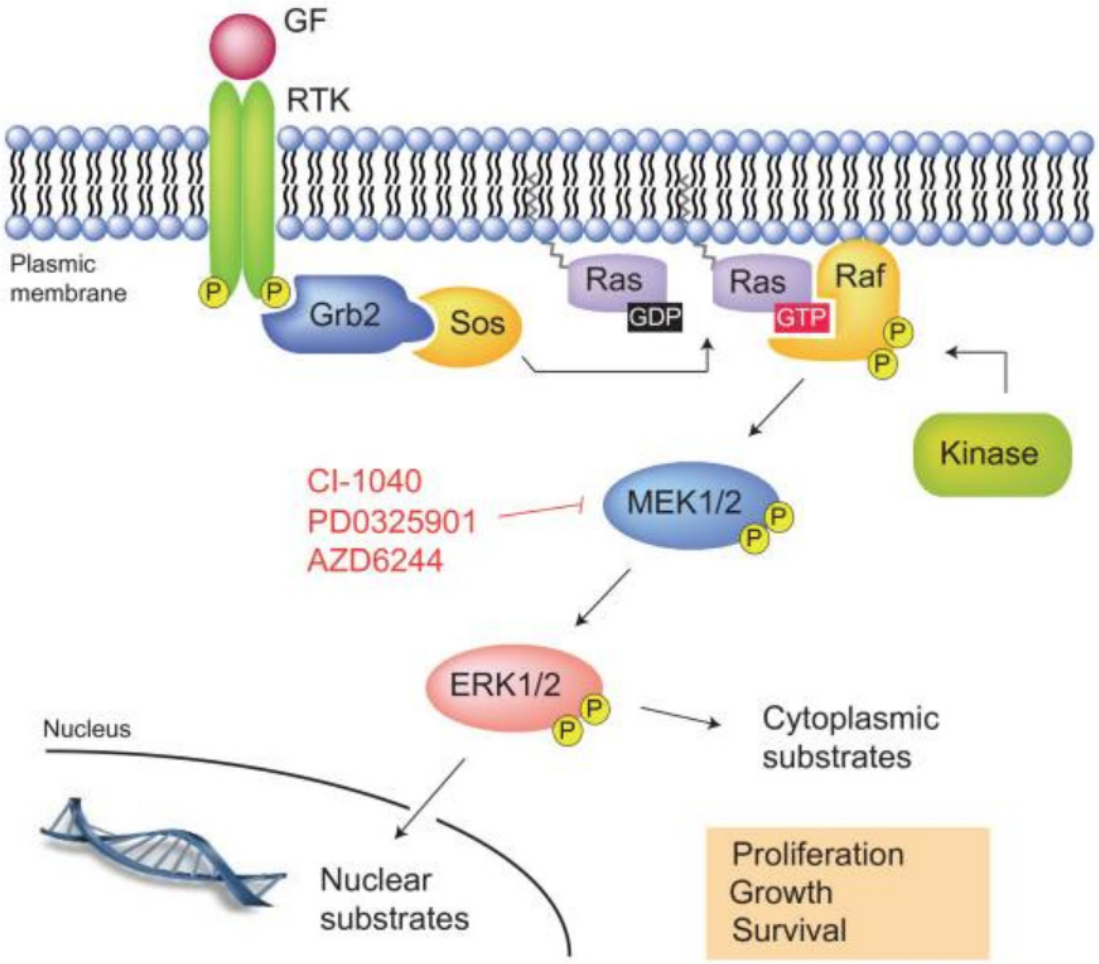

Figure 1.15: Schematic Representation of the Ras-Raf-MEK-ERK1/2 MAP kinase pathway. GF, growth factor; RTK, receptor tyrosine kinase. Adapted from [5].

ERK1 is phosphorylated at Thr202 and Tyr204 and ERK2 is phosphorylated at Thr183 and Tyr185, and both phosphorylation sites are required for maximal activity of ERK1/2 [180, 181]. ERK1 and ERK2 contain ~85% sequence identity, 100% similar catalysis and docking residues, are activated from identical stimuli, perform similar downstream functions inside the cell, and are co-expressed in almost all cell types [182-185]. However, ERK2 knockout mice are embryonic lethal, whereas ERK1 knockout mice are not and are fertile, pointing to ERK2 playing a more essential role in mouse embryo development [186-188]. Contradicting this ERK specific developmental assumption, is a study by Fremin et al., which demonstrated mice embryos developed normally in ERK2 deficient embryos by increasing ERK1 by an *Erk1* transgene [189]. Therefore, ERK1 and ERK2 may be functionally repetitive during mouse developmental stages as well as in a mature mouse, and any knockdown of one kinase, ERK1 or ERK2, led to observable effects merely because of a decrease in total kinase protein levels [184, 189, 190].

ERK1/2 can be anchored in the cytoplasm by various proteins, including MEKs and MAP kinase phosphatase 3 (MKP-3). However, ERK1/2 can translocate into the nucleus by way of passive diffusion, as the size of ERK1 (44 kDa) and ERK2 (42-kDa) is small enough to not require ATP or specialized protein transporters [191, 192]. This translocation process is dynamic and ERK1/2 do not contain nuclear export sequence, but rather ERK2 is exported by both energy- and carrier-independent

mechanisms, mediated in part by the exportin, Exportin 1 (XPO1 or CRM1) and the nuclear pore complex, specifically the nucleoporin, Tpr [193-196].

Extracellular stimuli can activate ERK1/2 in minutes which can be critical for the cell (and tissue/organ) depending on the biological response required to initiate. ERK1/2 has been shown to be involved with cell survival, cell death, differentiation, proliferation, migration, transcription, and translation among others [172, 197, 198]. To accomplish the above-mentioned biological responses, ERK1/2 phosphorylates various cellular substrates, and these substrates perform downstream cellular functions that ultimately provide the response for the specific stimulus. Currently, ERK1/2 was found to have 659 direct phospho-site targets on various substrates [199]. Among those substrate targets of ERK1/2 are upstream proteins involved in ERK1/2 activation, including Sos1, Raf, and MEK1. Interestingly, ERK1/2 phosphorylation of these upstream proteins decreases its own activation signal, by diminishing each substrates activity for continuing to stimulate the ERK1/2 signaling cascade [172, 200-203].

REFERENCES

1. Moore, P.K., R.K. Hsu, and K.D. Liu, *Management of Acute Kidney Injury: Core Curriculum 2018.* Am J Kidney Dis, 2018. **72**(1): p. 136-148.
2. Susantitaphong, P., et al., *World incidence of AKI: a meta-analysis.* Clin J Am Soc Nephrol, 2013. **8**(9): p. 1482-93.
3. Vaidya, V.S., et al., *Urinary biomarkers for sensitive and specific detection of acute kidney injury in humans.* Clin Transl Sci, 2008. **1**(3): p. 200-8.
4. Feng, J., et al., *Increasing Proliferation of Intrinsic Tubular Cells after Renal Ischemia-reperfusion Injury in Adult Rat.* Aging Dis, 2015. **6**(4): p. 228-35.
5. Fremin, C. and S. Meloche, *From basic research to clinical development of MEK1/2 inhibitors for cancer therapy.* J Hematol Oncol, 2010. **3**: p. 8.
6. Rasbach, K.A. and R.G. Schnellmann, *PGC-1alpha over-expression promotes recovery from mitochondrial dysfunction and cell injury.* Biochem Biophys Res Commun, 2007. **355**(3): p. 734-9.
7. Bonventre, J.V. and L. Yang, *Cellular pathophysiology of ischemic acute kidney injury.* J Clin Invest, 2011. **121**(11): p. 4210-21.
8. Kluge, M.A., J.L. Fetterman, and J.A. Vita, *Mitochondria and endothelial function.* Circ Res, 2013. **112**(8): p. 1171-88.
9. Lopes, J.A. and S. Jorge, *The RIFLE and AKIN classifications for acute kidney injury: a critical and comprehensive review.* Clin Kidney J, 2013. **6**(1): p. 8-14.
10. Hoste, E.A., et al., *RIFLE criteria for acute kidney injury are associated with hospital mortality in critically ill patients: a cohort analysis.* Crit Care, 2006. **10**(3): p. R73.
11. Lopes, J.A., et al., *Contemporary analysis of the influence of acute kidney injury after reduced intensity conditioning haematopoietic cell transplantation on long-term survival.* Bone Marrow Transplant, 2008. **42**(9): p. 619-26.
12. Ostermann, M. and R.W. Chang, *Acute kidney injury in the intensive care unit according to RIFLE.* Crit Care Med, 2007. **35**(8): p. 1837-43; quiz 1852.
13. Bagshaw, S.M., et al., *A multi-centre evaluation of the RIFLE criteria for early acute kidney injury in critically ill patients.* Nephrol Dial Transplant, 2008. **23**(4): p. 1203-10.
14. Bellomo, R., et al., *Acute renal failure - definition, outcome measures, animal models, fluid therapy and information technology needs: the Second International Consensus Conference of the Acute Dialysis Quality Initiative (ADQI) Group.* Crit Care, 2004. **8**(4): p. R204-12.
15. Venkataraman, R. and J.A. Kellum, *Defining acute renal failure: the RIFLE criteria.* J Intensive Care Med, 2007. **22**(4): p. 187-93.
16. Mishra, J., et al., *Neutrophil gelatinase-associated lipocalin (NGAL) as a biomarker for acute renal injury after cardiac surgery.* Lancet, 2005. **365**(9466): p. 1231-8.
17. Parikh, C.R., et al., *Urinary IL-18 is an early predictive biomarker of acute kidney injury after cardiac surgery.* Kidney Int, 2006. **70**(1): p. 199-203.
18. Abdel-Kader, K. and P.M. Palevsky, *Acute kidney injury in the elderly.* Clin Geriatr Med, 2009. **25**(3): p. 331-58.

19. Piccinni, P., et al., *Prospective multicenter study on epidemiology of acute kidney injury in the ICU: a critical care nephrology Italian collaborative effort (NEFROINT).* Minerva Anestesiol, 2011. **77**(11): p. 1072-83.
20. Hsu, C.Y., et al., *Community-based incidence of acute renal failure.* Kidney Int, 2007. **72**(2): p. 208-12.
21. Nash, K., A. Hafeez, and S. Hou, *Hospital-acquired renal insufficiency.* Am J Kidney Dis, 2002. **39**(5): p. 930-6.
22. Bagshaw, S.M., et al., *Changes in the incidence and outcome for early acute kidney injury in a cohort of Australian intensive care units.* Crit Care, 2007. **11**(3): p. R68.
23. Lassnigg, A., et al., *Minimal changes of serum creatinine predict prognosis in patients after cardiothoracic surgery: a prospective cohort study.* J Am Soc Nephrol, 2004. **15**(6): p. 1597-605.
24. Uchino, S., et al., *Acute renal failure in critically ill patients: a multinational, multicenter study.* JAMA, 2005. **294**(7): p. 813-8.
25. Investigators, R.R.T.S., et al., *Intensity of continuous renal-replacement therapy in critically ill patients.* N Engl J Med, 2009. **361**(17): p. 1627-38.
26. Vaara, S.T., et al., *Population-based incidence, mortality and quality of life in critically ill patients treated with renal replacement therapy: a nationwide retrospective cohort study in Finnish intensive care units.* Crit Care, 2012. **16**(1): p. R13.
27. Lafrance, J.P. and D.R. Miller, *Acute kidney injury associates with increased long-term mortality.* J Am Soc Nephrol, 2010. **21**(2): p. 345-52.
28. Chertow, G.M., et al., *Acute kidney injury, mortality, length of stay, and costs in hospitalized patients.* J Am Soc Nephrol, 2005. **16**(11): p. 3365-70.
29. Coca, S.G., et al., *Long-term risk of mortality and other adverse outcomes after acute kidney injury: a systematic review and meta-analysis.* Am J Kidney Dis, 2009. **53**(6): p. 961-73.
30. Chawla, L.S., et al., *The severity of acute kidney injury predicts progression to chronic kidney disease.* Kidney Int, 2011. **79**(12): p. 1361-9.
31. Wald, R., et al., *Chronic dialysis and death among survivors of acute kidney injury requiring dialysis.* JAMA, 2009. **302**(11): p. 1179-85.
32. Blake, C., et al., *Physical function, employment and quality of life in end-stage renal disease.* J Nephrol, 2000. **13**(2): p. 142-9.
33. Kaufman, J., et al., *Community-acquired acute renal failure.* Am J Kidney Dis, 1991. **17**(2): p. 191-8.
34. Hou, S.H., et al., *Hospital-acquired renal insufficiency: a prospective study.* Am J Med, 1983. **74**(2): p. 243-8.
35. Basile, D.P., M.D. Anderson, and T.A. Sutton, *Pathophysiology of acute kidney injury.* Compr Physiol, 2012. **2**(2): p. 1303-53.
36. Zarjou, A. and A. Agarwal, *Sepsis and acute kidney injury.* J Am Soc Nephrol, 2011. **22**(6): p. 999-1006.
37. Lopez-Novoa, J.M., et al., *New insights into the mechanism of aminoglycoside nephrotoxicity: an integrative point of view.* Kidney Int, 2011. **79**(1): p. 33-45.

38. Oliveira, J.F., et al., *Prevalence and risk factors for aminoglycoside nephrotoxicity in intensive care units.* Antimicrob Agents Chemother, 2009. **53**(7): p. 2887-91.
39. Gerlach, A.T., et al., *Risk factors for aminoglycoside-associated nephrotoxicity in surgical intensive care unit patients.* Int J Crit Illn Inj Sci, 2011. **1**(1): p. 17-21.
40. Miller, R.P., et al., *Mechanisms of Cisplatin nephrotoxicity.* Toxins (Basel), 2010. **2**(11): p. 2490-518.
41. Cullen, K.J., et al., *Mitochondria as a critical target of the chemotheraputic agent cisplatin in head and neck cancer.* J Bioenerg Biomembr, 2007. **39**(1): p. 43-50.
42. Qian, W., et al., *Mitochondrial density determines the cellular sensitivity to cisplatin-induced cell death.* Am J Physiol Cell Physiol, 2005. **289**(6): p. C1466-75.
43. Pistolesi, V., et al., *Contrast medium induced acute kidney injury: a narrative review*. J Nephrol, 2018.
44. Weisbord, S.D. and P.M. Palevsky, *Radiocontrast-induced acute renal failure.* J Intensive Care Med, 2005. **20**(2): p. 63-75.
45. Andreucci, M., et al., *Update on the renal toxicity of iodinated contrast drugs used in clinical medicine.* Drug Healthc Patient Saf, 2017. **9**: p. 25-37.
46. Ejaz, P., K. Bhojani, and V.R. Joshi, *NSAIDs and kidney.* J Assoc Physicians India, 2004. **52**: p. 632-40.
47. Dixit, M., et al., *Significant Acute Kidney Injury Due to Non-steroidal Anti-inflammatory Drugs: Inpatient Setting.* Pharmaceuticals (Basel), 2010. **3**(4): p. 1279-1285.
48. Bonventre, J.V. and J.M. Weinberg, *Recent advances in the pathophysiology of ischemic acute renal failure.* J Am Soc Nephrol, 2003. **14**(8): p. 2199-210.
49. Park, J.T., *Postoperative acute kidney injury.* Korean J Anesthesiol, 2017. **70**(3): p. 258-266.
50. Zarbock, A., H. Gomez, and J.A. Kellum, *Sepsis-induced acute kidney injury revisited: pathophysiology, prevention and future therapies.* Curr Opin Crit Care, 2014. **20**(6): p. 588-95.
51. Sharfuddin, A.A. and B.A. Molitoris, *Pathophysiology of ischemic acute kidney injury.* Nat Rev Nephrol, 2011. **7**(4): p. 189-200.
52. Sprague, A.H. and R.A. Khalil, *Inflammatory cytokines in vascular dysfunction and vascular disease.* Biochem Pharmacol, 2009. **78**(6): p. 539-52.
53. Goligorsky, M.S., *Pathogenesis of endothelial cell dysfunction in chronic kidney disease: a retrospective and what the future may hold.* Kidney Res Clin Pract, 2015. **34**(2): p. 76-82.
54. Kwon, O., S.M. Hong, and G. Ramesh, *Diminished NO generation by injured endothelium and loss of macula densa nNOS may contribute to sustained acute kidney injury after ischemia-reperfusion.* Am J Physiol Renal Physiol, 2009. **296**(1): p. F25-33.
55. Kurata, H., et al., *Protective effect of nitric oxide on ischemia/reperfusion-induced renal injury and endothelin-1 overproduction.* Eur J Pharmacol, 2005. **517**(3): p. 232-9.
56. Conger, J., *Hemodynamic factors in acute renal failure.* Adv Ren Replace Ther, 1997. **4**(2 Suppl 1): p. 25-37.

57. Shimizu, Y., et al., *Lymphocyte interactions with endothelial cells.* Immunol Today, 1992. **13**(3): p. 106-12.
58. Friedewald, J.J. and H. Rabb, *Inflammatory cells in ischemic acute renal failure.* Kidney Int, 2004. **66**(2): p. 486-91.
59. Liu, S., et al., *Novel cardiolipin therapeutic protects endothelial mitochondria during renal ischemia and mitigates microvascular rarefaction, inflammation, and fibrosis.* Am J Physiol Renal Physiol, 2014. **306**(9): p. F970-80.
60. Szeto, H.H., *First-in-class cardiolipin-protective compound as a therapeutic agent to restore mitochondrial bioenergetics.* Br J Pharmacol, 2014. **171**(8): p. 2029-50.
61. Lieberthal, W., S.A. Menza, and J.S. Levine, *Graded ATP depletion can cause necrosis or apoptosis of cultured mouse proximal tubular cells.* Am J Physiol, 1998. **274**(2 Pt 2): p. F315-27.
62. Breggia, A.C. and J. Himmelfarb, *Primary mouse renal tubular epithelial cells have variable injury tolerance to ischemic and chemical mediators of oxidative stress.* Oxid Med Cell Longev, 2008. **1**(1): p. 33-8.
63. Schrier, R.W., et al., *Acute renal failure: definitions, diagnosis, pathogenesis, and therapy.* J Clin Invest, 2004. **114**(1): p. 5-14.
64. Nakamura, M., et al., *Roles of renal proximal tubule transport in acid/base balance and blood pressure regulation.* Biomed Res Int, 2014. **2014**: p. 504808.
65. Nony, P.A. and R.G. Schnellmann, *Mechanisms of renal cell repair and regeneration after acute renal failure.* J Pharmacol Exp Ther, 2003. **304**(3): p. 905-12.
66. Papadimou, E., et al., *Direct reprogramming of human bone marrow stromal cells into functional renal cells using cell-free extracts.* Stem Cell Reports, 2015. **4**(4): p. 685-98.
67. Lin, F., et al., *Hematopoietic stem cells contribute to the regeneration of renal tubules after renal ischemia-reperfusion injury in mice.* J Am Soc Nephrol, 2003. **14**(5): p. 1188-99.
68. Humphreys, B.D. and J.V. Bonventre, *Mesenchymal stem cells in acute kidney injury.* Annu Rev Med, 2008. **59**: p. 311-25.
69. Bonventre, J.V., *Dedifferentiation and proliferation of surviving epithelial cells in acute renal failure.* J Am Soc Nephrol, 2003. **14 Suppl 1**: p. S55-61.
70. Kusaba, T., et al., *Differentiated kidney epithelial cells repair injured proximal tubule.* Proc Natl Acad Sci U S A, 2014. **111**(4): p. 1527-32.
71. Kramann, R., T. Kusaba, and B.D. Humphreys, *Who regenerates the kidney tubule?* Nephrol Dial Transplant, 2015. **30**(6): p. 903-10.
72. Kusaba, T. and B.D. Humphreys, *Controversies on the origin of proliferating epithelial cells after kidney injury.* Pediatr Nephrol, 2014. **29**(4): p. 673-9.
73. Venkatachalam, M.A., et al., *Acute kidney injury: a springboard for progression in chronic kidney disease.* Am J Physiol Renal Physiol, 2010. **298**(5): p. F1078-94.
74. Ralto, K.M. and S.M. Parikh, *Mitochondria in Acute Kidney Injury.* Semin Nephrol, 2016. **36**(1): p. 8-16.
75. Ishimoto, Y. and R. Inagi, *Mitochondria: a therapeutic target in acute kidney injury.* Nephrol Dial Transplant, 2016. **31**(7): p. 1062-9.

76. Brooks, C., et al., *Regulation of mitochondrial dynamics in acute kidney injury in cell culture and rodent models.* J Clin Invest, 2009. **119**(5): p. 1275-85.
77. Szeto, H.H., *Pharmacologic Approaches to Improve Mitochondrial Function in AKI and CKD.* J Am Soc Nephrol, 2017. **28**(10): p. 2856-2865.
78. Delbridge, M.S., et al., *The effect of body temperature in a rat model of renal ischemia-reperfusion injury.* Transplant Proc, 2007. **39**(10): p. 2983-5.
79. Wang, H.J., et al., *Ischemia/reperfusion-induced renal failure in rats as a model for evaluating cell therapies.* Ren Fail, 2012. **34**(10): p. 1324-32.
80. Skrypnyk, N.I., R.C. Harris, and M.P. de Caestecker, *Ischemia-reperfusion model of acute kidney injury and post injury fibrosis in mice.* J Vis Exp, 2013(78).
81. Heyman, S.N., et al., *Animal models of acute tubular necrosis.* Curr Opin Crit Care, 2002. **8**(6): p. 526-34.
82. Fu, Y., et al., *Rodent models of AKI-CKD transition.* Am J Physiol Renal Physiol, 2018.
83. Tesch, G.H., *Review: Serum and urine biomarkers of kidney disease: A pathophysiological perspective.* Nephrology (Carlton), 2010. **15**(6): p. 609-16.
84. Vaidya, V.S., M.A. Ferguson, and J.V. Bonventre, *Biomarkers of acute kidney injury.* Annu Rev Pharmacol Toxicol, 2008. **48**: p. 463-93.
85. Leelahavanichkul, A., et al., *Comparison of serum creatinine and serum cystatin C as biomarkers to detect sepsis-induced acute kidney injury and to predict mortality in CD-1 mice.* Am J Physiol Renal Physiol, 2014. **307**(8): p. F939-48.
86. Kashani, K., W. Cheungpasitporn, and C. Ronco, *Biomarkers of acute kidney injury: the pathway from discovery to clinical adoption.* Clin Chem Lab Med, 2017. **55**(8): p. 1074-1089.
87. Kjeldsen, L., et al., *Isolation and primary structure of NGAL, a novel protein associated with human neutrophil gelatinase.* J Biol Chem, 1993. **268**(14): p. 10425-32.
88. Cowland, J.B. and N. Borregaard, *Molecular characterization and pattern of tissue expression of the gene for neutrophil gelatinase-associated lipocalin from humans.* Genomics, 1997. **45**(1): p. 17-23.
89. Haase, M., et al., *The outcome of neutrophil gelatinase-associated lipocalin-positive subclinical acute kidney injury: a multicenter pooled analysis of prospective studies.* J Am Coll Cardiol, 2011. **57**(17): p. 1752-61.
90. Mishra, J., et al., *Identification of neutrophil gelatinase-associated lipocalin as a novel early urinary biomarker for ischemic renal injury.* J Am Soc Nephrol, 2003. **14**(10): p. 2534-43.
91. Mishra, J., et al., *Amelioration of ischemic acute renal injury by neutrophil gelatinase-associated lipocalin.* J Am Soc Nephrol, 2004. **15**(12): p. 3073-82.
92. Schaub, J.A. and C.R. Parikh, *Biomarkers of acute kidney injury and associations with short- and long-term outcomes.* F1000Res, 2016. **5**.
93. Zhou, F., et al., *Diagnostic value of neutrophil gelatinase-associated lipocalin for early diagnosis of cardiac surgery-associated acute kidney injury: a meta-analysis.* Eur J Cardiothorac Surg, 2016. **49**(3): p. 746-55.

94. Filho, L.T., et al., *Accuracy of neutrophil gelatinase-associated lipocalin for acute kidney injury diagnosis in children: systematic review and meta-analysis.* Pediatr Nephrol, 2017. **32**(10): p. 1979-1988.
95. Dai, X., et al., *Diagnostic value of neutrophil gelatinase-associated lipocalin, cystatin C, and soluble triggering receptor expressed on myeloid cells-1 in critically ill patients with sepsis-associated acute kidney injury.* Crit Care, 2015. **19**: p. 223.
96. Keatings, V.M. and P.J. Barnes, *Granulocyte activation markers in induced sputum: comparison between chronic obstructive pulmonary disease, asthma, and normal subjects.* Am J Respir Crit Care Med, 1997. **155**(2): p. 449-53.
97. Vijayan, A., et al., *Clinical Use of the Urine Biomarker [TIMP-2] x [IGFBP7] for Acute Kidney Injury Risk Assessment.* Am J Kidney Dis, 2016. **68**(1): p. 19-28.
98. Schinstock, C.A., et al., *Urinalysis is more specific and urinary neutrophil gelatinase-associated lipocalin is more sensitive for early detection of acute kidney injury.* Nephrol Dial Transplant, 2013. **28**(5): p. 1175-85.
99. Ichimura, T., et al., *Kidney injury molecule-1 (KIM-1), a putative epithelial cell adhesion molecule containing a novel immunoglobulin domain, is up-regulated in renal cells after injury.* J Biol Chem, 1998. **273**(7): p. 4135-42.
100. Vaidya, V.S., et al., *Urinary kidney injury molecule-1: a sensitive quantitative biomarker for early detection of kidney tubular injury.* Am J Physiol Renal Physiol, 2006. **290**(2): p. F517-29.
101. Shao, X., et al., *Diagnostic value of urinary kidney injury molecule 1 for acute kidney injury: a meta-analysis.* PLoS One, 2014. **9**(1): p. e84131.
102. Vaidya, V.S., et al., *A rapid urine test for early detection of kidney injury.* Kidney Int, 2009. **76**(1): p. 108-14.
103. Ichimura, T., et al., *Kidney injury molecule-1 is a phosphatidylserine receptor that confers a phagocytic phenotype on epithelial cells.* J Clin Invest, 2008. **118**(5): p. 1657-68.
104. Yang, L., et al., *KIM-1-mediated phagocytosis reduces acute injury to the kidney.* J Clin Invest, 2015. **125**(4): p. 1620-36.
105. Han, W.K., et al., *Kidney Injury Molecule-1 (KIM-1): a novel biomarker for human renal proximal tubule injury.* Kidney Int, 2002. **62**(1): p. 237-44.
106. Collier, J.B. and R.G. Schnellmann, *Extracellular Signal-Regulated Kinase 1/2 Regulates Mouse Kidney Injury Molecule-1 Expression Physiologically and Following Ischemic and Septic Renal Injury.* J Pharmacol Exp Ther, 2017. **363**(3): p. 419-427.
107. Arthur, J.M., et al., *Evaluation of 32 urine biomarkers to predict the progression of acute kidney injury after cardiac surgery.* Kidney Int, 2014. **85**(2): p. 431-8.
108. Alge, J.L. and J.M. Arthur, *Biomarkers of AKI: a review of mechanistic relevance and potential therapeutic implications.* Clin J Am Soc Nephrol, 2015. **10**(1): p. 147-55.
109. Lassnigg, A., et al., *Lack of renoprotective effects of dopamine and furosemide during cardiac surgery.* J Am Soc Nephrol, 2000. **11**(1): p. 97-104.
110. Stone, G.W., et al., *Fenoldopam mesylate for the prevention of contrast-induced nephropathy: a randomized controlled trial.* JAMA, 2003. **290**(17): p. 2284-91.

111. Kramer, B.K., et al., *Lack of renoprotective effect of theophylline during aortocoronary bypass surgery.* Nephrol Dial Transplant, 2002. **17**(5): p. 910-5.
112. Garg, A.X., et al., *Perioperative aspirin and clonidine and risk of acute kidney injury: a randomized clinical trial.* JAMA, 2014. **312**(21): p. 2254-64.
113. Loef, B.G., et al., *Effect of dexamethasone on perioperative renal function impairment during cardiac surgery with cardiopulmonary bypass.* Br J Anaesth, 2004. **93**(6): p. 793-8.
114. Haase, M., et al., *Phase II, randomized, controlled trial of high-dose N-acetylcysteine in high-risk cardiac surgery patients.* Crit Care Med, 2007. **35**(5): p. 1324-31.
115. Chen, H. and L.W. Busse, *Novel Therapies for Acute Kidney Injury.* Kidney Int Rep, 2017. **2**(5): p. 785-799.
116. Makris, K. and L. Spanou, *Acute Kidney Injury: Definition, Pathophysiology and Clinical Phenotypes.* Clin Biochem Rev, 2016. **37**(2): p. 85-98.
117. McStay, G.P., *Complex formation and turnover of mitochondrial transporters and ion channels.* J Bioenerg Biomembr, 2017. **49**(1): p. 101-111.
118. Mannella, C.A., W.J. Lederer, and M.S. Jafri, *The connection between inner membrane topology and mitochondrial function.* J Mol Cell Cardiol, 2013. **62**: p. 51-7.
119. Bogenhagen, D.F., *Mitochondrial DNA nucleoid structure.* Biochim Biophys Acta, 2012. **1819**(9-10): p. 914-20.
120. Gilkerson, R., et al., *The mitochondrial nucleoid: integrating mitochondrial DNA into cellular homeostasis.* Cold Spring Harb Perspect Biol, 2013. **5**(5): p. a011080.
121. Chinnery, P.F. and G. Hudson, *Mitochondrial genetics.* Br Med Bull, 2013. **106**: p. 135-59.
122. Stewart, J.B. and P.F. Chinnery, *The dynamics of mitochondrial DNA heteroplasmy: implications for human health and disease.* Nat Rev Genet, 2015. **16**(9): p. 530-42.
123. Miller, F.J., et al., *Precise determination of mitochondrial DNA copy number in human skeletal and cardiac muscle by a PCR-based assay: lack of change of copy number with age.* Nucleic Acids Res, 2003. **31**(11): p. e61.
124. Veltri, K.L., M. Espiritu, and G. Singh, *Distinct genomic copy number in mitochondria of different mammalian organs.* J Cell Physiol, 1990. **143**(1): p. 160-4.
125. Gottlieb, R.A. and A.B. Gustafsson, *Mitochondrial turnover in the heart.* Biochim Biophys Acta, 2011. **1813**(7): p. 1295-301.
126. Stallons, L.J., J.A. Funk, and R.G. Schnellmann, *Mitochondrial Homeostasis in Acute Organ Failure.* Curr Pathobiol Rep, 2013. **1**(3).
127. Kiryu-Seo, S., et al., *Mitochondrial fission is an acute and adaptive response in injured motor neurons.* Sci Rep, 2016. **6**: p. 28331.
128. Wai, T. and T. Langer, *Mitochondrial Dynamics and Metabolic Regulation.* Trends Endocrinol Metab, 2016. **27**(2): p. 105-117.
129. Kubli, D.A. and A.B. Gustafsson, *Mitochondria and mitophagy: the yin and yang of cell death control.* Circ Res, 2012. **111**(9): p. 1208-21.
130. Nisoli, E., et al., *Mitochondrial biogenesis as a cellular signaling framework.* Biochem Pharmacol, 2004. **67**(1): p. 1-15.

131. Jornayvaz, F.R. and G.I. Shulman, *Regulation of mitochondrial biogenesis.* Essays Biochem, 2010. **47**: p. 69-84.
132. Scarpulla, R.C., *Metabolic control of mitochondrial biogenesis through the PGC-1 family regulatory network.* Biochim Biophys Acta, 2011. **1813**(7): p. 1269-78.
133. Scarpulla, R.C., *Nucleus-encoded regulators of mitochondrial function: integration of respiratory chain expression, nutrient sensing and metabolic stress.* Biochim Biophys Acta, 2012. **1819**(9-10): p. 1088-97.
134. Weinberg, J.M., *Mitochondrial biogenesis in kidney disease.* J Am Soc Nephrol, 2011. **22**(3): p. 431-6.
135. Scarpulla, R.C., R.B. Vega, and D.P. Kelly, *Transcriptional integration of mitochondrial biogenesis.* Trends Endocrinol Metab, 2012. **23**(9): p. 459-66.
136. Virbasius, C.A., J.V. Virbasius, and R.C. Scarpulla, *NRF-1, an activator involved in nuclear-mitochondrial interactions, utilizes a new DNA-binding domain conserved in a family of developmental regulators.* Genes Dev, 1993. **7**(12A): p. 2431-45.
137. Kelly, D.P. and R.C. Scarpulla, *Transcriptional regulatory circuits controlling mitochondrial biogenesis and function.* Genes Dev, 2004. **18**(4): p. 357-68.
138. Huo, L. and R.C. Scarpulla, *Mitochondrial DNA instability and peri-implantation lethality associated with targeted disruption of nuclear respiratory factor 1 in mice.* Mol Cell Biol, 2001. **21**(2): p. 644-54.
139. Ristevski, S., et al., *The ETS transcription factor GABPalpha is essential for early embryogenesis.* Mol Cell Biol, 2004. **24**(13): p. 5844-9.
140. Rasbach, K.A. and R.G. Schnellmann, *Signaling of mitochondrial biogenesis following oxidant injury.* J Biol Chem, 2007. **282**(4): p. 2355-62.
141. Nowak, G., et al., *Recovery of cellular functions following oxidant injury.* Am J Physiol, 1998. **274**(3 Pt 2): p. F509-15.
142. Collier, J.B., et al., *Rapid Renal Regulation of Peroxisome Proliferator-activated Receptor gamma Coactivator-1alpha by Extracellular Signal-Regulated Kinase 1/2 in Physiological and Pathological Conditions.* J Biol Chem, 2016. **291**(52): p. 26850-26859.
143. Smith, J.A., et al., *Suppression of mitochondrial biogenesis through toll-like receptor 4-dependent mitogen-activated protein kinase kinase/extracellular signal-regulated kinase signaling in endotoxin-induced acute kidney injury.* J Pharmacol Exp Ther, 2015. **352**(2): p. 346-57.
144. Kukidome, D., et al., *Activation of AMP-activated protein kinase reduces hyperglycemia-induced mitochondrial reactive oxygen species production and promotes mitochondrial biogenesis in human umbilical vein endothelial cells.* Diabetes, 2006. **55**(1): p. 120-7.
145. Komen, J.C. and D.R. Thorburn, *Turn up the power - pharmacological activation of mitochondrial biogenesis in mouse models.* Br J Pharmacol, 2014. **171**(8): p. 1818-36.
146. Funk, J.A., S. Odejinmi, and R.G. Schnellmann, *SRT1720 induces mitochondrial biogenesis and rescues mitochondrial function after oxidant injury in renal proximal tubule cells.* J Pharmacol Exp Ther, 2010. **333**(2): p. 593-601.

147. Funk, J.A. and R.G. Schnellmann, *Accelerated recovery of renal mitochondrial and tubule homeostasis with SIRT1/PGC-1alpha activation following ischemia-reperfusion injury.* Toxicol Appl Pharmacol, 2013. **273**(2): p. 345-54.
148. Wills, L.P., et al., *The beta2-adrenoceptor agonist formoterol stimulates mitochondrial biogenesis.* J Pharmacol Exp Ther, 2012. **342**(1): p. 106-18.
149. Rasbach, K.A., et al., *5-hydroxytryptamine receptor stimulation of mitochondrial biogenesis.* J Pharmacol Exp Ther, 2010. **332**(2): p. 632-9.
150. Nisoli, E., et al., *Mitochondrial biogenesis by NO yields functionally active mitochondria in mammals.* Proc Natl Acad Sci U S A, 2004. **101**(47): p. 16507-12.
151. Whitaker, R.M., et al., *cGMP-selective phosphodiesterase inhibitors stimulate mitochondrial biogenesis and promote recovery from acute kidney injury.* J Pharmacol Exp Ther, 2013. **347**(3): p. 626-34.
152. Cameron, R.B., C.C. Beeson, and R.G. Schnellmann, *Development of Therapeutics That Induce Mitochondrial Biogenesis for the Treatment of Acute and Chronic Degenerative Diseases.* J Med Chem, 2016. **59**(23): p. 10411-10434.
153. Funk, J.A. and R.G. Schnellmann, *Persistent disruption of mitochondrial homeostasis after acute kidney injury.* Am J Physiol Renal Physiol, 2012. **302**(7): p. F853-64.
154. Stallons, L.J., R.M. Whitaker, and R.G. Schnellmann, *Suppressed mitochondrial biogenesis in folic acid-induced acute kidney injury and early fibrosis.* Toxicol Lett, 2014. **224**(3): p. 326-32.
155. Gibbs, W.S., et al., *5-HT1F receptor regulates mitochondrial homeostasis and its loss potentiates acute kidney injury and impairs renal recovery.* Am J Physiol Renal Physiol, 2018.
156. Whitaker, R.M., et al., *Mitochondrial Biogenesis as a Pharmacological Target: A New Approach to Acute and Chronic Diseases.* Annu Rev Pharmacol Toxicol, 2016. **56**: p. 229-49.
157. Chistiakov, D.A., et al., *Mitochondrial aging and age-related dysfunction of mitochondria.* Biomed Res Int, 2014. **2014**: p. 238463.
158. Koltai, E., et al., *Age-associated declines in mitochondrial biogenesis and protein quality control factors are minimized by exercise training.* Am J Physiol Regul Integr Comp Physiol, 2012. **303**(2): p. R127-34.
159. Valerio, A., et al., *TNF-alpha downregulates eNOS expression and mitochondrial biogenesis in fat and muscle of obese rodents.* J Clin Invest, 2006. **116**(10): p. 2791-8.
160. Sente, T., et al., *Tumor necrosis factor-alpha impairs adiponectin signalling, mitochondrial biogenesis, and myogenesis in primary human myotubes cultures.* Am J Physiol Heart Circ Physiol, 2016. **310**(9): p. H1164-75.
161. Delmotte, P., et al., *TNFalpha decreases mitochondrial movement in human airway smooth muscle.* Am J Physiol Lung Cell Mol Physiol, 2017. **313**(1): p. L166-L176.
162. Zhu, J.H., et al., *Impaired mitochondrial biogenesis contributes to depletion of functional mitochondria in chronic MPP+ toxicity: dual roles for ERK1/2.* Cell Death Dis, 2012. **3**: p. e312.

163. He, K. and E. Aizenman, *ERK signaling leads to mitochondrial dysfunction in extracellular zinc-induced neurotoxicity.* J Neurochem, 2010. **114**(2): p. 452-61.
164. Park, C.B., et al., *MTERF3 is a negative regulator of mammalian mtDNA transcription.* Cell, 2007. **130**(2): p. 273-85.
165. Wang, K.Z., et al., *ERK-mediated phosphorylation of TFAM downregulates mitochondrial transcription: implications for Parkinson's disease.* Mitochondrion, 2014. **17**: p. 132-40.
166. Nowak, G., *Protein kinase C-alpha and ERK1/2 mediate mitochondrial dysfunction, decreases in active Na+ transport, and cisplatin-induced apoptosis in renal cells.* J Biol Chem, 2002. **277**(45): p. 43377-88.
167. Nowak, G., et al., *Activation of ERK1/2 pathway mediates oxidant-induced decreases in mitochondrial function in renal cells.* Am J Physiol Renal Physiol, 2006. **291**(4): p. F840-55.
168. Nahorski, S.R., *Pharmacology of intracellular signalling pathways.* Br J Pharmacol, 2006. **147 Suppl 1**: p. S38-45.
169. Zhang, K. and B. Cui, *Optogenetic control of intracellular signaling pathways.* Trends Biotechnol, 2015. **33**(2): p. 92-100.
170. Lorton, D. and D.L. Bellinger, *Molecular mechanisms underlying beta-adrenergic receptor-mediated cross-talk between sympathetic neurons and immune cells.* Int J Mol Sci, 2015. **16**(3): p. 5635-65.
171. Haeusler, R.A., T.E. McGraw, and D. Accili, *Biochemical and cellular properties of insulin receptor signalling.* Nat Rev Mol Cell Biol, 2018. **19**(1): p. 31-44.
172. Eblen, S.T., *Extracellular-Regulated Kinases: Signaling From Ras to ERK Substrates to Control Biological Outcomes.* Adv Cancer Res, 2018. **138**: p. 99-142.
173. Maher, P.A. and E.B. Pasquale, *Tyrosine phosphorylated proteins in different tissues during chick embryo development.* J Cell Biol, 1988. **106**(5): p. 1747-55.
174. Lemmon, M.A. and J. Schlessinger, *Cell signaling by receptor tyrosine kinases.* Cell, 2010. **141**(7): p. 1117-34.
175. Pierre, S., A.S. Bats, and X. Coumoul, *Understanding SOS (Son of Sevenless).* Biochem Pharmacol, 2011. **82**(9): p. 1049-56.
176. Weber, C.K., et al., *Active Ras induces heterodimerization of cRaf and BRaf.* Cancer Res, 2001. **61**(9): p. 3595-8.
177. Chaudhary, A., et al., *Phosphatidylinositol 3-kinase regulates Raf1 through Pak phosphorylation of serine 338.* Curr Biol, 2000. **10**(9): p. 551-4.
178. Mason, C.S., et al., *Serine and tyrosine phosphorylations cooperate in Raf-1, but not B-Raf activation.* EMBO J, 1999. **18**(8): p. 2137-48.
179. Alessi, D.R., et al., *Identification of the sites in MAP kinase kinase-1 phosphorylated by p74raf-1.* EMBO J, 1994. **13**(7): p. 1610-9.
180. Ahn, N.G., et al., *Multiple components in an epidermal growth factor-stimulated protein kinase cascade. In vitro activation of a myelin basic protein/microtubule-associated protein 2 kinase.* J Biol Chem, 1991. **266**(7): p. 4220-7.

181. Payne, D.M., et al., *Identification of the regulatory phosphorylation sites in pp42/mitogen-activated protein kinase (MAP kinase).* EMBO J, 1991. **10**(4): p. 885-92.
182. Woodson, E.N. and D.H. Kedes, *Distinct roles for extracellular signal-regulated kinase 1 (ERK1) and ERK2 in the structure and production of a primate gammaherpesvirus.* J Virol, 2012. **86**(18): p. 9721-36.
183. Boulton, T.G., et al., *ERKs: a family of protein-serine/threonine kinases that are activated and tyrosine phosphorylated in response to insulin and NGF.* Cell, 1991. **65**(4): p. 663-75.
184. Busca, R., et al., *ERK1 and ERK2 present functional redundancy in tetrapods despite higher evolution rate of ERK1.* BMC Evol Biol, 2015. **15**: p. 179.
185. Saba-El-Leil, M.K., C. Fremin, and S. Meloche, *Redundancy in the World of MAP Kinases: All for One.* Front Cell Dev Biol, 2016. **4**: p. 67.
186. Pages, G., et al., *Defective thymocyte maturation in p44 MAP kinase (Erk 1) knockout mice.* Science, 1999. **286**(5443): p. 1374-7.
187. Hatano, N., et al., *Essential role for ERK2 mitogen-activated protein kinase in placental development.* Genes Cells, 2003. **8**(11): p. 847-56.
188. Saba-El-Leil, M.K., et al., *An essential function of the mitogen-activated protein kinase Erk2 in mouse trophoblast development.* EMBO Rep, 2003. **4**(10): p. 964-8.
189. Fremin, C., et al., *Functional Redundancy of ERK1 and ERK2 MAP Kinases during Development.* Cell Rep, 2015. **12**(6): p. 913-21.
190. Busca, R., J. Pouyssegur, and P. Lenormand, *ERK1 and ERK2 Map Kinases: Specific Roles or Functional Redundancy?* Front Cell Dev Biol, 2016. **4**: p. 53.
191. Fukuda, M., Y. Gotoh, and E. Nishida, *Interaction of MAP kinase with MAP kinase kinase: its possible role in the control of nucleocytoplasmic transport of MAP kinase.* EMBO J, 1997. **16**(8): p. 1901-8.
192. Gonzalez, F.A., et al., *Serum-induced translocation of mitogen-activated protein kinase to the cell surface ruffling membrane and the nucleus.* J Cell Biol, 1993. **122**(5): p. 1089-101.
193. Ranganathan, A., M.N. Yazicioglu, and M.H. Cobb, *The nuclear localization of ERK2 occurs by mechanisms both independent of and dependent on energy.* J Biol Chem, 2006. **281**(23): p. 15645-52.
194. Whitehurst, A.W., et al., *ERK2 enters the nucleus by a carrier-independent mechanism.* Proc Natl Acad Sci U S A, 2002. **99**(11): p. 7496-501.
195. Jivan, A., A. Ranganathan, and M.H. Cobb, *Reconstitution of the nuclear transport of the MAP kinase ERK2.* Methods Mol Biol, 2010. **661**: p. 273-85.
196. Vomastek, T., et al., *Extracellular signal-regulated kinase 2 (ERK2) phosphorylation sites and docking domain on the nuclear pore complex protein Tpr cooperatively regulate ERK2-Tpr interaction.* Mol Cell Biol, 2008. **28**(22): p. 6954-66.
197. Shaul, Y.D. and R. Seger, *The MEK/ERK cascade: from signaling specificity to diverse functions.* Biochim Biophys Acta, 2007. **1773**(8): p. 1213-26.
198. Wortzel, I. and R. Seger, *The ERK Cascade: Distinct Functions within Various Subcellular Organelles.* Genes Cancer, 2011. **2**(3): p. 195-209.

199. Unal, E.B., F. Uhlitz, and N. Bluthgen, *A compendium of ERK targets.* FEBS Lett, 2017. **591**(17): p. 2607-2615.
200. Eblen, S.T., et al., *Mitogen-activated protein kinase feedback phosphorylation regulates MEK1 complex formation and activation during cellular adhesion.* Mol Cell Biol, 2004. **24**(6): p. 2308-17.
201. Dougherty, M.K., et al., *Regulation of Raf-1 by direct feedback phosphorylation.* Mol Cell, 2005. **17**(2): p. 215-24.
202. Brummer, T., et al., *Identification of novel ERK-mediated feedback phosphorylation sites at the C-terminus of B-Raf.* Oncogene, 2003. **22**(55): p. 8823-34.
203. Cherniack, A.D., J.K. Klarlund, and M.P. Czech, *Phosphorylation of the Ras nucleotide exchange factor son of sevenless by mitogen-activated protein kinase.* J Biol Chem, 1994. **269**(7): p. 4717-20.

CHAPTER TWO:

Rapid Renal Regulation of Peroxisome Proliferator-activated Receptor γ Coactivator-1α by Extracellular Signal-Regulated Kinase 1/2 in Physiological and Pathological Conditions

ABSTRACT

Previous studies have shown that extracellular signal-regulated kinase 1/2 (ERK1/2) directly inhibits mitochondrial function during cellular injury. We evaluated the role of ERK1/2 on the expression of peroxisome proliferator-activated receptor γ coactivator-1α (PGC-1α) gene, a master regulator of mitochondrial function. The potent and specific MEK1/2 inhibitor trametinib rapidly blocked ERK1/2 phosphorylation, decreased cytosolic and nuclear FOXO3a/1 phosphorylation, and increased PGC-1α gene expression and its downstream mitochondrial biogenesis (MB) targets under physiological conditions in the kidney cortex and in primary renal cell cultures. The epidermal growth factor receptor (EGFR) inhibitor erlotinib blocked ERK1/2 phosphorylation and increased PGC-1α gene expression similar to treatment with trametinib, linking EGFR activation and FOXO3a/1 inactivation to the down-regulation of PGC-1α and MB through ERK1/2. Pretreatment with trametinib blocked early ERK1/2 phosphorylation following ischemia/reperfusion kidney injury and attenuated the down-regulation of PGC-1α and downstream target genes. These results demonstrate that ERK1/2 rapidly regulates mitochondrial function through a novel pathway, EGFR/ERK1/2/FOXO3a/1/PGC-1α, under physiological and pathological conditions. As such, ERK1/2 down-regulates mitochondrial function directly by phosphorylation of upstream regulators of PGC-1α and subsequently decreasing MB.

Introduction

ERK1/2 is a major player in various cell signaling pathways, including proliferation, differentiation, senescence, cell injury and recovery, and apoptosis. ERK1/2 becomes activated through a variety of extracellular stimuli, including receptor tyrosine kinases (RTK) such as the epidermal growth factor receptor (EGFR), which leads to the activation of mitogen-activated protein kinase kinase (MEK) (1,2). EGFR agonists activate intrinsic tyrosine kinase activity within the cytoplasmic domain of the receptor, initiating the recruitment of Ras, a GTPase, which allows for interaction with downstream effectors, including the Raf protein kinases. Raf phosphorylates MEK1/2, which phosphorylates ERK1/2. ERK1/2 is thought to be the only substrate for MEK1/2 phosphorylation, which has allowed for MEK1/2 inhibitors to be used specifically for ERK1/2 inactivation (3,4).

ERK1/2 is also activated by cell stressors, including reactive oxygen species (ROS). Utilizing H_2O_2 injury in human renal cells, ERK1/2 inhibition was shown to decrease necrosis and apoptosis (5), while in a cisplatin-induced cell injury model ERK1/2 inhibition reduced caspase 3 activation and apoptosis (6). In renal proximal tubular cells (RPTC), phosphorylated ERK1/2 was shown to reduce mitochondrial respiration and ATP production by decreasing complex I electron transport chain activity in response to tert-butyl hydroperoxide (TBHP), a model oxidant (7). Nowak, et al., also showed that expression of a constitutively active MEK1 increased ERK1/2 activation and decreased basal and uncoupled oxygen consumption, a measure of electron transport chain activity (7). Zhuang, et al., demonstrated that H_2O_2 treatment of RPTC led to a high level of ERK1/2 phosphorylation and loss of mitochondrial membrane potential (MMP) which

was attenuated by treating with a MEK/ERK1/2 inhibitor. Finally, Fe^{2+}-induced mitochondrial swelling was shown to occur through activation of the ERK1/2 pathway (8). These findings illustrate that ERK1/2 decreases mitochondrial function in response to injury.

The kidney is a high-energy consuming organ and its cells have an abundance of mitochondria to meet ATP demand, especially within the proximal tubules (9). Previous studies demonstrated that rapid and persistent disruption of mitochondria homeostasis is an important contributor to the pathology of renal ischemia/reperfusion (IR) injury (10,11). PGC-1α is thought to be the master regulator of mitochondria biogenesis (MB) and is enriched in tissues with high metabolic demand, such as the heart, skeletal muscle, and kidney (12,13). The role of ERK1/2 activation and subsequent regulation of PGC-1α and downstream targets involved in mitochondrial homeostasis and dysfunction remains limited.

Physiological and pathological stimuli, such as exercise, caloric restriction, hypoxia, sepsis, and ischemia/reperfusion (IR) are known to alter PGC-1α expression (9,14). IR-induced renal injury rapidly suppresses MB, PGC-1α and its direct downstream targets at the transcriptional and protein level (10,11,13). However, the mechanism(s) by which PGC-1α is transcriptionally suppressed after injury has not been determined. Therefore, we examined the role of ERK1/2 in renal PGC-1α transcription under physiological and pathophysiological conditions in primary cultures of RPTC and in the renal cortex of mice. We determined that ERK1/2 regulates PGC-1α in RPTC and in the renal cortex of mice at a physiological level through phosphorylation of the transcription factors

FOXO3a/1. EGFR was found to be the upstream activator of ERK1/2 under basal conditions, negatively regulating PGC-1α transcription. Finally, under the pathophysiological condition of IR-induced AKI in mice, ERK1/2 activation was responsible for the initial decrease in PGC-1α mRNA expression and the decrease in kidney function as measured by serum creatinine. By inhibiting ERK1/2 activation we attenuated the early decrease in PGC-1α and prevented the decrease in kidney function. This research is significant because PGC-1α is the key regulator for MB and by sustaining mitochondrial homeostasis ERK1/2 inhibition may be a potential therapeutic to prevent further injury and/or increase recovery where early mitochondrial dysfunction is observed.

RESULTS

ERK1/2 Inhibition Increases PGC-1α and MB Proteins mRNA in RPTC.

To test the hypothesis that ERK1/2 regulates PGC-1α and MB at a physiological level, we utilized the pharmacological MEK1/2 inhibitor trametinib and primary cultures of rabbit RPTC. Trametinib has been well-characterized as a potent and specific inhibitor of MEK1/2 with an IC_{50} of 0.92 to 3.4 nM in various cell lines and shows limited inhibitory activity against at least 98 other kinases (15,16). RPTC were treated with 0.3, 1, or 10 nM trametinib, and at 10 nM ERK1/2 phosphorylation was completely inhibited after 4 hr (Figure 2.1A). Trametinib (10 nM) completely inhibited ERK1/2 phosphorylation within 10 min and continued to inhibit for 24 hr (data not shown) without altering total ERK1/2 (Figure 2.1A). PGC-1α mRNA expression increased 1.8-fold at 1 hr and 2.8-fold at 4 hr before decreasing to control levels at 24 hr after trametinib exposure (Figure 2.1B). The increase in PGC-1α mRNA was linked to increased nuclear-encoded mediators of MB and gene targets of PGC-1α, including mitochondrial transcription factor A (TFAM), nuclear respiratory factor-1 (NRF1), and NADH Dehydrogenase (Ubiquinone) Fe-S Protein 1 (NDUFS1) at 1, 4 and 24 hr after trametinib treatment (Figure 2.1C-E). These results reveal that ERK1/2 represses PGC-1α mRNA expression and its downstream target genes under physiological conditions and that inhibition of ERK1/2 activation results in a rapid induction of PGC-1α mRNA and other downstream MB genes.

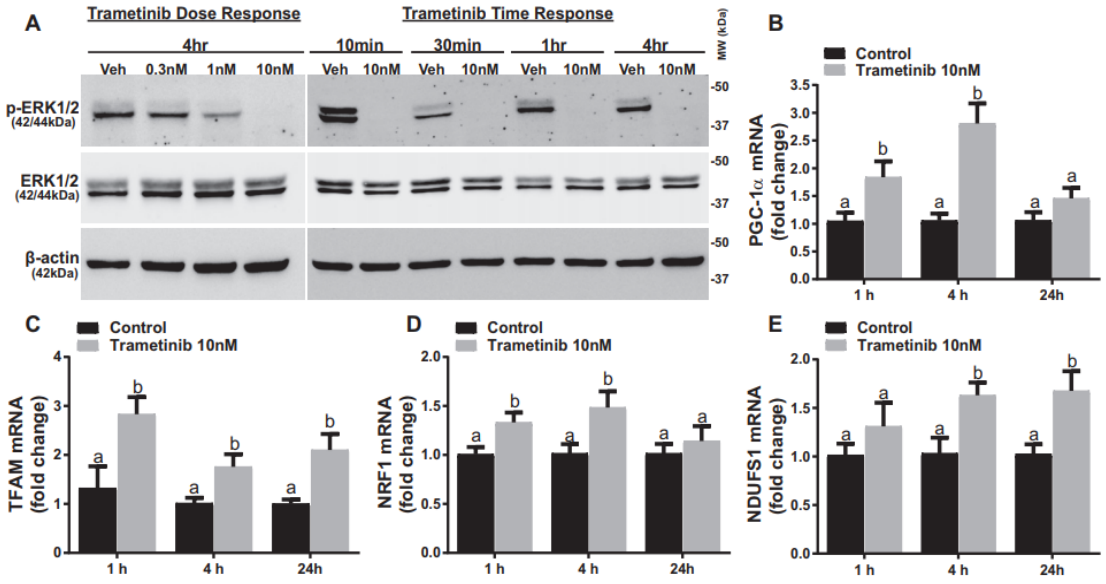

Figure 2.1: ERK1/2 inhibition increases levels of PGC-1 and downstream targets of MB mRNA. A, immunoblotting analysis of phosphorylated ERK1/2 (p-ERK1/2) in RPTC in response to increasing concentrations of trametinib at 4 h and increasing time of exposure to 10 nM trametinib. Veh, vehicle; MW, molecular weight. B–E, mRNA expression of PGC-1, TFAM, NDUFS1, and NRF1 at 1, 4, and 24 h after treatment with 10 nM trametinib. Data are represented as mean S.E., n > 5. Different superscripts indicate statistically significant differences ($p < 0.05$).

ERK1/2 Regulates PGC-1α Through Phosphorylation of FOXO3a Independent of p38 and AKT Kinases in RPTC.

We analyzed the phosphorylation levels of FOXO3a in RPTC 30 min after trametinib treatment since FOXO3a is a direct transcriptional regulator of PGC-1α (17-19). Phosphorylation of the ERK1/2 phosphorylation site, serine 294, on FOXO3a decreased 54% at 30 min in RPTC treated with trametinib (Figure 2.2A-B). Other kinases, such as p38 and AKT are known to target FOXO3a for phosphorylation (20,21); however, p38 and AKT phosphorylation did not change in the presence of trametinib (Figure 2.2C). To exert its transcriptional effects, FOXO3a shuttles between the cytosol and the nucleus (22). Phosphorylation of FOXO3a inactivates the protein by preventing it from entering the nucleus and increases the rate of export from the nucleus to the cytosol where it may be degraded (23). Therefore, phosphorylation of FOXO3a decreases its ability to bind to promoters and increase gene expression (20,23,24). Nuclear phosphorylated FOXO3a decreased 60% in the trametinib-treated RPTC at 30 min with no alteration in total FOXO3a nor the loading control, lamin B1 (Figure 2.2D-E). In summary, phosphorylated ERK1/2, but not AKT or p38, phosphorylates FOXO3a, which inactivates FOXO3a in the nucleus, and prevents FOXO3a from increasing PGC-1α expression physiologically. This dynamic control of FOXO3a by ERK1/2 regulates PGC-1α rapidly leading to a decrease/increase MB gene regulation.

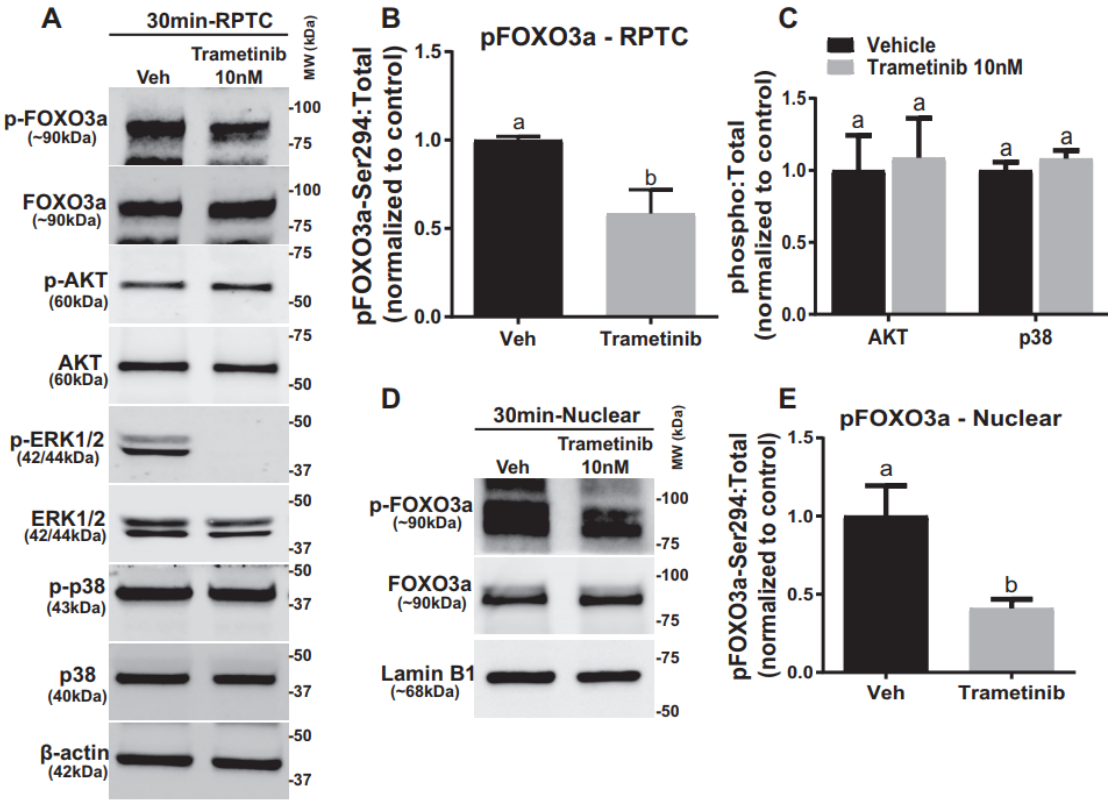

Figure 2.2: ERK1/2 regulates PGC-1 through phosphorylation of FOXO3a independent of p38 and AKT kinases in RPTC. A, representative immunoblot of pFOXO3a after 10 nM trametinib treatment in RPTC. p, phosphorylated; Veh, vehicle; MW, molecular weight. B, densitometry analysis of phosphorylated FOXO3a, with -actin as loading control. C, densitometry analysis of p38 and AKT kinases. D, representative immunoblot of phosphorylated and total FOXO3a in the nucleus. E, densitometry analysis of phosphorylated FOXO3a in the nucleus following ERK1/2 inhibition. Data are represented as mean S.E., n > 5. Different superscripts indicate statistically significant differences ($p < 0.05$).

EGFR Inhibition Increases PGC-1α mRNA Expression by Preventing ERK1/2 Activation in RPTC.

EGFR is known to regulate the activity of the ERK1/2 signaling cascade (1,25,26). To determine whether ERK1/2 inhibition of PGC-1α mRNA was mediated by the EGFR in RPTC, we utilized the EGFR inhibitor erlotinib, a direct inhibitor of the intracellular kinase domain of the EGFR that prevents autophosphorylation and signal transduction (26). Within 1 hr of erlotinib treatment (100 nM and 1 μM), ERK1/2 phosphorylation was blocked without a change in total ERK1/2 protein and remained decreased 4 hr post treatment (Figure 2.3A). PGC-1α mRNA expression was increased at 4 hr by 2.4- and 2.8-fold in the 100 nM and 1 μM erlotinib groups, respectively (Figure 2.3B). NRF1 was also up 2.4-fold by 4 hr after EGFR inhibition (Figure 2.3C). We conclude that EGFR inhibition with erlotinib leads to an upregulation of PGC-1α mRNA through inactivation of ERK1/2. It should be noted that the 4 hr increases in PGC-1α mRNA expression are very similar to the increases observed using trametinib (Figure 2.1B). In summary, under physiological conditions the activation of the EGFR/ERK1/2/FOXO3a pathway regulates PGC-1α and MB genes within 1 hr.

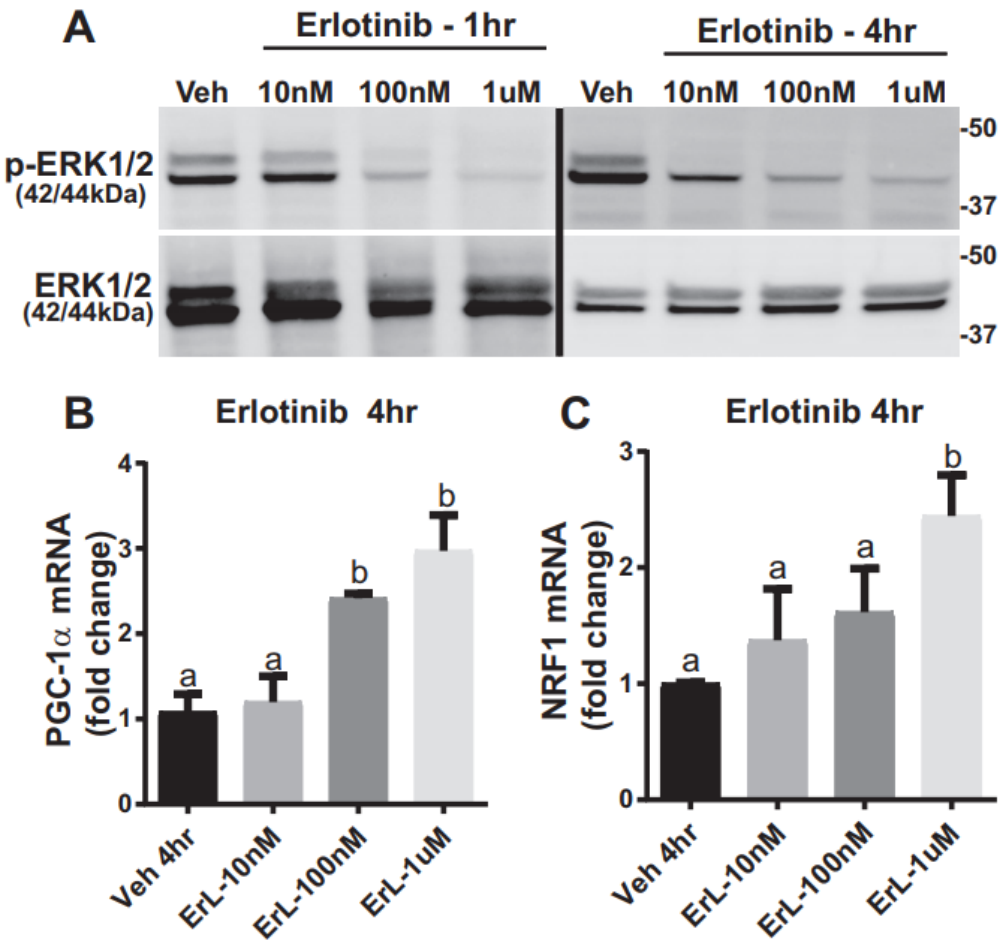

Figure 2.3: EGFR inhibition increases PGC-1 mRNA expression by preventing ERK1/2 activation in RPTC. A, representative immunoblot of phosphorylated ERK1/2 after treatment with increasing concentrations of erlotinib (ErL) at 1 and 4 h in RPTC. p, phosphorylated; Veh, vehicle. B and C, mRNA expression of PGC-1 (B) and NRF1 (C) following increasing concentrations of erlotinib at 4 h. Data are represented as mean S.E., n > 5. Different superscripts indicate statistically significant differences ($p < 0.05$).

ERK1/2 Physiologically Regulates PGC-1α Expression and Protein by Altering FOXO1 Phosphorylation in the Mouse Kidney.

Our laboratory and others have previously reported that a 1 mg/kg dose of trametinib inhibits ERK1/2 phosphorylation in mice (16,27). We verified that trametinib (1 mg/kg, i.p.) inhibited ERK1/2 phosphorylation at 4 hr post-injection in the renal cortex with no change to total ERK1/2 protein (Figure 2.4A). PGC-1α mRNA expression in the renal cortex increased 1.5-fold 4 hr after ERK1/2 inhibition, corresponding with the observations made *in vitro* (Figure 2.4B). Likewise, targets of PGC-1α were also upregulated at 4 hr with NRF1 mRNA elevated by 1.8-fold and TFAM mRNA up 1.2-fold (Figure 2.4C). Cytochrome c oxidase I (COX1) mRNA, a mitochondrial encoded gene, one of the subunits of respiratory complex IV, was also upregulated 1.4-fold following ERK1/2 inhibition with trametinib (Figure 2.4C). The increase in MB gene expression due to ERK1/2 inhibition resulted in increases in PGC-1α and TFAM proteins of 1.6-fold and 1.3-fold, respectively, at 4 hr in the trametinib group (Figure 2.4B, D-E).

After failing to detect FOXO3a in the mouse renal cortex (data not shown), we examined FOXO1. FOXO3a and FOXO1 are similar transcription factors and share overlapping activities, including regulating PGC-1α (20). FOXO1 phosphorylation at the phosphorylation site, serine 329, was decreased in the trametinib group (28,29)(Figure 2.5A-B). Total FOXO1 protein did not change in response to ERK1/2 inhibition (Figure 2.5A). Neither AKT and p38 phosphorylation nor total AKT and p38 proteins changed in the trametinib group (Figure 2.5C). Trametinib treatment decreased nuclear phosphorylated FOXO1 to total FOXO1 32%, 4 hr after trametinib (Figure

2.5D-E). FOXO1 mRNA was also upregulated at 4 hr post ERK1/2 inhibition (Figure 2.5F). Further evidence that ERK1/2 inhibition results in increased FOXO1 gene transcription was revealed by increases in catalase and mitochondrial superoxide dismutase 2 (SOD2), two genes regulated by FOXO1 (Figure 2.5F) (30,31). We conclude that ERK1/2 regulates the activity of FOXO1 within the nucleus and controls the basal level of PGC-1α mRNA and subsequent PGC-1α protein levels, as well as downstream MB genes in the kidney.

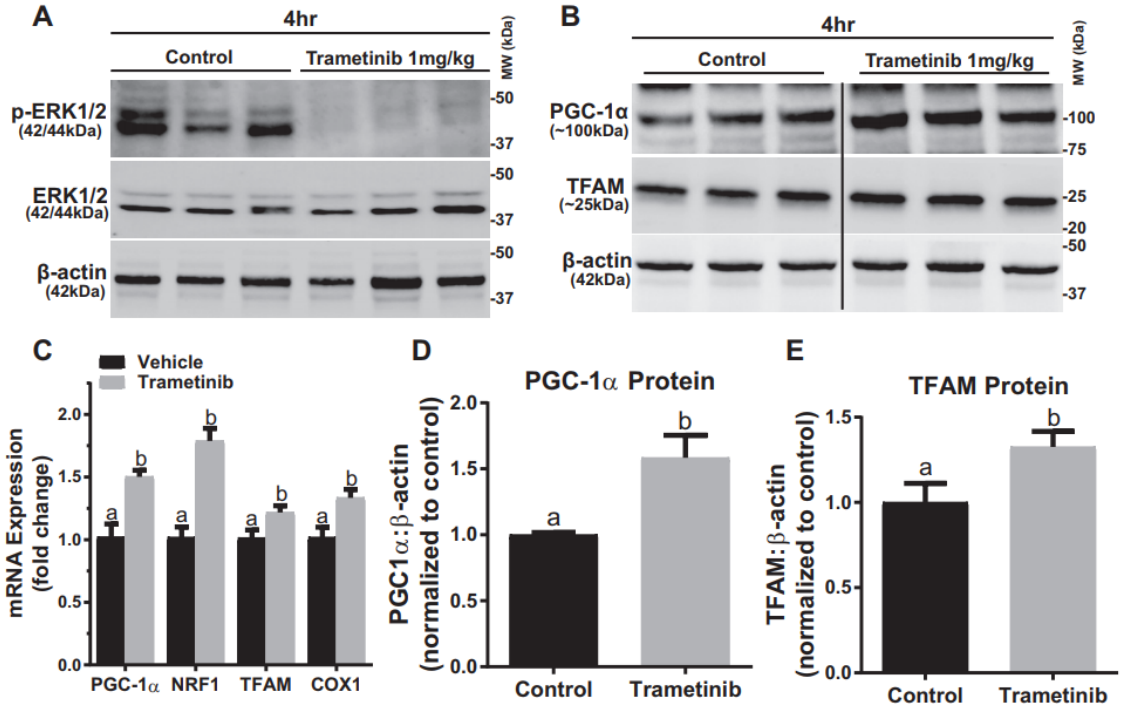

Figure 2.4: ERK1/2 physiologically regulates PGC-1 expression and protein in mouse kidney. A, representative immunoblot of phosphorylated ERK1/2 after treatment with trametinib in mouse kidney cortex. p, phosphorylated; MW, molecular weight. B, representative immunoblot of PGC-1 and TFAM proteins after treatment with trametinib in the kidney cortex. The black line represents the splicing of the blot from the same membrane. C, mRNA expression of PGC-1, NRF1, TFAM, and COX 1 following trametinib administration at 4 h. D and E, densitometry analysis of PGC-1 (D) and TFAM (E) protein at 4 h following trametinib. Data are represented as mean S.E., $n > 5$. Different superscripts indicate statistically significant differences ($p < 0.05$).

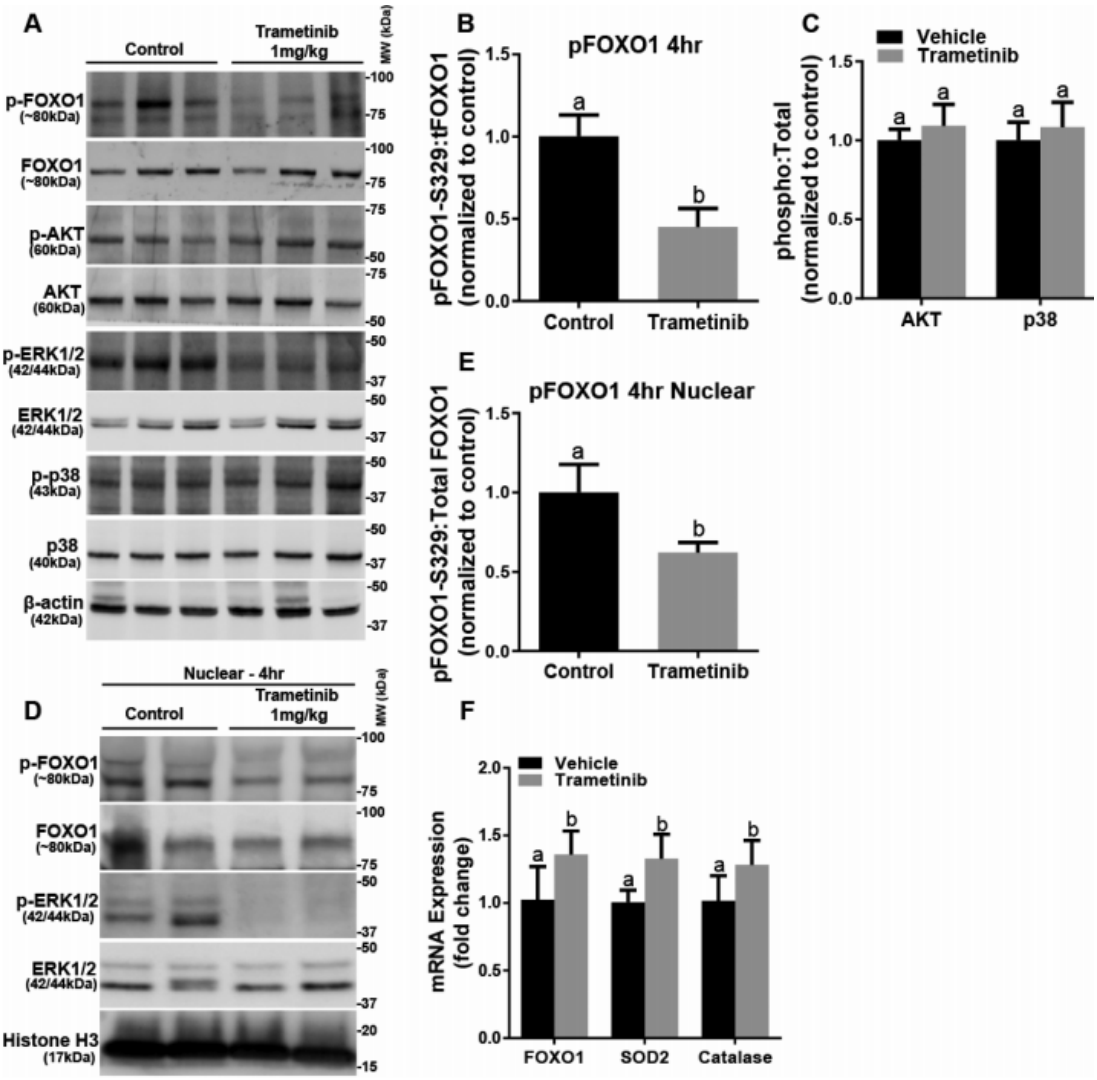

Figure 2.5: FOXO1 phosphorylation in the cortex and nuclear phosphorylation decrease after ERK1/2 inhibition. A, representative immunoblot of phosphorylated FOXO1 and ERK1/2, AKT, and p38 kinases following trametinib administration. p, phosphorylated; MW, molecular weight. B, densitometry analysis of phosphorylated FOXO1 when compared with total FOXO1. C, densitometry analysis of phosphorylated AKT to total AKT, and phosphorylated p38 to total p38 after trametinib treatment. D, representative immunoblot of nuclear phosphorylated FOXO1 and ERK1/2 after trametinib treatment in mouse kidney cortex. E, densitometry analysis of phosphorylated FOXO1 when compared with total FOXO1 after inhibition of ERK1/2 in the nucleus. F, mRNA expression of FOXO1, SOD2, and catalase at 4 h following trametinib administration. Data are represented as mean S.E., n > 4. Different superscripts indicate statistically significant differences ($p < 0.05$).

ERK1/2 Inhibition During AKI Attenuates an Increase in Serum Creatinine and Decreases in PGC-1α and NRF1 Expression.

To examine the role of ERK1/2 on PGC-1α in the renal cortex under injurious conditions, we pretreated mice with trametinib or vehicle for 1 hr and then subjected mice to bilateral IR surgery or sham surgery for 18 min to induce AKI and kidneys were collected 3 hr later. IR-induced AKI decreases PGC-1α mRNA expression, as well as other mitochondrial genes and proteins (32). Trametinib prevented the increase in ERK1/2 phosphorylation following the IR (Figure 2.6A). PGC-1α mRNA decreased 41% in IR mice after 3 hr and trametinib attenuated this decrease (Figure 2.6B). Interestingly, trametinib pretreatment increased NRF1 expression following IR compared to sham, whereas IR alone resulted in 13% decrease in NRF1 compared to sham (Figure 2.6B). At the protein level both PGC-1α and TFAM proteins increased 1.7- and 2.4-fold, respectively (Figure 2.6C-D).

Serum creatinine, a marker of renal dysfunction increased 4-fold in the IR group at 3 hr and was attenuated in the trametinib pretreatment group (Fig 6E). We demonstrate that by inhibiting ERK1/2 phosphorylation prior to inducing IR AKI we attenuated the decreases in PGC-1α and NRF1 mRNA, as well as increasing mitochondrial related proteins PGC-1α and TFAM 3 hr post-surgery. By maintaining mitochondrial function due to ERK1/2 inhibition kidney dysfunction was prevented at 3 hr.

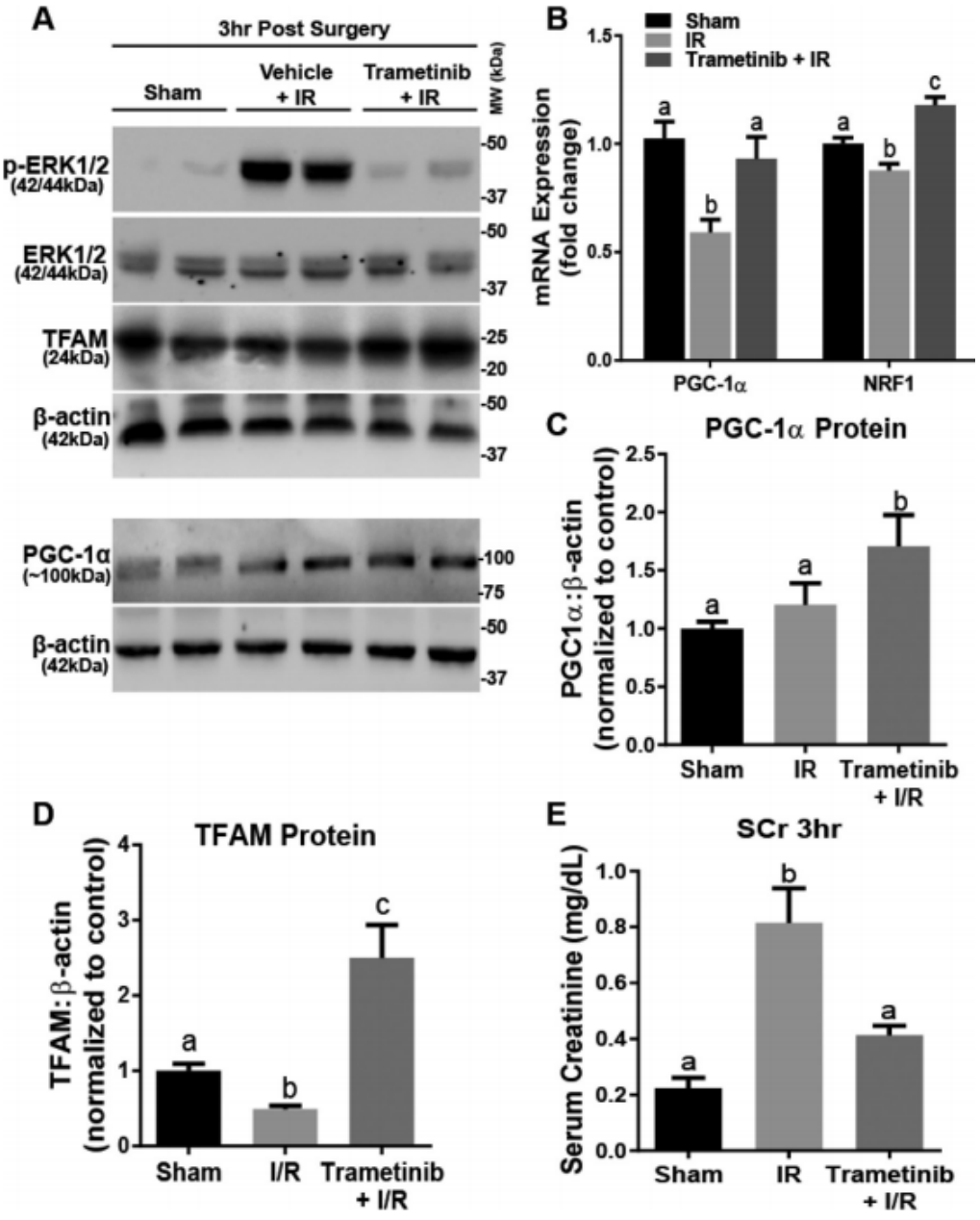

Figure 2.6: ERK1/2 inhibition during AKI attenuates an increase in serum creatinine and increases PGC-1 and TFAM proteins. A, representative immunoblot of phosphorylated ERK1/2, total ERK1/2, TFAM, and PGC-1 following IR AKI. p, phosphorylated; MW, molecular weight. B, mRNA expression of PGC-1 and NRF1 following IR AKI at 3 h after IR in the kidney cortex. C and D, densitometry analysis of PGC-1 (C) and TFAM (D) proteins following 3 h IR. E, serum creatinine was assessed 3 h after IR AKI. Data are represented as mean S.E., n > 5. Different superscripts indicate statistically significant differences ($p < 0.05$).

Erlotinib Blocks ERK1/2 Phosphorylation in Naïve Mice and Following IR, Preventing Decreases in PGC-1α and NRF1 Expression.

To elucidate the role of EGFR on ERK1/2 and PGC-1α and MB genes in the renal cortex, erlotinib (50 mg/kg i.p.) was administered to naïve mice (33). Erlotinib decreased ERK1/2 phosphorylation by 45% in the kidney cortex 4 hr after administration (Figure 2.7A-B). Mice given erlotinib had 1.3-fold higher PGC-1α mRNA and 1.4-fold higher FOXO1 mRNA expression (Figure 2.7C). To elucidate if the EGFR is the upstream receptor required for the ERK1/2 activation that downregulates PGC-1α following IR AKI we pretreated with erlotinib prior to inducing IR AKI. We observed attenuation in the increase of phosphorylated ERK1/2 at 3 hr compared to IR alone (Figure 2.7D-E). Very similar to the results obtained in the trametinib experiments (Figure 2.6B-C), we observed attenuation of PGC-1α and NRF1 mRNA compared to the IR group, as well as an increase in PGC-1α protein (Figure 2.7F-G). The erlotinib group also prevented the 5-fold increase in serum creatinine seen in the IR group (Figure 2.7H). These data reveal that EGFR actively regulates ERK1/2 phosphorylation in the kidney, and as a consequence, EGFR regulates renal PGC-1α mRNA at a physiological and pathophysiological level. In summary, EGFR is the upstream receptor regulator of basal ERK1/2 phosphorylation in the renal cortex that controls PGC-1α mRNA and MB genes.

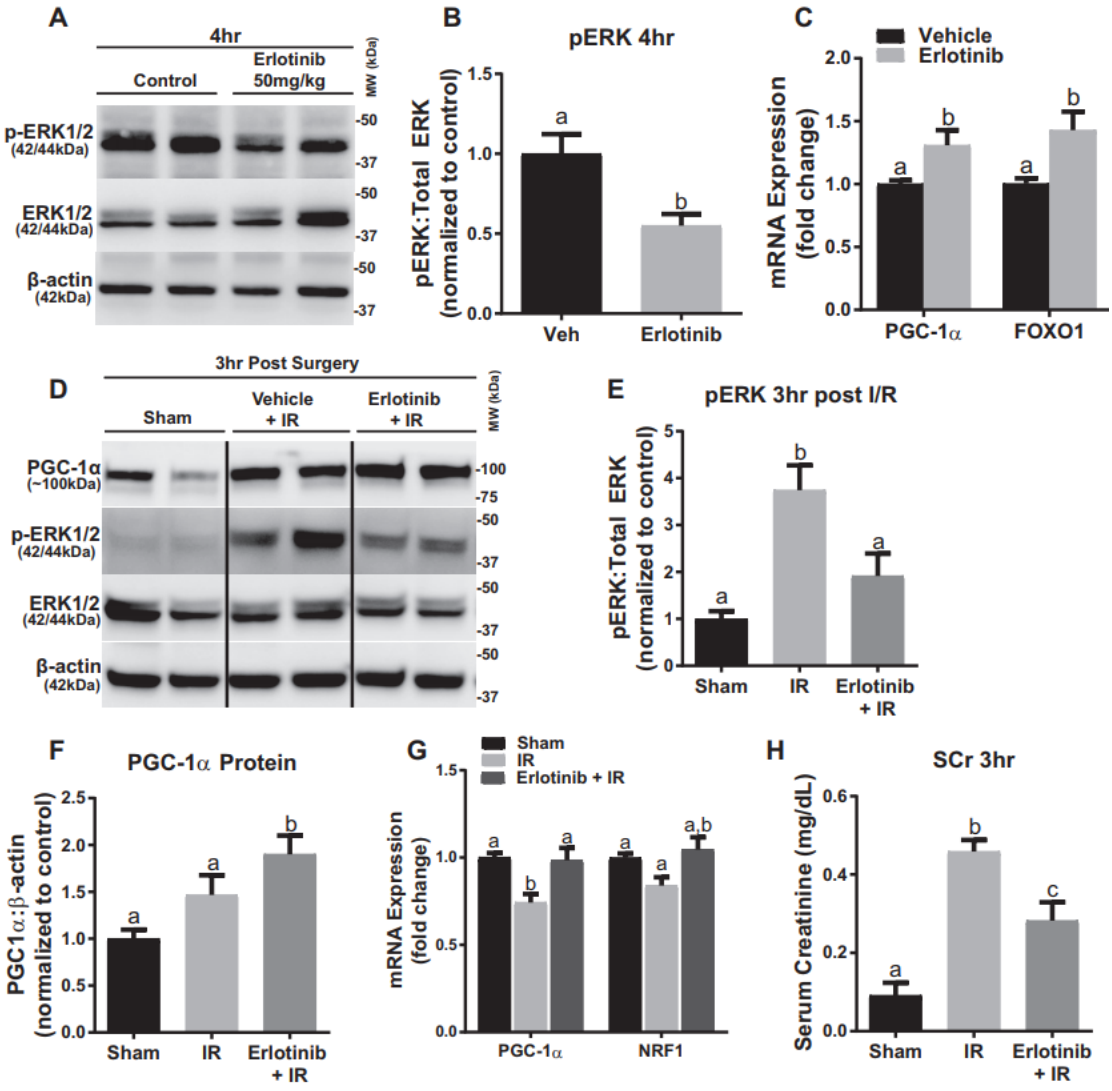

Figure 2.7: Erlotinib blocks ERK1/2 phosphorylation in naïve mice and following IR, preventing decreases in PGC-1α and NRF1 expression. A, representative immunoblot of phosphorylated ERK1/2 after 4 h of treatment with erlotinib in mouse kidney cortex. p, phosphorylated; MW, molecular weight. B, densitometry analysis of phosphorylated ERK1/2 when compared with total ERK1/2 following 4 h of erlotinib treatment. C, mRNA expression of PGC-1α and FOXO1 at 4 h in mouse cortex following erlotinib treatment. D, representative immunoblot of phosphorylated ERK1/2 and total ERK1/2, as well as PGC-1α following IR AKI. E, densitometry analysis of phosphorylated ERK1/2 when compared with total ERK1/2 following 3 h of IR AKI. F, densitometry analysis of PGC-1α protein when compared with β-actin following 3 h of IR AKI. G, mRNA expression of PGC-1α and NRF1 following 3 h of IR AKI. H, serum creatinine was assessed 3 h after IR AKI. Data are represented as mean S.E., n > 4. Different superscripts indicate statistically significant differences ($p < 0.05$).

DISCUSSION

In this study we identified ERK1/2 as an important and rapid regulator of PGC-1α gene transcription in RPTC and in mouse kidney under physiological and pathological conditions. In RPTC, we showed trametinib inhibits ERK1/2 phosphorylation within 10 min leading to an increase in PGC-1α mRNA expression which was sufficient to up-regulate mitochondrial genes involved in MB. In addition, we determined that EGFR was the upstream activator of ERK1/2 in both RPTC and renal cortex. Thus, the EGFR/ERK1/2/FOXO(3a/1) pathway is an important negative regulator of PGC-1α and its downstream targets, including MB genes.

Previous studies revealed that ERK1/2 down regulates mitochondrial function by decreasing basal and uncoupled oxygen consumption following TBHP exposure in RPTC (7). Furthermore, ATP production was reduced 40% in RPTC due to ERK1/2 activation by TBHP, and by inhibiting ERK1/2 ATP remained at control levels. In contrast, ERK1/2 inhibition was found to decrease ATP production and cause a rapid loss of mitochondrial membrane potential in alveolar macrophages (34), but not in primary cultures of tracheobronchial epithelial cells or lung fibroblasts. A decrease in oxygen consumption through inhibition of complex I in HL-60 cells was found to occur by ERK1/2 inhibition (35). Overall, ERK1/2 decreases mitochondrial function by three mechanisms: 1) post-translation modifications that decrease electron transport chain activity, 2) down regulation of PGC-1α and mitochondrial gene expression, and 3) decreased expression of mitochondrial protectants (i.e. SOD2). However, ERK1/2 appears to regulate mitochondrial functions differently in various cell types and the

differences may be based on the level of oxidative phosphorylation that occurs in each cell type. RPTC used by Nowak et al. and in our studies derive all their energy from oxidative phosphorylation, similar to that found in kidney cortex.

In RPTC, FOXO3a phosphorylation was decreased 30 min post trametinib treatment. These results are consistent with previous studies that show ERK1/2 regulates phosphorylation of FOXO3a (23,36). Phosphorylation is a key determinant of FOXO3a localization and its regulation of PGC-1α (37-39). Yang et al., showed that ERK1/2 phosphorylation of FOXO3a promotes a FOXO3a degradation pathway mediated by the E3 ubiquitin ligase MDM2 (23). We show that ERK1/2 inhibition decreased phosphorylated FOXO3a in the nucleus, allowing greater FOXO3a and PGC-1α expression physiologically. This FOXO3a dependent increase in PGC-1α was also shown during endothelial oxidative stress (19).

It is not clear the pathway ERK1/2 is being regulated by under these basal conditions. Using the specific EGFR inhibitor erlotinib, ERK1/2 phosphorylation was blocked and PGC-1α mRNA increased. Thus, EGFR appears to be a key regulator of ERK1/2 which in turn regulates the basal level of PGC-1α mRNA and its downstream mitochondrial genes. Nevertheless, it remains to be determined what is activating the EGFR under these conditions. Possible candidates include EGFR ligands, TGFα and HB-EGF, and/or transactivation pathways (ADAM17, ANGII, TWEAK/Fn14) (4,40). Inhibiting ERK1/2 increased PGC-1α mRNA, as well as TFAM, NRF1, and COX1. The increase in COX1 demonstrates that ERK1/2 is not only increasing nuclear-

encoded gene expression, but also mitochondrial-encoded gene expression. This response is similar to findings in melanoma cell lines after treatment with various ERK cascade inhibitors in which an increase in PGC-1α gene expression was observed (41). Because FOXO3a was not expressed in naïve mouse renal cortex we shifted focus to FOXO1. FOXO3a and FOXO1 share similar DNA-binding domains, have overlapping gene expressions (42), and are both directly phosphorylated by ERK1/2 (43). Phosphorylation of FOXO1 decreased in the nucleus due to ERK1/2 inhibition, which resulted in an increase in downstream targets of FOXO1 (e.g. catalase and SOD2) and PGC-1α in the kidney cortex.

During IR-induced AKI in mice, ERK1/2 is highly phosphorylated with accompanying decreases in PGC-1α and NRF1, as well as a decline in kidney function at 3 hr post IR surgery. Inhibiting phosphorylated ERK1/2 pre-surgery attenuated the PGC-1α and NRF1 mRNA decreases and prevented an increase in serum creatinine. We have previously shown that PGC-1α is rapidly decreased following diverse models of AKI in mice and rats and these results implicate ERK1/2 as the mediator behind this transcriptional suppression.

In conclusion we determined the role of ERK1/2 in the physiological and pathological regulation of renal PGC-1α and MB. We linked EGFR activation and FOXO3a/1 inactivation to the downregulation of PGC-1α and MB, through ERK1/2 signaling. PGC-1α physiological regulation appears to be structured so that changes can occur very rapidly when necessary. Finally, ERK1/2 inhibition may have potential in

preventing mitochondrial dysfunction as a therapeutic strategy in organ dysfunction. Because mitochondrial injury/recovery and biogenesis can occur throughout different tissues of the body due to various injury insults we think this therapeutic potential of inhibiting early activation of ERK1/2 to prevent downregulation of MB may be applicable to other organs with further studies required.

EXPERIMENTAL PROCEDURES

In Vitro Studies

Female New Zealand White rabbits (2 kg) were purchased from Charles River (Oakwood, MI/Canada). Renal proximal tubule cells (RPTC) were isolated using the iron oxide perfusion method and grown in 35-mm tissue culture dishes under improved conditions similar to what is observed *in vivo*, as described previously (44). The culture medium was a 1:1 mixture of Dulbecco's modified Eagle's medium/F-12 (without glucose, phenol red, or sodium pyruvate) supplemented with 15 mM HEPES buffer, 2.5 mM L-glutamine, 1 uM pyridoxine HCl, 15 mM sodium bicarbonate, and 6 mM lactate. Hydrocortisone (50 nM), selenium (5 ng/ml), human transferrin (5 ug/ml), bovine insulin (10 nM), and L-ascorbic acid-2-phosphate (50 uM) were added to fresh culture medium. Confluent RPTC were used for all experiments. RPTC monolayers were treated with various compounds or vehicle (DMSO) for time points indicated.

In Vivo Studies

Trametinib (GSK1120212, (15)) was purchased from Selleckchem Chemicals (Houston, TX). Eight-to-nine week old male C57BL/6 mice (20–25 g) mice received an injection of trametinib (1 mg/kg i.p.) or vehicle control (DMSO). Four hr after injection kidneys were collected and flash frozen for further analysis.

Mice were assigned to 3 groups: 1) Sham, 2) I/R + Vehicle, 3) I/R + Trametinib. Vehicle or trametinib were administered i.p 1 hr before surgery. I/R grouped mice were subjected to I/R surgery by bilateral renal pedicle clamping for 18 min as described previously (32). Briefly, the renal artery and vein were isolated and blood flow was

occluded with a vascular clamp for 18min while maintaining a constant body temperature of 36~37°C. Sham mice were treated exactly the same as I/R mice without the clamping of the renal pedicles. Mice were euthanized at 3 h after surgery, and blood and kidneys (flash frozen in liquid nitrogen) were collected for analysis.

RT-qPCR Analysis of mRNA Expression

Total RNA was isolated from renal cortical tissue with TRIzol reagent (Life Technologies). The iScript Advanced cDNA Synthesis Kit (Bio-Rad) was used according to the manufacturer's protocol. The generated cDNA was used with the SsoAdvanced Universal SYBR Green Supermix reagent (Bio-Rad). The relative mRNA expression of all genes was determined by the $2^{-\Delta\Delta Ct}$ method, and mouse Actin RNA and rabbit tubulin RNA were used as reference genes for normalization (Table 1 for Primer pairs).

Immunoblot Analysis

Protein was extracted from renal cortex using RIPA assay buffer (50 mM Tris-HCl, 150 mM NaCl, 0.1% SDS, 0.5% sodium deoxycholate, 1% Triton X-100, pH 7.4) with protease inhibitor cocktail (1:100), 1 mM sodium fluoride, and 1 mM sodium orthovanadate (Sigma-Aldrich).

Mouse tissue and rabbit primary cells nuclear and cytosolic fraction lysates were prepared as previously described with modifications (11). Briefly, a piece of kidney cortex was homogenized in sucrose isolation (ISO) buffer (250 mM sucrose, 1 mM EGTA, 10 mM HEPES, 1 mg/ml fatty acid-free BSA [pH 7.4]) with a dounce tissue

grinder. Lysates were centrifuged at 1000 x g for 10 min. The 1st pellet was re-washed two separate times in ISO buffer and resuspended in RIPA. The 1st supernatant was centrifuged at 10,000 x g for 5 min for further purification of the cytosol fraction. Histone H3 and/or Lamin B1 were used as loading control for nuclear lysate immunoblots, and alpha-tubulin was used for loading control of cytosolic lysates. Equal protein quantities (20–60 μg) were loaded onto 4–15% SDS-PAGE gels, resolved by gel electrophoresis, and transferred onto nitrocellulose or PVDF membranes (Bio-Rad). Membranes were blocked in 5% bovine serum albumin or 5% milk in TBST and incubated overnight with primary antibody at 4°C with gently agitation. Primary antibodies used in these studies included (all from Cell Signaling) phospho-ERK1/2 (1:1000) [#4370], total ERK1/2 (1:1000) [#4695], AKT (1:1000) [#9272], phospho-AKT (1:1000) [#4060], phospho-p38 (1:1000) [#4511], p38 MAPK (1:1000) [#8690], EGF Receptor (1:1000) [#4267], phospho-EGFR Tyr1173 (1:750) [#4407s], phospho-EGFR Tyr1068 (1:1000) [#3777s], total FOXO3a (1:1000), phospho Ser294-FOXO3a (1:1000) [#5538], and total FOXO1 (1:1000) [#2880] Danvers, MA. Phospho S329-FOXO1 (1:1000; Abcam) [ab192201], TFAM (1:1000; Abcam) [ab131607], lamin B1 (1:1000; Abcam) [ab16048], kidney injury molecule-1 (KIM-1) (1:1000; R&D systems, Minneapolis, MN) [AF1817], histone H3 (1:2000) [#9715], PGC-1α (1:1000; Abcam) [ab54481], and β-actin (1:2000; Santa Cruz Biotechnology, Dallas, TX) [sc-47778]. Membranes were incubated with the appropriate horseradish peroxidase–conjugated secondary antibody before visualization using enhanced chemiluminescence (Thermo Scientific) and the GE ImageQuant LAS4000 (GE Life Sciences). Optical density was determined using the ImageJ software from NIH.

Statistical Analysis

All data are shown as mean ± S.E.M. When comparing two experimental groups, an unpaired, two-tailed *t* test or Mann-Whitney U was used to determine statistical differences. A one-way analysis of variance (ANOVA) followed by Tukey's post hoc test was performed for comparisons of multiple groups. $P < 0.05$ was considered statistically significant. All statistical tests were performed using GraphPad Prism software (GraphPad Software, San Diego, CA).

REFERENCES

1. Daub, H., Weiss, F. U., Wallasch, C., and Ullrich, A. (1996) Role of transactivation of the EGF receptor in signalling by G-protein-coupled receptors. *Nature* **379**, 557-560
2. Luttrell, L. M., Della Rocca, G. J., van Biesen, T., Luttrell, D. K., and Lefkowitz, R. J. (1997) Gbetagamma subunits mediate Src-dependent phosphorylation of the epidermal growth factor receptor. A scaffold for G protein-coupled receptor-mediated Ras activation. *The Journal of biological chemistry* **272**, 4637-4644
3. Wortzel, I., and Seger, R. (2011) The ERK Cascade: Distinct Functions within Various Subcellular Organelles. *Genes & cancer* **2**, 195-209
4. Forrester, S. J., Kawai, T., O'Brien, S., Thomas, W., Harris, R. C., and Eguchi, S. (2016) Epidermal Growth Factor Receptor Transactivation: Mechanisms, Pathophysiology, and Potential Therapies in the Cardiovascular System. *Annual review of pharmacology and toxicology* **56**, 627-653
5. Sabbatini, M., Santillo, M., Pisani, A., Paterno, R., Uccello, F., Seru, R., Matrone, G., Spagnuolo, G., Andreucci, M., Serio, V., Esposito, P., Cianciaruso, B., Fuiano, G., and Avvedimento, E. V. (2006) Inhibition of Ras/ERK1/2 signaling protects against postischemic renal injury. *American journal of physiology. Renal physiology* **290**, F1408-1415
6. Nowak, G. (2002) Protein kinase C-alpha and ERK1/2 mediate mitochondrial dysfunction, decreases in active Na+ transport, and cisplatin-induced apoptosis in renal cells. *The Journal of biological chemistry* **277**, 43377-43388
7. Nowak, G., Clifton, G. L., Godwin, M. L., and Bakajsova, D. (2006) Activation of ERK1/2 pathway mediates oxidant-induced decreases in mitochondrial function in renal cells. *American journal of physiology. Renal physiology* **291**, F840-855
8. Zhuang, S., Kinsey, G. R., Yan, Y., Han, J., and Schnellmann, R. G. (2008) Extracellular signal-regulated kinase activation mediates mitochondrial dysfunction and necrosis induced by hydrogen peroxide in renal proximal tubular cells. *The Journal of pharmacology and experimental therapeutics* **325**, 732-740
9. Lameire, N. H., Bagga, A., Cruz, D., De Maeseneer, J., Endre, Z., Kellum, J. A., Liu, K. D., Mehta, R. L., Pannu, N., Van Biesen, W., and Vanholder, R. (2013) Acute kidney injury: an increasing global concern. *Lancet (London, England)* **382**, 170-179
10. Stallons, L. J., Funk, J. A., and Schnellmann, R. G. (2013) Mitochondrial Homeostasis in Acute Organ Failure. *Current pathobiology reports* **1**
11. Funk, J. A., and Schnellmann, R. G. (2013) Accelerated recovery of renal mitochondrial and tubule homeostasis with SIRT1/PGC-1alpha activation following ischemia-reperfusion injury. *Toxicology and applied pharmacology* **273**, 345-354
12. Scarpulla, R. C. (2008) Transcriptional paradigms in mammalian mitochondrial biogenesis and function. *Physiological reviews* **88**, 611-638
13. Puigserver, P., and Spiegelman, B. M. (2003) Peroxisome proliferator-activated receptor-gamma coactivator 1 alpha (PGC-1 alpha): transcriptional coactivator and metabolic regulator. *Endocrine reviews* **24**, 78-90

14. Che, R., Yuan, Y., Huang, S., and Zhang, A. (2014) Mitochondrial dysfunction in the pathophysiology of renal diseases. *American journal of physiology. Renal physiology* **306**, F367-378
15. Gilmartin, A. G., Bleam, M. R., Groy, A., Moss, K. G., Minthorn, E. A., Kulkarni, S. G., Rominger, C. M., Erskine, S., Fisher, K. E., Yang, J., Zappacosta, F., Annan, R., Sutton, D., and Laquerre, S. G. (2011) GSK1120212 (JTP-74057) is an inhibitor of MEK activity and activation with favorable pharmacokinetic properties for sustained in vivo pathway inhibition. *Clinical cancer research : an official journal of the American Association for Cancer Research* **17**, 989-1000
16. Yamaguchi, T., Kakefuda, R., Tajima, N., Sowa, Y., and Sakai, T. (2011) Antitumor activities of JTP-74057 (GSK1120212), a novel MEK1/2 inhibitor, on colorectal cancer cell lines in vitro and in vivo. *International journal of oncology* **39**, 23-31
17. Borniquel, S., Garcia-Quintans, N., Valle, I., Olmos, Y., Wild, B., Martinez-Granero, F., Soria, E., Lamas, S., and Monsalve, M. (2010) Inactivation of Foxo3a and subsequent downregulation of PGC-1 alpha mediate nitric oxide-induced endothelial cell migration. *Molecular and cellular biology* **30**, 4035-4044
18. Daitoku, H., Yamagata, K., Matsuzaki, H., Hatta, M., and Fukamizu, A. (2003) Regulation of PGC-1 promoter activity by protein kinase B and the forkhead transcription factor FKHR. *Diabetes* **52**, 642-649
19. Olmos, Y., Valle, I., Borniquel, S., Tierrez, A., Soria, E., Lamas, S., and Monsalve, M. (2009) Mutual dependence of Foxo3a and PGC-1alpha in the induction of oxidative stress genes. *The Journal of biological chemistry* **284**, 14476-14484
20. Tzivion, G., Dobson, M., and Ramakrishnan, G. (2011) FoxO transcription factors; Regulation by AKT and 14-3-3 proteins. *Biochimica et biophysica acta* **1813**, 1938-1945
21. Ho, K. K., McGuire, V. A., Koo, C. Y., Muir, K. W., de Olano, N., Maifoshie, E., Kelly, D. J., McGovern, U. B., Monteiro, L. J., Gomes, A. R., Nebreda, A. R., Campbell, D. G., Arthur, J. S., and Lam, E. W. (2012) Phosphorylation of FOXO3a on Ser-7 by p38 promotes its nuclear localization in response to doxorubicin. *The Journal of biological chemistry* **287**, 1545-1555
22. Schachter, T. N., Shen, T., Liu, Y., and Schneider, M. F. (2012) Kinetics of nuclear-cytoplasmic translocation of Foxo1 and Foxo3A in adult skeletal muscle fibers. *American journal of physiology. Cell physiology* **303**, C977-990
23. Yang, J. Y., Zong, C. S., Xia, W., Yamaguchi, H., Ding, Q., Xie, X., Lang, J. Y., Lai, C. C., Chang, C. J., Huang, W. C., Huang, H., Kuo, H. P., Lee, D. F., Li, L. Y., Lien, H. C., Cheng, X., Chang, K. J., Hsiao, C. D., Tsai, F. J., Tsai, C. H., Sahin, A. A., Muller, W. J., Mills, G. B., Yu, D., Hortobagyi, G. N., and Hung, M. C. (2008) ERK promotes tumorigenesis by inhibiting FOXO3a via MDM2-mediated degradation. *Nature cell biology* **10**, 138-148
24. Tseng, A. H., Wu, L. H., Shieh, S. S., and Wang, D. L. (2014) SIRT3 interactions with FOXO3 acetylation, phosphorylation and ubiquitinylation mediate endothelial cell responses to hypoxia. *The Biochemical journal* **464**, 157-168

25. Pierce, K. L., Luttrell, L. M., and Lefkowitz, R. J. (2001) New mechanisms in heptahelical receptor signaling to mitogen activated protein kinase cascades. *Oncogene* **20**, 1532-1539
26. Raymond, E., Faivre, S., and Armand, J. P. (2000) Epidermal growth factor receptor tyrosine kinase as a target for anticancer therapy. *Drugs* **60 Suppl 1**, 15-23; discussion 41-12
27. Smith, J. A., Stallons, L. J., Collier, J. B., Chavin, K. D., and Schnellmann, R. G. (2015) Suppression of mitochondrial biogenesis through toll-like receptor 4-dependent mitogen-activated protein kinase kinase/extracellular signal-regulated kinase signaling in endotoxin-induced acute kidney injury. *The Journal of pharmacology and experimental therapeutics* **352**, 346-357
28. Zhao, Y., Wang, Y., and Zhu, W. G. (2011) Applications of post-translational modifications of FoxO family proteins in biological functions. *Journal of molecular cell biology* **3**, 276-282
29. Woods, Y. L., Rena, G., Morrice, N., Barthel, A., Becker, W., Guo, S., Unterman, T. G., and Cohen, P. (2001) The kinase DYRK1A phosphorylates the transcription factor FKHR at Ser329 in vitro, a novel in vivo phosphorylation site. *The Biochemical journal* **355**, 597-607
30. Sengupta, A., Molkentin, J. D., Paik, J. H., DePinho, R. A., and Yutzey, K. E. (2011) FoxO transcription factors promote cardiomyocyte survival upon induction of oxidative stress. *The Journal of biological chemistry* **286**, 7468-7478
31. Greer, E. L., and Brunet, A. (2005) FOXO transcription factors at the interface between longevity and tumor suppression. *Oncogene* **24**, 7410-7425
32. Funk, J. A., and Schnellmann, R. G. (2012) Persistent disruption of mitochondrial homeostasis after acute kidney injury. *American journal of physiology. Renal physiology* **302**, F853-864
33. Friess, T., Scheuer, W., and Hasmann, M. (2006) Erlotinib antitumor activity in non-small cell lung cancer models is independent of HER1 and HER2 overexpression. *Anticancer research* **26**, 3505-3512
34. Monick, M. M., Powers, L. S., Barrett, C. W., Hinde, S., Ashare, A., Groskreutz, D. J., Nyunoya, T., Coleman, M., Spitz, D. R., and Hunninghake, G. W. (2008) Constitutive ERK MAPK activity regulates macrophage ATP production and mitochondrial integrity. *Journal of immunology (Baltimore, Md. : 1950)* **180**, 7485-7496
35. Ripple, M. O., Kim, N., and Springett, R. (2013) Acute mitochondrial inhibition by mitogen-activated protein kinase/extracellular signal-regulated kinase kinase (MEK) 1/2 inhibitors regulates proliferation. *The Journal of biological chemistry* **288**, 2933-2940
36. Roy, S. K., Srivastava, R. K., and Shankar, S. (2010) Inhibition of PI3K/AKT and MAPK/ERK pathways causes activation of FOXO transcription factor, leading to cell cycle arrest and apoptosis in pancreatic cancer. *Journal of molecular signaling* **5**, 10
37. Van Der Heide, L. P., Hoekman, M. F., and Smidt, M. P. (2004) The ins and outs of FoxO shuttling: mechanisms of FoxO translocation and transcriptional regulation. *The Biochemical journal* **380**, 297-309

38. Southgate, R. J., Bruce, C. R., Carey, A. L., Steinberg, G. R., Walder, K., Monks, R., Watt, M. J., Hawley, J. A., Birnbaum, M. J., and Febbraio, M. A. (2005) PGC-1alpha gene expression is down-regulated by Akt- mediated phosphorylation and nuclear exclusion of FoxO1 in insulin-stimulated skeletal muscle. *FASEB journal : official publication of the Federation of American Societies for Experimental Biology* **19**, 2072-2074
39. Link, W., Oyarzabal, J., Serelde, B. G., Albarran, M. I., Rabal, O., Cebria, A., Alfonso, P., Fominaya, J., Renner, O., Peregrina, S., Soilan, D., Ceballos, P. A., Hernandez, A. I., Lorenzo, M., Pevarello, P., Granda, T. G., Kurz, G., Carnero, A., and Bischoff, J. R. (2009) Chemical interrogation of FOXO3a nuclear translocation identifies potent and selective inhibitors of phosphoinositide 3-kinases. *The Journal of biological chemistry* **284**, 28392-28400
40. Rayego-Mateos, S., Morgado-Pascual, J. L., Sanz, A. B., Ramos, A. M., Eguchi, S., Batlle, D., Pato, J., Keri, G., Egido, J., Ortiz, A., and Ruiz-Ortega, M. (2013) TWEAK transactivation of the epidermal growth factor receptor mediates renal inflammation. *The Journal of pathology* **231**, 480-494
41. Haq, R., Shoag, J., Andreu-Perez, P., Yokoyama, S., Edelman, H., Rowe, G. C., Frederick, D. T., Hurley, A. D., Nellore, A., Kung, A. L., Wargo, J. A., Song, J. S., Fisher, D. E., Arany, Z., and Widlund, H. R. (2013) Oncogenic BRAF regulates oxidative metabolism via PGC1alpha and MITF. *Cancer cell* **23**, 302-315
42. Furuyama, T., Nakazawa, T., Nakano, I., and Mori, N. (2000) Identification of the differential distribution patterns of mRNAs and consensus binding sequences for mouse DAF-16 homologues. *The Biochemical journal* **349**, 629-634
43. Asada, S., Daitoku, H., Matsuzaki, H., Saito, T., Sudo, T., Mukai, H., Iwashita, S., Kako, K., Kishi, T., Kasuya, Y., and Fukamizu, A. (2007) Mitogen-activated protein kinases, Erk and p38, phosphorylate and regulate Foxo1. *Cellular signalling* **19**, 519-527
44. Nowak, G., and Schnellmann, R. G. (1996) L-ascorbic acid regulates growth and metabolism of renal cells: improvements in cell culture. *The American journal of physiology* **271**, C2072-2080

CHAPTER THREE:

Extracellular Signal-Regulated Kinase 1/2 Regulates Mouse Kidney Injury Molecule-1 Expression Physiologically and Following Ischemic and Septic Renal Injury.

ABSTRACT

The upregulation of kidney injury molecule-1 (KIM-1) has been extensively studied in various renal diseases and following acute injury; however, the initial mechanisms controlling KIM-1 expression remain limited. In this study, KIM-1 expression was examined in mouse renal cell cultures and in two different models of acute kidney injury (AKI), ischemia reperfusion (IR)–induced and lipopolysaccharide (LPS)-induced sepsis. KIM-1 mRNA increased in both AKI models, and pharmacological inhibition of extracellular signal–regulated kinase 1/2 (ERK1/2) signaling attenuated injury-induced KIM-1 expression in the renal cortex. Toll-like receptor 4 knockout (TLR4KO) mice exhibited reduced ERK1/2 phosphorylation and attenuated KIM-1 mRNA after LPS exposure. TLR4KO mice were not protected from IR-induced ERK1/2 phosphorylation and upregulation of KIM-1 mRNA. Following renal IR injury, phosphorylation of signal transducer and activator of transcription 3 (STAT3) at serine 727 and tyrosine 705 increased downstream from ERK1/2 activation. Because phosphorylated STAT3 is a transcriptional upregulator of KIM-1 and inhibition of ERK1/2 attenuated increases in STAT3 phosphorylation, we suggest an ERK1/2-STAT3-KIM-1 pathway following renal injury. Finally, ERK1/2 inhibition in naive mice decreased KIM-1 mRNA and nuclear STAT3 phosphorylation in the cortex, indicating homeostatic regulation of KIM-1. These findings reveal renal ERK1/2 as an important initial regulator of KIM-1 expression in IR and septic AKI and at a physiologic level (Figure 3.7 – Visual Abstract).

INTRODUCTION

KIM-1 is a type I transmembrane glycoprotein that is rapidly upregulated at the gene and protein level following various types of injury to the kidney [1-3]. For example, KIM-1 is increased in IR, cisplatin, sepsis, folic acid, aristolochic acid and gentamicin-induced injuries, as well as occurring in disease states, such as renal cell carcinoma, polycystic kidney disease, hyperoxaluria, and hypertension [4-7].

The ectodomain, which contains an Ig-like domain and a glycosylated mucin domain, is cleaved by the metalloproteinase ADAM17 at the cellular membrane [3, 8, 9]. Membrane bound KIM-1 and cleaved KIM-1 increase with worsening renal injury [10]. KIM-1 is located on the apical surface of renal proximal tubule epithelial cells and recognizes phosphatidylserine and oxidized lipoprotein epitopes on the surface of apoptotic bodies [11].

The extracellular signal-regulated kinase 1/2 (ERK1/2) is a mitogen-activated protein kinase (MAPK) that is phosphorylated rapidly following renal injury [12-14]. We previously demonstrated ERK1/2 phosphorylation is elevated 3 hr post IR injury and 1 hr post LPS induced AKI [15, 16]. Further exploration of the ERK1/2 pathway was performed utilizing a specific MEK1/2 inhibitor, trametinib, which inhibits the increase in ERK1/2 phosphorylation, since MEK1/2 is directly upstream of ERK1/2 [17, 18]. Interestingly, inhibiting LPS induced ERK1/2 phosphorylation prevented KIM-1 mRNA upregulation at 3 and 18 hr post LPS administration. Smith et al. confirmed ERK1/2 inhibition attenuates the upregulation of KIM-1 mRNA following injury

utilizing trametinib treatment 6 hr post cecal ligation and puncture (CLP) surgery, a model of sepsis [19].

ERK1/2 and KIM-1 were studied in vitro using a porcine kidney epithelial cell line, LLC-PK1, transfected with human KIM-1 [20]. KIM-1 protein promoted cell migration and proliferation through activation of the ERK1/2 pathway, and inhibiting ERK1/2 attenuated these processes. Recently, KIM-1 was shown to modulate macrophages by promoting an M1 phenotype and macrophage migration by MAPK pathways, including ERK, p38, and JNK [6]. It is clear that ERK1/2 and KIM-1 are activated and upregulated shortly after kidney injury, however a direct connection between ERK1/2 and KIM-1 has received limited study.

Ajay et al. used a combination of bioinformatics, in vitro, and in vivo experiments to determine that signal transducer and activator of transcription-3 (STAT3) phosphorylation at serine 727 (S727) and tyrosine 705 (Y705) increases KIM-1 transcription by binding to the KIM-1 specific promoter [21]. Checkpoint kinase 1 (Chk1) was upregulated following IR injury due to DNA damage which phosphorylated STAT3 and subsequently regulated KIM-1 expression [21]. Interestingly, ERK2 was the most enriched upstream kinase identified that was associated with the highest upregulated transcription factors following IR injury [21-23]. Given this information and our previous data demonstrating ERK1/2 is rapidly phosphorylated post IR injury, we hypothesized early ERK1/2 activation following injury preferentially regulates KIM-1 expression.

MATERIALS AND METHODS

In Vitro Studies.

A transgenic kidney proximal tubule (TK) cell line originally isolated from 8Tg(SV40E)Bri7 mice and developed by Ernest and Bello-Reuss, was used in all in vitro experiments [24, 25]. TK cells were grown in 35-mm tissue culture dishes. The culture medium was a 1:1 mixture of Dulbecco's modified Eagle's medium/F-12 (without phenol red, or sodium pyruvate) supplemented with 5mM glucose, 10% FBS, 15 mM HEPES buffer, 2.5 mM L-glutamine, 1 uM pyridoxine HCl, 15 mM sodium bicarbonate, and 6 mM lactate. Hydrocortisone (50 nM), selenium (5 ng/ml), human transferrin (5 ug/ml), bovine insulin (10 nM), and L-ascorbic acid-2-phosphate (50 uM) were added to fresh culture medium. 90-95% confluent TK cells were used for all experiments, and FBS was removed from culture media 24 hr before experimentation. TK cell monolayers were treated HU (Fisher Scientific- AC151680050), TBHP (Sigma- #458139), and H2O2 (Sigma- H1009) or vehicle (DMSO-Sigma) for time points indicated. Different TK cell passages used on different days represent the "N" value for the in vitro studies.

Naïve and AKI Studies.

Trametinib (GSK1120212, [18]) was purchased from Selleckchem Chemicals (Houston, TX). Eight-to-nine week old male C57BL/6 mice (20–25 g) were acquired from Charles River Laboratories (Frederick, MD) and received an injection of trametinib (1 mg/kg i.p.) or vehicle control (NEOBEE M-5 – Fisher Scientific). Four hr after injection kidneys were collected and flash frozen in liquid nitrogen for further analysis.

For IR AKI, mice were assigned to 3 groups: 1) Sham, 2) IR + Vehicle, 3) IR + Trametinib. Vehicle or trametinib were administered i.p 1 hr before surgery. For TLR4KO IR AKI mice were assigned to 4 groups: 1) WT sham, 2) TLR4KO SHAM, 3) WT IR, 4) TLR4KO IR. IR grouped mice were subjected to IR surgery by bilateral renal pedicle clamping for 18.5 min as described previously [26]. Briefly, the renal artery and vein were isolated and blood flow was occluded with a vascular clamp for 18.5 min while maintaining a constant body temperature of 36~37°C. Sham mice were treated exactly the same as IR mice, except without the clamping of the renal pedicles. Mice were euthanized at 3 or 24 hr after surgery, and blood and kidneys (flash frozen in liquid nitrogen) were collected for analysis.

For LPS model of sepsis, eight week old male C57BL/6 mice (20–25 g) were given an i.p injection of 10 mg/kg LPS derived from Escherichia coli serotype O111:B4 (Sigma-Aldrich, St. Louis, MO). Control mice received an i.p injection of an equal volume of 0.9% normal saline. Mice received an injection of GSK1120212 (1 mg/kg i.p.) or vehicle control 1 hr before administration of LPS. Mice were euthanized at 18 hr after LPS exposure, and kidneys and blood were collected for analysis. Experiments with TLR4KO mice were graciously donated by Dr. Kenneth D. Chavin and generated by crossing C57BL/10ScN mice with the tlr4LPS-d mutation onto the C57BL/6 background for at least five generations [16, 27]. All studies were conducted in accordance with the recommendations in the Guide for the Care and Use of Laboratory Animals of the National Institutes of Health. Animal use was approved by the Institutional Animal Care and Use Committee at the Medical University of South Carolina.

Serum Creatinine Measurement.

Blood was collected by retro-orbital bleeding puncture and allowed to sit at room temperature for 30 minutes. The samples were centrifuged at 10,000 rpm for 10 min to separate the serum. Serum creatinine (SCr) was determined using the Creatinine Enzymatic Reagent Assay kit (Pointe Scientific, Canton, MI) [c7548-120] based on the manufacturer's directions. All values are expressed as serum creatinine concentration in milligrams per deciliter.

RT-qPCR Analysis of mRNA Expression.

Total RNA was isolated from renal cortical tissue with TRIzol reagent (Life Technologies). The iScript Advanced cDNA Synthesis Kit (Bio-Rad) was used according to the manufacturer's protocol. The generated cDNA was used with the SsoAdvanced Universal SYBR Green Supermix reagent (Bio-Rad). The relative mRNA expression of all genes was determined by the $2^{-\Delta\Delta Ct}$ method, and mouse Actin RNA and rabbit tubulin RNA were used as reference genes for normalization. KIM-1 primer sequences used were Fwd- 5'-GCATCTCTAAGCGTGGTTGC-3' and Rev- 5'-TCAGCTCGGGAATGCACAA-3'.

Immunoblot Analysis.

Protein was extracted from renal cortex using RIPA assay buffer (50 mM Tris-HCl, 150 mM NaCl, 0.1% SDS, 0.5% sodium deoxycholate, 1% Triton X-100, pH 7.4) with

protease inhibitor cocktail (1:100), 1 mM sodium fluoride, and 1 mM sodium orthovanadate (Sigma-Aldrich).

Mouse tissue nuclear and cytosolic fraction lysates were prepared as previously described (24096033, 27875304). Briefly, a piece of kidney cortex was homogenized in sucrose isolation (ISO) buffer (250 mM sucrose, 1 mM EGTA, 10 mM HEPES, 1 mg/ml fatty acid-free BSA [pH 7.4]) added fresh, with a dounce tissue grinder. Lysates were centrifuged at 1000 x g for 10 min. The 1st pellet was pushed through 25G needle 3 times and re-washed three separate times in ISO buffer and resuspended in RIPA. The 1st supernatant was centrifuged at 10,000 x g for 5 min for further purification of the cytosol fraction. Histone H3 and/or Lamin B1 were used as loading control for nuclear lysate immunoblots, and alpha-tubulin was used for loading control of cytosolic lysates. Equal protein quantities (10–60 μg) were loaded onto 4–15% SDS-PAGE gels, resolved by gel electrophoresis, and transferred onto nitrocellulose membranes (Bio-Rad). Membranes were blocked in 5% bovine serum albumin or 5% milk in TBST and incubated overnight with primary antibody at 4°C with gently agitation. Primary antibodies used in these studies included phospho-ERK1/2 (1:1000) [#4370], total ERK1/2 (1:1000) [#4695], phospho-Chk1 (1:1000) [#12302], Chk1 (1:1000) [#2360], phospho-STAT3-Tyr705 (1:1000) [#9145], phospho-STAT3-Ser727 (1:1000) [#94994], total STAT3 (1:1000) [#9139], Histone H3 (1:2000) [#9715] all from Cell Signaling Technology, Danvers, MA. lamin B1 (1:1000; Abcam) [ab16048], phospho-Chk1 (1:800) [AF2054], kidney injury molecule-1 (KIM-1) (1:1000) [AF1817] from R&D systems, Minneapolis, MN. β-actin (1:2000; Santa Cruz Biotechnology, Dallas, TX) [sc-47778].

Membranes were incubated with the appropriate horseradish peroxidase–conjugated secondary antibody before visualization using enhanced chemiluminescence (Thermo Scientific) and the GE ImageQuant LAS4000 (GE Life Sciences). Optical density was determined using the ImageJ software from NIH and Image Studio Lite from LI-COR.

Statistical Analysis.

All data are shown as mean ± S.E.M. When comparing two experimental groups, an unpaired, two-tailed t test or Mann-Whitney U was used to determine statistical differences. A one-way analysis of variance (ANOVA) followed by Tukey's post hoc test was performed for comparisons of multiple groups. $P < 0.05$ was considered statistically significant. All statistical tests were performed using GraphPad Prism software (GraphPad Software, San Diego, CA).

RESULTS

ERK1/2 Increases KIM-1 mRNA Following Toxicant Exposure in Mouse Renal Cells.

To confirm KIM-1 expression is upregulated following toxicant exposure, cultured transgenic mouse kidney proximal tubule (TK) cells were treated with 1 and 10 mM hydroxyurea (HU), 0.1 and 1 mM hydrogen peroxide (H2O2), and 350 and 700 μM tert-butyl hydroperoxide (TBHP) for 24 hr. HU causes cellular injury by inhibiting DNA synthesis and causing DNA damage [28], while H2O2 and TBHP are model oxidants that lead to oxidative stress causing protein, lipid, and DNA damage [29]. Each toxicant increased KIM-1 mRNA with increasing concentration (Figure 3.1A). KIM-1 mRNA increased 8-, 3-, and 3-fold in response to 10 mM HU, 1 mM H2O2, and 700 μM TBHP, respectively (Figure 3.1A). A 1 hr pretreatment with trametinib prevented HU, H2O2, and TBHP induced KIM-1 mRNA increases (Figure 3.1B). Interestingly, TK cells treated with trametinib alone showed a 54% decrease in KIM-1 mRNA compared to vehicle control cells at 24 hr (Figure 3.1B). These data reveal a regulatory role for ERK1/2 on KIM-1 mRNA under control conditions and following DNA and oxidative damage.

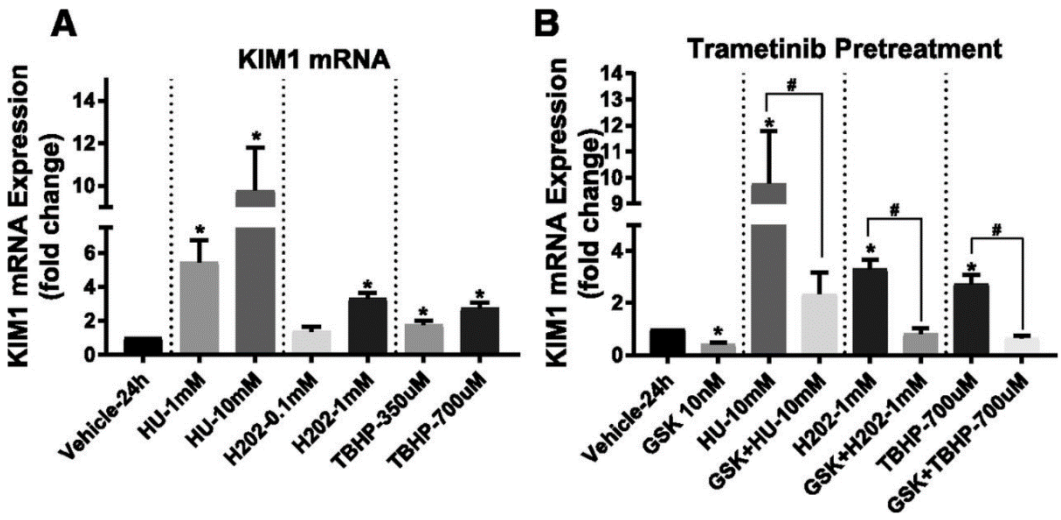

Figure 3.1: ERK1/2 increases KIM-1 mRNA after toxicant exposure in mouse TKPT cells. (A) KIM-1 mRNA expression after 24 hr following exposure to HU, H2O2, and TBHP. (B) KIM-1 mRNA measured after 24 hr post toxicant administration with or without 1 hour trametinib (GSK) pretreatment. Data are represented as mean ± S.E.M., n ≥ 4. Superscripts indicate statistically significant differences ($P < 0.05$);*, significantly different than vehicle control; #, significance between same toxicant groups.

Early ERK1/2 Activation Mediates STAT3 Phosphorylation Induced KIM-1 mRNA Upregulation Following IR AKI.

KIM-1 mRNA increased 4.7-fold 3 hr post IR AKI compared to sham controls (Figure 3.2A). Trametinib attenuated the KIM-1 mRNA and serum creatinine increases when administered 1 hr before IR surgery (Figure 3.2A, 2B). The phosphorylated ERK1/2 to total ERK1/2 ratio increased 4.5-fold in the IR groups compared to sham (Figure 3.2C, 2D). Trametinib also completely inhibited ERK1/2 phosphorylation increases following AKI, as observed previously [15, 16].

Ajay et al. (2014) reported that Chk1 phosphorylation is elevated 3 hr post IR AKI. In contrast, we did not observe any change in phosphorylated Chk1 to total Chk1 ratio following IR injury in the presence or absence of trametinib. However, transcription factor STAT3 phosphorylation at both activating sites, S727 and Y705, increased 2.5- and 3.5-fold after renal IR, respectively (Figure 3.2C, 2E-H) and pretreatment with trametinib partially blocked the increase in phosphorylation of STAT3 at S727 and Y705 (Figure 3.2G, 2H). These findings suggest that inhibiting ERK1/2 phosphorylation prevents KIM-1 mRNA upregulation 3 hr post IR AKI by preventing STAT3 phosphorylation at S727 and Y705.

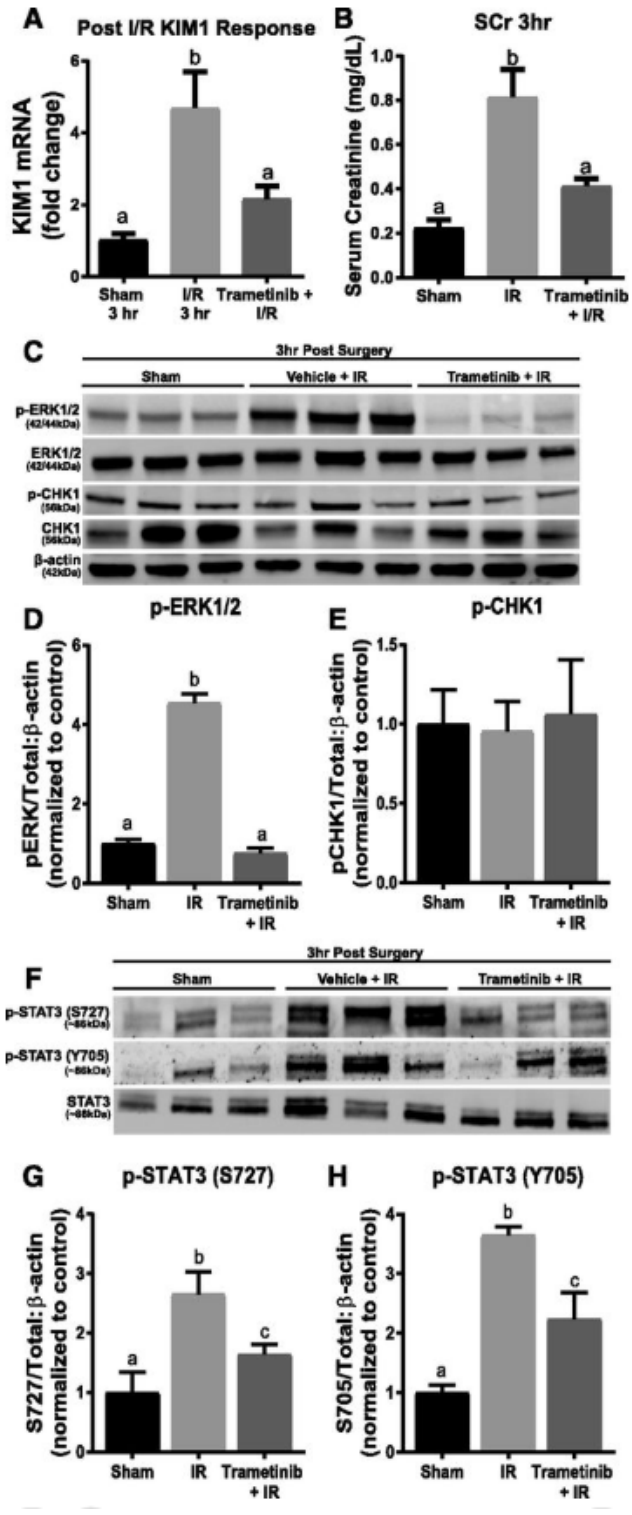

Figure 3.2: ERK1/2 mediates STAT3 phosphorylation and KIM-1 mRNA upregulation following 3 hr of IR AKI. (A) KIM-1 mRNA expression following IR AKI after 3 hr. (B) Serum creatinine was assessed 3 hr after IR AKI. (C) Representative immunoblot of phosphorylated ERK1/2, total ERK1/2, phosphorylated Chk1, and total Chk1 following 3 hr of IR AKI. (D) Densitometry analysis of phosphorylated ERK1/2 compared with total ERK1/2. (E) Densitometry analysis of phosphorylated Chk1 compared with total Chk1. (F) Representative immunoblot of phosphorylated STAT3 (S727 and Y705) and total STAT3 following 3 hr of IR AKI. (G and H) Densitometry analysis of phosphorylated STAT3 (S727 and Y705) compared with total STAT3. Data are represented as mean ± S.E.M., n = 6. Different superscripts indicate statistically significant differences ($P < 0.05$).

ERK1/2 Inhibition Suppresses KIM-1 mRNA and Protein 24 hr Following IR AKI. At 24 hr, KIM-1 mRNA was ~280-fold higher in the IR group compared to sham controls (Figure 3.3A). Trametinib partially blocked the increase in KIM-1 mRNA (~120-fold higher compared to sham) compared to the IR mice (Figure 3.3A). Serum creatinine increased to 1.1 mg/dL in the IR group and pretreatment with trametinib attenuated this rise in serum creatinine at 24 hr (Figure 3.3B). STAT3 phosphorylation at S727 and Y705 increased following renal IR injury and trametinib pretreatment blocked these increases (Figure 3.3D, G-H). Chk1 phosphorylation decreased in the IR group at 24 hr and ERK1/2 inhibition had no influence on Chk1 phosphorylation (Figure 3.3D, 3.3F). Trametinib inhibited ERK1/2 phosphorylation throughout the 24 hr period after IR surgery (Figure 3.3D, 3.3E). The IR group showed a large upregulation in KIM-1 kidney cortex protein that was markedly reduced in the presence of trametinib at 24 hr (Figure 3.3C). Because KIM-1 is cleaved from the cell surface, KIM-1 protein was measured in the serum to detect any changes in cleavage regulation [30]. Serum KIM-1 protein was high in the IR group and was markedly reduced in the trametinib group (Figure 3.3C). These findings reveal ERK1/2 remains activated 24 hr following IR AKI, which corresponds to increased phosphorylation of STAT3 at S727 and Y705, and leads to increases in KIM-1 mRNA and protein. This correlates with our observations of STAT3 phosphorylation at S727 and Y705 in the trametinib group compared to the IR group in our 3 hr study (Figure 3.2F-H). It is clear, however, that ERK1/2 and STAT3 are not the only pathway responsible for the later increases in KIM-1 mRNA, as the trametinib group is only partially attenuated at 24 hr (Figure 3.3A).

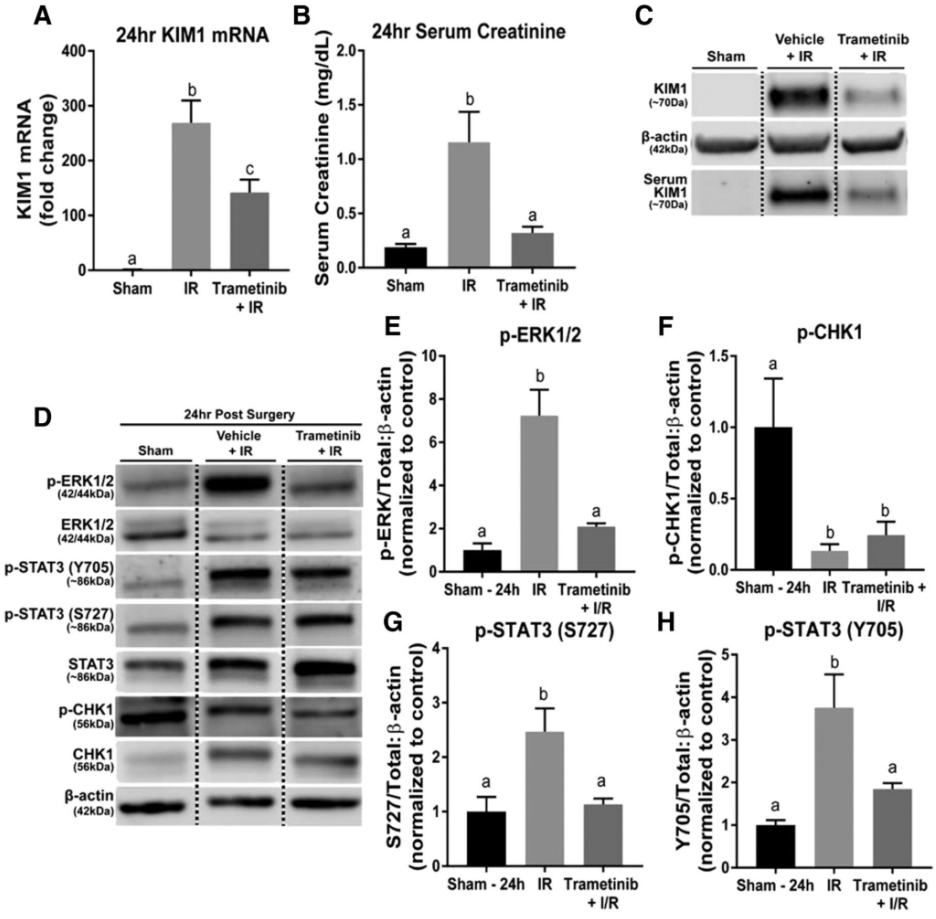

Figure 3.3: ERK1/2 mediates KIM-1 mRNA and protein increases and STAT3 phosphorylation following 24 hr of IR AKI. (A) KIM-1 mRNA expression following IR AKI after 24 hr. (B) Serum creatinine was assessed 24 hr after IR AKI. (C) Representative immunoblot of renal KIM-1 and serum KIM-1 (n = 2 for serum KIM-1) following 24 hr of IR AKI. (D) Representative immunoblot of phosphorylated ERK1/2, total ERK1/2, phosphorylated STAT3 (S727 and Y705), total STAT3, phosphorylated Chk1, and total Chk1 following IR AKI. (E–H) Densitometry analysis of phosphorylated (E) ERK1/2 to total ERK1/2; (F) p-Chk1 to total Chk1; (G) p-STAT3 S727 to total STAT3; (H) p-STAT3 Y705 to total STAT3. Data are represented as mean ± S.E.M., $n \geq 5$, except where indicated. Different superscripts indicate statistically significant differences ($P < 0.05$).

ERK1/2 Increases KIM-1 mRNA in Sepsis Induced AKI and Requires TLR4.

Previously, we demonstrated LPS-induced AKI requires TLR4 mediated ERK1/2 activation at the initiation of injury to impair kidney function through mitochondrial dysfunction and inflammatory cytokines [16]. Similarly, partial attenuation of KIM-1 mRNA upregulation through ERK1/2 inhibition prior to LPS administration at 18 hrs was observed [16]. Here, trametinib treatment prevented KIM-1 protein upregulation within the kidney cortex compared to LPS alone at 18 hr (Figure 3.4A). ERK1/2 phosphorylation was inhibited in the trametinib + LPS group compared to the control and LPS group, whereas the LPS group was not different from controls (Figure 3.4A, 4B). To further illustrate pharmacological ERK1/2 inhibition downregulates KIM-1 expression, ERK1/2 phosphorylation was studied following LPS in TLR4KO mice, as TLR4 is required for LPS-induced kidney dysfunction [16]. TLR4KO mice had reduced ERK1/2 phosphorylation compared to WT mice administered LPS (Figure 3.4D, F). LPS induced increases in KIM-1 mRNA and KIM-1 protein were attenuated in LPS treated TLR4KO mice, connecting ERK1/2 activation and KIM-1 to TLR4 (Figure 3.4D, E). For confirmation, TLR4 mRNA expression in the TLR4KO mice was negligible compared to WT TLR4 mRNA expression (Figure 3.4C).

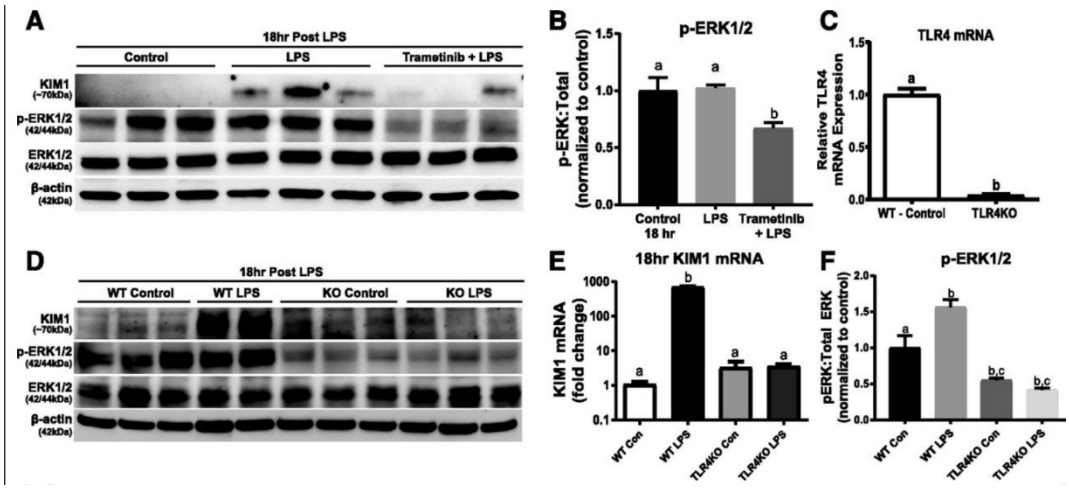

Figure 3.4: ERK1/2 increases KIM-1 mRNA and protein in LPS-induced AKI through TLR4 after 18 hr. (A) Representative immunoblot of KIM-1, phosphorylated ERK1/2, and total ERK1/2 following LPS-induced AKI. (B) Densitometry analysis of phosphorylated ERK1/2 compared with total ERK1/2. (C) TLR4 mRNA measured in WT mice kidney and TLR4KO mice kidney. (D) Representative immunoblot of KIM-1, phosphorylated ERK1/2, and total ERK1/2 following LPS-induced AKI in WT and TLR4KO mice. (E) KIM-1 mRNA measured in the kidneys of WT and TLR4KO mice following LPS-induced AKI after 18 hr. (F) Densitometry analysis of renal phosphorylated ERK1/2 compared with total ERK1/2 in the LPS-treated WT and TLR4KO mice. Data are represented as mean ± S.E.M., $n \geq 3$. Different superscripts indicate statistically significant differences ($P < 0.05$).

TLR4 is Not Required for IR-Induced ERK1/2 Phosphorylation and KIM-1 mRNA Upregulation.

To determine if ERK1/2 and KIM-1 are regulated by TLR4 during initiation of injury following IR AKI, TLR4KO mice were subjected to IR surgeries and KIM-1 alterations were observed at 3 hr. The WT and TLR4KO mice had similar increases in phosphorylated ERK1/2 following IR AKI compared to their sham controls (Figure 3.5A, 5C). Interestingly, KIM-1 mRNA was markedly elevated in the TLR4KO IR mice and WT IR mice trended upward (Figure 3.5B). The above findings demonstrate that IR AKI induced KIM-1 upregulation and ERK1/2 activation are TLR4 independent.

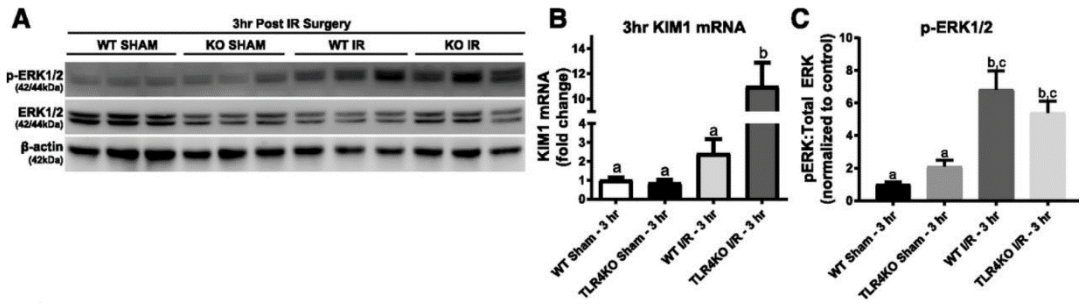

Figure 3.5: TLR4 is not required for IR-induced ERK1/2 phosphorylation and KIM-1 mRNA upregulation. (A) Representative immunoblot of phosphorylated ERK1/2 and total ERK1/2 following IR-induced AKI after 3 hr in WT and TLR4KO mice. (B) KIM-1 mRNA measured in the kidneys of WT and TLR4KO mice following IR-induced AKI after 3 hr. (C) Densitometry analysis of renal phosphorylated ERK1/2 compared with total ERK1/2 in the WT and TLR4KO mice following IR-induced AKI. Data are represented as mean ± S.E.M., $n \geq 3$. Different superscripts indicate statistically significant differences ($P < 0.05$).

ERK1/2 Inhibition Decreases KIM-1 mRNA, and Nuclear and Cytosolic STAT3 Phosphorylation Under Physiological Conditions.

To determine if ERK1/2 regulates KIM-1 at a physiological level, naïve mice were treated with trametinib or vehicle for 4 hr. Unexpectedly, trametinib treated mice had ~55% lower KIM-1 mRNA compared to vehicle control mice (Figure 3.6A). The trametinib group had reduced ERK1/2 phosphorylation in the nucleus and cytosol (Figure 3.6G, H). Nuclear STAT3 phosphorylation at sites Y705 and S727 were down in the trametinib group 55% and 46%, respectively, compared to the vehicle control group (Figure 3.6B-D). Phosphorylated Y705 and S727 on STAT3 in the cytosol was also reduced in the trametinib group (Figure 3.6E, F). To confirm that trametinib was inhibiting nuclear STAT3 phosphorylation, and subsequently KIM-1 mRNA downregulation, cytosol and nuclear fractions were isolated and confirmed for purity using α-tubulin and lamin B1 (Figure 3.6H). The purified fractions demonstrated that inhibition of physiological ERK1/2 phosphorylation results in a decrease in KIM-1 mRNA through reducing STAT3 phosphorylation at Y705 and S727 in the kidney. By decreasing active STAT3 within the nucleus there is potential for less KIM-1 promoter binding, resulting in lower KIM-1 mRNA expression.

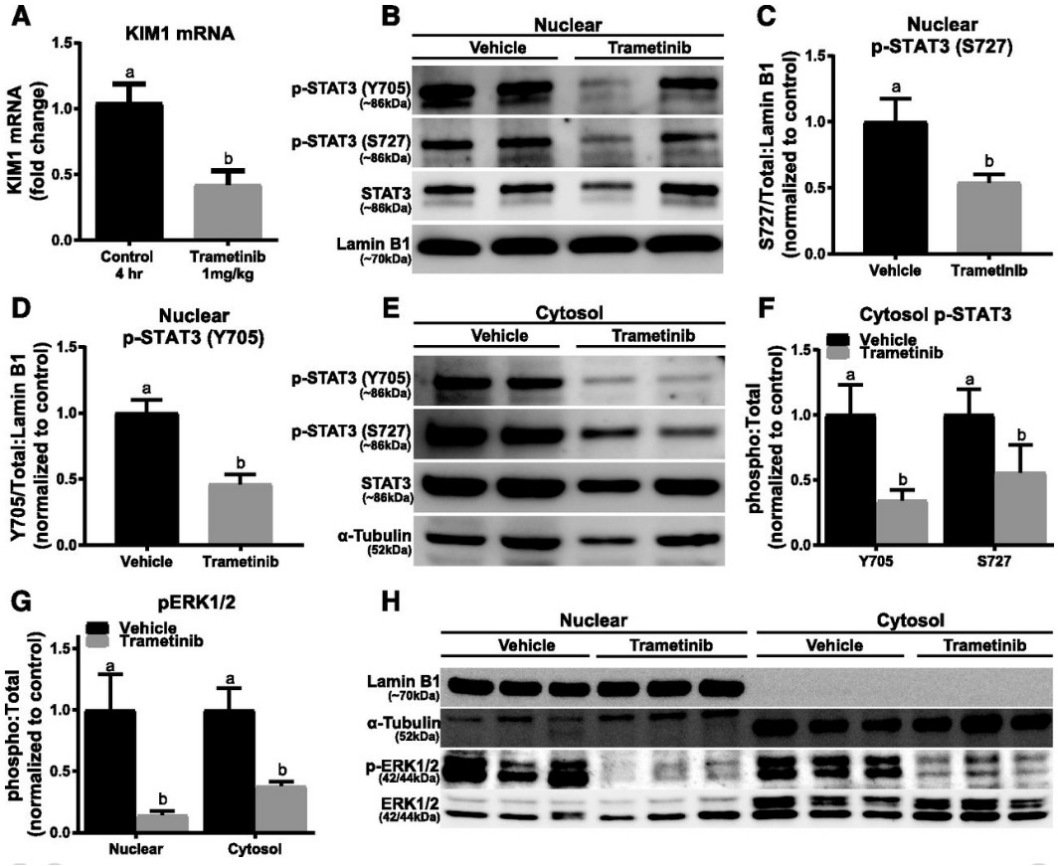

Figure 3.6: ERK1/2 inhibition decreases KIM-1 mRNA and nuclear and cytosolic STAT3 phosphorylation under physiologic conditions in naive mice. (A) Representative immunoblot of nuclear phosphorylated STAT3 (S727 and Y705) and total STAT3 in naive mice after 4-hour treatment with trametinib. (B) KIM-1 mRNA measured at 4 hr post-treatment with trametinib. (C and D) Densitometry analysis of nuclear phosphorylated STAT3 (S727 and Y705) compared with total STAT3. (E) Representative immunoblot of cytosol phosphorylated STAT3 (S727 and Y705) and total STAT3 in naive mice after 4-hour treatment with trametinib. (F) Densitometry analysis of cytosol phosphorylated STAT3 (S727 and Y705) compared with total STAT3. (G) Densitometry analysis of nuclear and cytosol phosphorylated ERK1/2 compared with total ERK1/2. (H) Representative and verification renal immunoblot of nuclear and cytosol control proteins with and without trametinib treatment. Data are represented as mean ± S.E.M., $n \geq 6$. Different superscripts indicate statistically significant differences ($P < 0.05$).

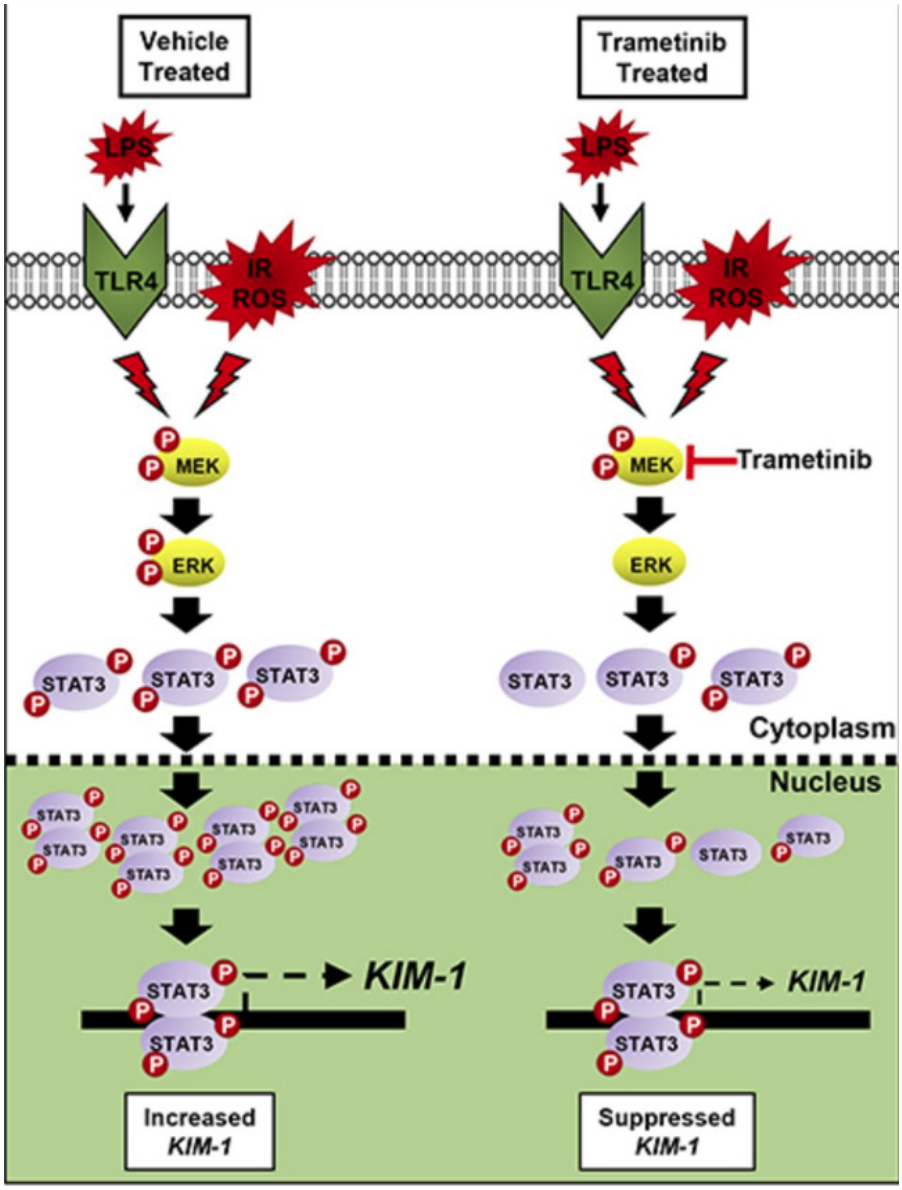

Figure 3.7: Visual Abstract. Proposed mechanism of IR, LPS, and ROS-induced renal damage that initiates ERK1/2 and STAT3 phosphorylation. STAT3 then binds to the KIM-1 promoter and increases KIM-1 mRNA. By preventing ERK1/2 phosphorylation following renal injury, STAT3 phosphorylation is decreased, leading to less phosphorylated STAT3 within the nucleus, and subsequently less KIM-1 mRNA increases post injury.

DISCUSSION

In this study, ERK1/2 was identified as a regulator of KIM-1 expression. ERK1/2 inhibition prevented KIM-1 transcription in vitro following toxicant exposure, and attenuated increases in KIM-1 mRNA and protein in IR AKI. STAT3 phosphorylation at S727 and Y705 decreased as a result of ERK1/2 inhibition, leading to less KIM-1 expression. In sepsis-induced AKI, TLR4 was required for activation of ERK1/2 and KIM-1 upregulation. In contrast, ERK1/2 phosphorylation following IR AKI was not dependent on TLR4. Interestingly, in naïve mice ERK1/2 regulates KIM-1 mRNA by physiological STAT3 phosphorylation in the nucleus. We suggest ERK1/2 regulates renal KIM-1 expression at a physiological level and initially during pathological renal injury by phosphorylation of STAT3.

The discovery that KIM-1 is the most upregulated gene following AKI led to an increase in KIM-1 renal research [2, 3, 31]. Ajay et al. explored the signaling pathway that results in upregulation of renal KIM-1 transcription. They reported KIM-1 transcriptional regulation by Chk1-STAT3 interaction following AKI-induced DNA damage. Chk1 was revealed as an upstream kinase of STAT3 and phosphorylation at S727 and Y705 on STAT3 was required for KIM-1 upregulation [21]. Phosphorylated STAT3 increased following AKI and was found to bind to the KIM-1 promoter, therefore increasing KIM-1 mRNA and protein [21]. While our studies support the work of Ajay et al., important differences were observed. (1) Chk1 phosphorylation did not increase following IR AKI at 3 and 24 hr. (2) ERK1/2 was responsible for the STAT3 phosphorylation after IR. (3) Our IR experimental design utilized mice rather than rats for AKI. Chk1 phosphorylation did not increase in the renal cortex in our

experiments, yet, KIM-1 mRNA and renal dysfunction was observed. Nevertheless, STAT3 phosphorylation was verified to increase following renal injury, and a reduction in phosphorylated STAT3 attenuated KIM-1 mRNA. However, ERK1/2 was demonstrated as the key initial regulator of STAT3 phosphorylation following renal injury, rather than Chk1.

We previously published work demonstrating that inhibiting the rapid activation of ERK1/2 following renal injury prevents and/or attenuates injury and dysfunction through restoration of mitochondrial function, renal microvascular perfusion, and attenuation of pro-inflammatory cytokines [15, 16, 19]. Here, ERK1/2 involvement with STAT3 after renal injury was observed. STAT3 phosphorylation is activated early in tubule cells following injury, although the exact role in kidney dysfunction and recovery varies in different AKI models [32, 33]. For example, in HgCl2, IR, and aristolochic acid induced AKI, early STAT3 phosphorylation was protective [34, 35]. In contrast, inhibition of STAT3 phosphorylation in polycystic kidney disease, unilateral ureteral obstruction, and HIV-associated nephropathy has shown beneficial outcomes [36-38]. Our findings suggest that prevention of renal IR-induced STAT3 phosphorylation through ERK1/2 inhibition attenuates serum creatinine and KIM-1 expression.

Previous experiments demonstrated activated ERK1/2 phosphorylates STAT3 at S727, while at the same time decreasing STAT3 Y705 phosphorylation [39-41]. However, in our study both S727 and Y705 phosphorylation increased following IR injury and decreased with pretreatment with trametinib, suggesting ERK1/2 is responsible for phosphorylating both sites. At 24 hr following IR AKI, a partial reduction of KIM-1

mRNA in the trametinib group was observed, along with a complete attenuation of serum creatinine elevation compared to the IR group. KIM-1 protein levels were substantially lower in the trametinib treated mice, both in the kidney cortex and in the circulatory system, as KIM-1 can be detected in the blood. This occurrence has been recognized due to the loss of cell polarity, microvascular permeability dysfunction, disruption of cell-cell adhesion junctions, and basement membrane cell detachment [6, 30].

ERK1/2 phosphorylation was found to regulate KIM-1 expression in a second AKI model. LPS-induced AKI increased ERK1/2 phosphorylation and KIM-1 protein, whereas trametinib prevented ERK1/2 activation and attenuated the KIM-1 protein increase. Further characterization of the ERK1/2-KIM-1 pathway was demonstrated by utilization of TLR4KO mice. TLR4 is required for LPS-induced ERK1/2 phosphorylation and subsequently, KIM-1 mRNA upregulation [16]. ERK1/2 is rapidly phosphorylated following LPS at 1 and 3 hr, however in this study, at 18 hr post-LPS phosphorylated ERK1/2 was not different than the control group, most likely stemming from a prompt compensatory mechanism. Nonetheless, 18 hr after CLP, which is a slower developing sepsis model, ERK1/2 phosphorylation is still highly phosphorylated compared to controls [16, 19]. To verify that TLR4 signaling was not regulating KIM-1 expression directly, the TLR4KO mice underwent IR AKI and were compared to the wild type mice. There were no differences in ERK1/2 phosphorylation between the TLR4KO IR group and the WT IR group, and the TLR4KO group had increased KIM-1 mRNA. Thus, TLR4 is required for LPS induced ERK1/2 activation and increase in KIM-1 mRNA, yet in IR AKI TLR4 is not required since ERK1/2 is activated via other

non-TLR4 upstream pathways. Therefore, we view ERK1/2 phosphorylation as a key event controlling KIM-1 regulation, and is activated through different pathways in different diseases.

To determine if ERK1/2 regulated KIM-1 at a physiological level, trametinib was administered to naïve mice. Although KIM-1 is expressed at very low levels in healthy non-injured kidneys, there is a physiological basal level of detection [3, 42]. In the absence of an injury, inhibiting physiological ERK1/2 phosphorylation resulted in the downregulation of KIM-1 mRNA. This observation correlates with our in vitro results that demonstrated trametinib treatment in mouse TK cells decreased KIM-1 mRNA. Phosphorylated Chk1 was not altered in the trametinib treated mice (data not shown). ERK1/2 phosphorylation was inhibited in the nuclear and cytosolic fractions of the kidney cortex, which decreased STAT3 Y705 and S727 phosphorylation in the nucleus. Therefore, less active STAT3 is able to bind to the KIM-1 promoter, corresponding to the KIM-1 mRNA reduction observed.

We have provided evidence that STAT3 phosphorylated at Y705 and S727 are partially responsible for renal KIM-1 upregulation, and that ERK1/2 involvement is upstream of STAT3. These findings provide further evidence that initial ERK1/2 activation is a key regulator of various pathways following renal injury, which may lead to the discovery of potential pharmacological based therapies.

REFERENCES

1. Amin, R.P., et al., *Identification of putative gene based markers of renal toxicity.* Environ Health Perspect, 2004. **112**(4): p. 465-79.
2. Vaidya, V.S., et al., *Kidney injury molecule-1 outperforms traditional biomarkers of kidney injury in preclinical biomarker qualification studies.* Nat Biotechnol, 2010. **28**(5): p. 478-85.
3. Ichimura, T., et al., *Kidney injury molecule-1 (KIM-1), a putative epithelial cell adhesion molecule containing a novel immunoglobulin domain, is up-regulated in renal cells after injury.* J Biol Chem, 1998. **273**(7): p. 4135-42.
4. Ichimura, T. and S. Mou, *Kidney injury molecule-1 in acute kidney injury and renal repair: a review.* Zhong Xi Yi Jie He Xue Bao, 2008. **6**(5): p. 533-8.
5. Khandrika, L., et al., *Kidney injury molecule-1 is up-regulated in renal epithelial cells in response to oxalate in vitro and in renal tissues in response to hyperoxaluria in vivo.* PLoS One, 2012. **7**(9): p. e44174.
6. Tian, L., et al., *Kidney Injury Molecule-1 is Elevated in Nephropathy and Mediates Macrophage Activation via the Mapk Signalling Pathway.* Cell Physiol Biochem, 2017. **41**(2): p. 769-783.
7. Han, W.K., et al., *Human kidney injury molecule-1 is a tissue and urinary tumor marker of renal cell carcinoma.* J Am Soc Nephrol, 2005. **16**(4): p. 1126-34.
8. Bailly, V., et al., *Shedding of kidney injury molecule-1, a putative adhesion protein involved in renal regeneration.* J Biol Chem, 2002. **277**(42): p. 39739-48.
9. Gandhi, R., et al., *Accelerated receptor shedding inhibits kidney injury molecule-1 (KIM-1)-mediated efferocytosis.* Am J Physiol Renal Physiol, 2014. **307**(2): p. F205-21.
10. Zhang, Z., B.D. Humphreys, and J.V. Bonventre, *Shedding of the urinary biomarker kidney injury molecule-1 (KIM-1) is regulated by MAP kinases and juxtamembrane region.* J Am Soc Nephrol, 2007. **18**(10): p. 2704-14.
11. Ichimura, T., et al., *Kidney injury molecule-1 is a phosphatidylserine receptor that confers a phagocytic phenotype on epithelial cells.* J Clin Invest, 2008. **118**(5): p. 1657-68.
12. Arany, I., et al., *Cisplatin-induced cell death is EGFR/src/ERK signaling dependent in mouse proximal tubule cells.* Am J Physiol Renal Physiol, 2004. **287**(3): p. F543-9.
13. Masaki, T., et al., *Activation of the ERK pathway precedes tubular proliferation in the obstructed rat kidney.* Kidney Int, 2003. **63**(4): p. 1256-64.
14. Masaki, T., et al., *Activation of the extracellular-signal regulated protein kinase pathway in human glomerulopathies.* J Am Soc Nephrol, 2004. **15**(7): p. 1835-43.
15. Collier, J.B., et al., *Rapid Renal Regulation of Peroxisome Proliferator-activated Receptor gamma Coactivator-1alpha by Extracellular Signal-Regulated Kinase 1/2 in Physiological and Pathological Conditions.* J Biol Chem, 2016. **291**(52): p. 26850-26859.
16. Smith, J.A., et al., *Suppression of mitochondrial biogenesis through toll-like receptor 4-dependent mitogen-activated protein kinase kinase/extracellular signal-regulated kinase signaling in endotoxin-induced acute kidney injury.* J Pharmacol Exp Ther, 2015. **352**(2): p. 346-57.
17. Yamaguchi, T., et al., *Antitumor activities of JTP-74057 (GSK1120212), a novel MEK1/2 inhibitor, on colorectal cancer cell lines in vitro and in vivo.* Int J Oncol, 2011. **39**(1): p. 23-31.

18. Gilmartin, A.G., et al., *GSK1120212 (JTP-74057) is an inhibitor of MEK activity and activation with favorable pharmacokinetic properties for sustained in vivo pathway inhibition.* Clin Cancer Res, 2011. **17**(5): p. 989-1000.
19. Smith, J.A., P.R. Mayeux, and R.G. Schnellmann, *Delayed Mitogen-Activated Protein Kinase/Extracellular Signal-Regulated Kinase Inhibition by Trametinib Attenuates Systemic Inflammatory Responses and Multiple Organ Injury in Murine Sepsis.* Crit Care Med, 2016. **44**(8): p. e711-20.
20. Zhang, Z. and C.X. Cai, *Kidney injury molecule-1 (KIM-1) mediates renal epithelial cell repair via ERK MAPK signaling pathway.* Mol Cell Biochem, 2016. **416**(1-2): p. 109-16.
21. Ajay, A.K., et al., *A bioinformatics approach identifies signal transducer and activator of transcription-3 and checkpoint kinase 1 as upstream regulators of kidney injury molecule-1 after kidney injury.* J Am Soc Nephrol, 2014. **25**(1): p. 105-18.
22. Berger, S.I., J.M. Posner, and A. Ma'ayan, *Genes2Networks: connecting lists of gene symbols using mammalian protein interactions databases.* BMC Bioinformatics, 2007. **8**: p. 372.
23. Lachmann, A. and A. Ma'ayan, *KEA: kinase enrichment analysis.* Bioinformatics, 2009. **25**(5): p. 684-6.
24. Ernest, S. and E. Bello-Reuss, *Expression and function of P-glycoprotein in a mouse kidney cell line.* Am J Physiol, 1995. **269**(2 Pt 1): p. C323-33.
25. MacKay, K., et al., *Glomerular epithelial, mesangial, and endothelial cell lines from transgenic mice.* Kidney Int, 1988. **33**(3): p. 677-84.
26. Funk, J.A. and R.G. Schnellmann, *Persistent disruption of mitochondrial homeostasis after acute kidney injury.* Am J Physiol Renal Physiol, 2012. **302**(7): p. F853-64.
27. Ellett, J.D., et al., *Toll-like receptor 4 is a key mediator of murine steatotic liver warm ischemia/reperfusion injury.* Liver Transpl, 2009. **15**(9): p. 1101-9.
28. Singh, A. and Y.J. Xu, *The Cell Killing Mechanisms of Hydroxyurea.* Genes (Basel), 2016. **7**(11).
29. Nowak, G., et al., *Activation of ERK1/2 pathway mediates oxidant-induced decreases in mitochondrial function in renal cells.* Am J Physiol Renal Physiol, 2006. **291**(4): p. F840-55.
30. Sabbisetti, V.S., et al., *Blood kidney injury molecule-1 is a biomarker of acute and chronic kidney injury and predicts progression to ESRD in type I diabetes.* J Am Soc Nephrol, 2014. **25**(10): p. 2177-86.
31. Vaidya, V.S., et al., *Urinary kidney injury molecule-1: a sensitive quantitative biomarker for early detection of kidney tubular injury.* Am J Physiol Renal Physiol, 2006. **290**(2): p. F517-29.
32. Talbot, J.J., et al., *Polycystin-1 regulates STAT activity by a dual mechanism.* Proc Natl Acad Sci U S A, 2011. **108**(19): p. 7985-90.
33. Brosius, F.C., 3rd and J.C. He, *JAK inhibition and progressive kidney disease.* Curr Opin Nephrol Hypertens, 2015. **24**(1): p. 88-95.
34. Nechemia-Arbely, Y., et al., *IL-6/IL-6R axis plays a critical role in acute kidney injury.* J Am Soc Nephrol, 2008. **19**(6): p. 1106-15.
35. Zhou, L., et al., *Activation of p53 promotes renal injury in acute aristolochic acid nephropathy.* J Am Soc Nephrol, 2010. **21**(1): p. 31-41.
36. Takakura, A., et al., *Pyrimethamine inhibits adult polycystic kidney disease by modulating STAT signaling pathways.* Hum Mol Genet, 2011. **20**(21): p. 4143-54.

37. Pang, M., et al., *A novel STAT3 inhibitor, S3I-201, attenuates renal interstitial fibroblast activation and interstitial fibrosis in obstructive nephropathy.* Kidney Int, 2010. **78**(3): p. 257-68.
38. Gu, L., et al., *Deletion of podocyte STAT3 mitigates the entire spectrum of HIV-1-associated nephropathy.* Aids, 2013. **27**(7): p. 1091-8.
39. Gough, D.J., L. Koetz, and D.E. Levy, *The MEK-ERK pathway is necessary for serine phosphorylation of mitochondrial STAT3 and Ras-mediated transformation.* PLoS One, 2013. **8**(11): p. e83395.
40. Kanai, M., et al., *Differentiation-inducing factor-1 (DIF-1) inhibits STAT3 activity involved in gastric cancer cell proliferation via MEK-ERK-dependent pathway.* Oncogene, 2003. **22**(4): p. 548-54.
41. Booz, G.W., J.N. Day, and K.M. Baker, *Angiotensin II effects on STAT3 phosphorylation in cardiomyocytes: evidence for Erk-dependent Tyr705 dephosphorylation.* Basic Res Cardiol, 2003. **98**(1): p. 33-8.
42. van Timmeren, M.M., et al., *Tubular kidney injury molecule-1 in protein-overload nephropathy.* Am J Physiol Renal Physiol, 2006. **291**(2): p. F456-64.

CHAPTER FOUR:

ERK1/2 Regulates NAD^+ Metabolism During Acute Kidney Injury Through microRNA-34a-Mediated NAMPT Expression

ABSTRACT

Prior studies have established the important role of extracellular signal-regulated kinase 1/2 (ERK1/2) as a mediator of acute kidney injury (AKI). We demonstrated rapid ERK1/2 activation induced renal dysfunction following ischemia/reperfusion (IR)-induced AKI and downregulated the mitochondrial biogenesis (MB) regulator, peroxisome proliferator-activated receptor γ coactivator-1α (PGC-1α) in mice. In this study, ERK1/2 regulation of cellular NAD^+ and PGC-1α were explored. Inhibition of ERK1/2 activation using the MEK1/2 inhibitor, trametinib, attenuated renal cortical NAD^+ depletion after AKI in mice. The rate-limiting NAD biosynthesis salvage enzyme, NAMPT, decreased following AKI, and this decrease was prevented by ERK1/2 inhibition. The microRNA miR-34a decreased with the inhibition of ERK1/2, leading to increased NAMPT protein. Treating mice with a miR34a mimic prevented increases in NAMPT protein in the renal cortex in the presence of ERK1/2 inhibition. In addition, ERK1/2 activation increased acetylated PGC-1α, the less active form, whereas inhibition of ERK1/2 activation prevented an increase in acetylated PGC-1α after AKI through SIRT1 and NAD^+ attenuation. These results implicate IR-induced ERK1/2 activation as an important contributor to the downregulation of both PGC-1α and NAD^+ pathways that ultimately decrease cellular metabolism and renal function. Inhibition of ERK1/2 activation prior to the initiation of IR injury attenuated decreases in PGC-1α and NAD^+ and prevented kidney function.

INTRODUCTION

Extracellular regulated kinases 1/2 (ERK1/2) are protein-serine/threonine kinases that are activated through phosphorylation by the upstream mitogen-activated protein kinase kinase 1/2 (MEK1/2) [1, 2]. This signaling pathway is initiated by various extracellular stimuli and intracellular signaling that ultimately targets several physiological and pathological pathways [3, 4]. Many reviews have covered the cellular processes that ERK1/2 is known to participate, such as proliferation, differentiation, cell survival, migration, death, and metabolism [2, 5-9]. Because ERK1/2 regulates a broad array of processes, and many of these processes are seemingly opposite in nature, context is very important in ERK1/2 signaling.

We previously demonstrated rapid ERK1/2 activation following renal ischemia-reperfusion (IR) injury downregulates mitochondrial biogenesis (MB) by decreasing PGC-1α, the master regulator of MB, and the downstream targets of MB expression in renal cortical epithelial cells [10]. This is especially relevant as epithelial cells of the proximal tubules have a high mitochondrial content to produce ATP that drives various transport processes. This is not unique to the epithelial cells of the kidney, as the epithelium of the intestine, lung (alveolar type II cell), and the liver (hepatocytes) require mitochondria for their energy demands [11-14]. To meet the energy demands, renal proximal tubules rely on mitochondrial oxidative phosphorylation exclusively and any mitochondrial dysfunction can disrupt the energy balance resulting in cellular injury/death and prevent recovery from injury [15, 16].

PGC-1α is a transcriptional coactivator involved in the regulation of cellular and mitochondrial metabolism through a number of pathways that include MB,

mitochondrial dynamics, and mitophagy [17-19]. PGC-1α is enriched in tissues with high mitochondrial content and energy demands, such as the heart, skeletal muscle, and kidney [20-22]. Specifically, PGC-1α is highly expressed in the renal cortical epithelial cells and has been demonstrated to play a vital protective role in multiple diverse renal diseases, including sepsis, IR injury, diabetes, and fibrosis [19].

Using the potent and specific MEK1/2 inhibitor, trametinib, we blocked ERK1/2 phosphorylation in the kidney of naive mice and observed increases in PGC-1α and downstream targets of PGC-1α, including nuclear-encoded mitochondrial transcription factor A (TFAM) and nuclear respiratory factor-1 (NRF1), and the mitochondrial-encoded electron transport chain protein cytochrome c oxidase I (COX1) [10]. ERK1/2 activation due to IR injury was inhibited by trametinib pretreatment, and attenuated PGC-1α mRNA and protein loss, ultimately preventing a rise in serum creatinine, a marker of renal dysfunction. Similarly, ERK1/2 inhibition also prevented the downregulation of renal PGC-1α in a lipopolysaccharide (LPS)-induced sepsis model in mice and attenuated kidney dysfunction [23].

Overexpression of PGC-1α in cultures of primary rabbit renal proximal tubule epithelial cells (RPTC) promoted mitochondrial and cellular recovery following oxidant injury [24]. Similar results were obtained in RPTC using a pharmacological compound, formoterol, which acts through the β_2-adrenergic receptor to increase PGC-1α expression leading to an increase in maximal oxygen consumption rate and MB. *In vivo* PGC-1α upregulation using formoterol increased mitochondrial electron transport chain proteins and improved renal recovery following IR injury [25, 26].

NAD^+ is a vital coenzyme used in cellular energy metabolism, redox signaling, and contributes to overall cellular health [27, 28]. NAD^+ is often depleted during injury or disease, and restoration or prevention of this depletion averts worsening injury and often promotes recovery [29]. The kidney is highly susceptible to NAD^+ depletion as it has the lowest NAD^+ half-life at ~30 min, yet is also among the highest NAD^+ containing organs [30].

Tran et al. reported a connection between PGC-1α and nicotinamide adenine dinucleotide (NAD) metabolism [31, 32]. Utilizing both PGC-1α knockout and overexpressing transgenic mice, the group determined that PGC-1α is required for less severe AKI, including improved renal recovery and increased survival. Additionally, the group found that PGC-1α-mediated AKI protection was largely due to the prevention of NAD^+ depletion through upregulation of the de novo NAD^+ pathway. Exogenous nicotinamide (NAM) administered to PGC-1α KO mice improved renal function after injury by increasing the NAD^+ pool [31].

The importance of NAD^+ in the kidney was also confirmed by Guan et al., by preventing NAD^+ depletion and renal dysfunction in both cisplatin and IR injury-induced AKI in 3 and 20 month old mice by administering nicotinamide mononucleotide (NMN), a NAD^+ precursor [33]. NMN also restored NAD^+ and SIRT1 levels [33]. Age associated AKI microarray data pointed to MAPK signaling as an important contributor following cisplatin injury, possibly connecting MAPK signaling and NAD. However, less is known about the interactions between ERK1/2 and NAD^+ metabolism in the proximal tubules and kidney. Considering the important roles of ERK1/2, PGC-1α, and NAD^+ physiologically and pathologically, and our previous

reports of ERK1/2 regulation on renal PGC-1α, we hypothesized early ERK1/2 activation following IR-induced AKI regulates NAD^+ metabolism.

MATERIALS AND METHODS

In Vitro Studies.

Female New Zealand White rabbits (2 kg) were purchased from Charles River (Oakwood, MI/Canada). Renal proximal tubule cells (RPTC) were isolated using the iron oxide perfusion method and grown in 35-mm tissue culture dishes under improved conditions similar to what is observed in vivo [34]. The culture medium was a 1:1 mixture of Dulbecco's modified Eagle's medium/F-12 (without glucose, phenol red, or sodium pyruvate) supplemented with 15 mM HEPES buffer, 2.5 mM L-glutamine, 1 uM pyridoxine HCl, 15 mM sodium bicarbonate, and 6 mM lactate. Hydrocortisone (50 nM), selenium (5 ng/ml), human transferrin (5 ug/ml), bovine insulin (10 nM), and L-ascorbic acid-2-phosphate (50 uM) were added to fresh culture medium. Confluent RPTC were used for all experiments. RPTC monolayers were treated with various compounds or vehicle (DMSO).

Naïve and AKI Studies.

Trametinib (GSK1120212 [35]) was purchased from Selleckchem Chemicals (Houston, TX). Eight-to-nine week old male C57BL/6 mice (20–25 g) were acquired from Charles River Laboratories (Frederick, MD) and received an injection of trametinib (1 mg/kg) or vehicle control (NEOBEE M-5 – Fisher Scientific) intraperitoneally (ip). Four hr after injection, kidneys were collected and flash frozen in liquid nitrogen for further analysis.

For IRI-induced AKI, mice were assigned to 3 groups: 1) Sham, 2) IR + Vehicle, 3) IR + trametinib. Vehicle or trametinib were administered ip 1 hr before surgery. In some experiments (Figure 3.5), mice were pretreated 48 and 24 hr before IR surgery with vehicle, FK866 (20 mg/kg) (Selleckchem) [S2799], or NMN (500 mg/kg) (Sigma-Aldrich) [N3501] by ip injection [36]. IRI mice were subjected to ischemia/reperfusion surgery by bilateral renal pedicle clamping for 18.5 min as described previously [37]. Briefly, the renal artery and vein were isolated and blood flow was occluded with a vascular clamp while maintaining a constant body temperature of 36.5~37.5°C. Sham mice were treated the same as IRI mice, except the renal pedicles were not clamped. Mice were euthanized at 3 or 24 hr after surgery, and blood and kidneys (flash frozen in liquid nitrogen) were collected for analysis.

Retro-Orbital Injection of microRNA 34a Mimic.

Polyplus transfection (Illkirch, France) delivery reagent, in vivo-jetPEI, was used for delivering microRNA 34a mimic to the kidney. Preparation of delivery reagent was carried out according to manufacturer's instructions. A 5% glucose solution mixed with

in vivo-jetPEI was added to a 5% glucose solution containing mirVana miRNA 34a mimic. Combined solutions were vortexed and allowed to incubate at RT for 15-20 min. Retro-orbital injection was performed using a solution containing 40 ug of miR34a mimic and a N/P ratio of 8. An ip injection of vehicle control (NEOBEE M-5) or trametinib (1 mg/kg) was administered 2 hr later. Mice were euthanized 6 hr following retro-orbital injection. Mice were assigned 3 groups: 1) jetPEI (retro-orbital) + Vehicle (ip), 2) miR34a mimic + Vehicle, 3) miR34a mimic + trametinib.

Serum Creatinine Measurement.

Serum creatinine (SCr) was determined using the Creatinine Enzymatic Reagent Assay kit (Pointe Scientific, Canton, MI) [c7548-120] based on the manufacturer's directions. All values are expressed as serum creatinine concentration in milligrams per deciliter.

RT-qPCR Analysis of mRNA and microRNA Expression.

Total RNA was isolated from renal cortical tissue with TRIzol reagent (Life Technologies). The iScript Advanced cDNA Synthesis Kit (Bio-Rad) was used according to the manufacturer's protocol. The generated cDNA was used with the SsoAdvanced Universal SYBR Green Supermix reagent (Bio-Rad). The relative mRNA expression of all genes was determined by the $2^{-\Delta\Delta Ct}$ method, and mouse actin RNA and rabbit tubulin RNA were used as reference genes for normalization (see Table 1 for Primer pairs). For microRNA the MystiCq microRNA cDNA synthesis kit was used according to the manufacturer's instructions (Sigma-Aldrich) [MIRRT]. MystiCq

SYBR green (Sigma-Aldrich) [MIRRM00] and universal PCR primer (Sigma-Aldrich) [MIRUP] were used for RT-qPCR. The relative microRNA expression was determined by the $2^{-\Delta\Delta Ct}$ method, and the mouse small nucleolar RNA, SNORD48 was used as a reference small non-coding RNA for normalization (Sigma-Aldrich) [MIRCP00007].

Immunoblot Analysis.

Protein was extracted from renal cortex using RIPA assay buffer (50 mM Tris-HCl, 150 mM NaCl, 0.1% SDS, 0.5% sodium deoxycholate, 1% Triton X-100, pH 7.4). Protease inhibitor cocktail (1:100), 1 mM sodium fluoride, and 1 mM sodium orthovanadate (Sigma-Aldrich) and nicotinamide and 4-phenylbutyrate were added fresh before each extraction.

Equal protein quantities (10–60 μg) were loaded onto 4–15% SDS-PAGE gels, resolved by gel electrophoresis, and transferred onto nitrocellulose membranes (Bio-Rad). Membranes were blocked in 5% bovine serum albumin or 5% milk in TBST and incubated overnight with primary antibody at 4°C with gentle agitation. Primary antibodies used in these studies included phospho-ERK1/2 (1:1000) [#4370], total ERK1/2 (1:1000) [#4695]. β-actin (1:2000; Santa Cruz Biotechnology, Dallas, TX) [sc-47778].

Membranes were incubated with the appropriate horseradish peroxidase–conjugated secondary antibody before visualization using enhanced chemiluminescence (Thermo Scientific) and the GE ImageQuant LAS4000 (GE Life Sciences). Optical density was determined using the ImageJ software from NIH and Image Studio Lite from LI-COR.

Immunoprecipitation.

Following protein extraction, protein quantification was performed using Pierce 660 nm Assay (ThermoFisher Scientific) [22660]. Equal amounts of protein from every group were utilized according to the instructions from Dynabeads Protein G Immunoprecipitation Kit (ThermoFisher Scientific). Immunoprecipitation was

performed using acetylated-lysine antibody (1:100; Cell Signaling) [#9441]. PGC-1α antibody (1:1000; abcam) [ab54481] was used for immunoblotting pull-down and input. Veriblot (1:400; abcam) [ab131366] was used for detection of immunoblotted target protein before visualization using enhanced chemiluminescence (Thermo Scientific) and the GE ImageQuant LAS4000 (GE Life Sciences).

Respirometry Assay:

Oxygen consumption rate (OCR) was determined using a Seahorse Bioscience XF-96 instrument as previously described (20465991). RPTC were plated at 18,000 cells per well and grown for 36 hr before a 24 hr treatment. The XF-96 protocol consists of five measurements of basal OCR (1 measurement/2.5 min), injection of carbonyl cyanide-4-(trifluoromethoxy) phenylhydrazone (FCCP) (Sigma) [#C2920], and four measurements of uncoupled OCR (1 measurement/2.5 min).

NAD^+ and NADH measurement.

Quantification of NAD^+ and NADH were carried out using the NAD/NADH Assay Kit (abcam) [#ab65348] according to the manufacturer's instructions. NAD^+ and NADH values were normalized to kidney cortex wet weight.

NAMPT Activity Assay.

To quantify the enzymatic activity of NAMPT in kidney cortex, protein extracts were assayed according to the manufacturer's instructions using the Cyclex NAMPT Colorimetric Assay Kit (MBL International) [#CY-1251].

Statistical Analysis.

All data are shown as mean ± S.E.M. When comparing two experimental groups, an unpaired, two-tailed t test or Mann-Whitney U was used to determine statistical differences. A one-way analysis of variance (ANOVA) followed by Tukey's post hoc test was performed for comparisons of multiple groups. $P < 0.05$ was considered statistically significant. All statistical tests were performed using GraphPad Prism software (GraphPad Software, San Diego, CA).

RESULTS

ERK1/2 Inhibition Prevents IR-Induced Downregulation of PGC-1α and Downstream MB Targets, and Attenuates Kidney Dysfunction.

The effect of ERK1/2 activation and inhibition on PGC-1α signaling in the renal cortex 24 hr after renal IR injury was examined. We previously demonstrated the potent and selective MEK1/2 inhibitor trametinib blocks ERK1/2 activation in this model [10] and confirmed ERK1/2 phosphorylation increased in the IR group and was blocked by trametinib, without a change in total ERK1/2 (Figure 4.1A). PGC-1α mRNA and protein decreased ~70% and ~55%, respectively, 24 hr after IR injury (Figure 4.1 B,C). Pretreatment with trametinib 1 hr before IR injury partially prevented this decrease in PGC-1α mRNA and protein at 24 hr (Figure 4.1 B,C). MB proteins involved in PGC-1α signaling and the mitochondrial electron transport chain such as nuclear-encoded NDUFS1 and NDUFB8, and the mitochondrial-encoded COX1 decreased after IR injury and were completely attenuated by trametinib pretreatment (Figure 4.1 A,B). Specific downstream transcriptional targets of PGC-1α, including TFAM, superoxide dismutase 2 (SOD2), and forkhead box protein O1 (FOXO1) mRNA, that were previously demonstrated to be regulated by ERK1/2 [10] were reduced ~70% after 24 hr and was partially attenuated by trametinib (Figure 4.1 C). In addition, the renal dysfunction marker, serum creatinine, increased ~10-fold after IR and trametinib completely prevented the increase in serum creatinine, and the loss of renal function in response to IR injury (Figure 4.1 D). PGC-1α signaling has been shown to play a critical role in MB, and preventing and restoring renal function in settings of AKI [10, 25, 31, 38]. MB proteins and mRNA were consistently decreased 24 hr after injury and

trametinib pretreatment partially or completely prevented the decreases, ultimately, preventing a rise in serum creatinine.

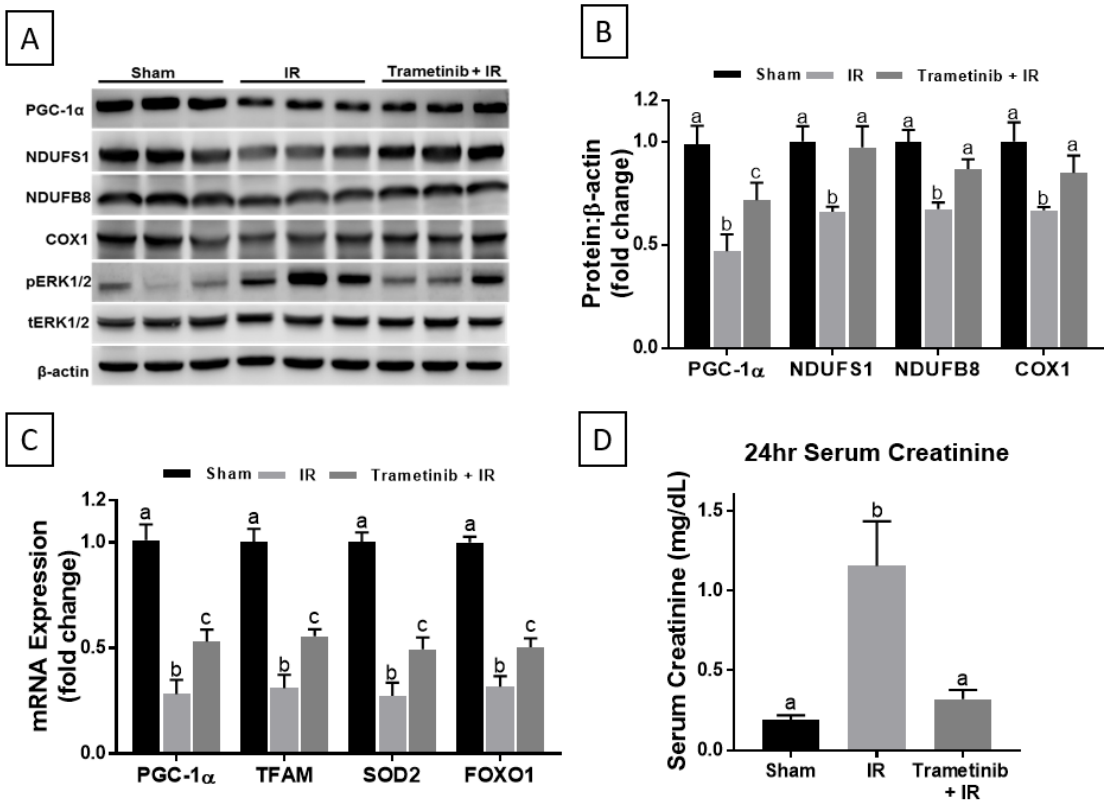

Figure 4.1: ERK1/2 Inhibition Prevents IR-Induced Downregulation of PGC-1α and Downstream MB Targets, and Attenuates Kidney Dysfunction. A) Representative immunoblot of phosphorylated ERK1/2 and PGC-1α following 24 hr of IR AKI. B) Densitometry analysis of PGC-1α, NDYFS1, NDUFB8 and COX1. C) PGC-1α mRNA expression following IR AKI after 24 hr. D) Serum creatinine was assessed 24 hr after IR AKI. Data are represented as mean ± S.E.M., $n \geq 4$. Different superscripts indicate statistically significant differences ($P < 0.05$), where 'b' is different from 'a' and 'c' is different from 'a' and 'b'.

ERK1/2 Inhibition Attenuates PGC-1α Acetylation Increases Following 24 hr AKI. Because PGC-1α acetylation status alters its activity, particularly following an acute injury [39-42], we used acetylated-lysine immunoprecipitation to look at PGC-1α acetylation. In the IR group, PGC-1α was more acetylated, meaning less active, compared to the sham group (Figure 4.2 A). However, in the trametinib + IR group there was less acetylated PGC-1α compared to the IR group and not different than the sham group (Figure 4.2 A). PGC-1α is a major target of deacetylation [43, 44] for the NAD-dependent deacetylase, SIRT1. SIRT1 deacetylation of PGC-1α has been reported to play a critical role during AKI [39, 40]. After IR injury SIRT1 protein was decreased and this decrease was prevented in the trametinib + IR group (Figure 4.2 B). SIRT1 mRNA was downregulated at 24 hr after IR injury and was not altered in the trametinib + IR group (Figure 4.2 B). These results reveal that trametinib pretreatment preserves PGC-1α in a more active state by preventing PGC-1α acetylation following 24 hr IR injury and may be explained by the prevention of SIRT1 protein loss due to trametinib.

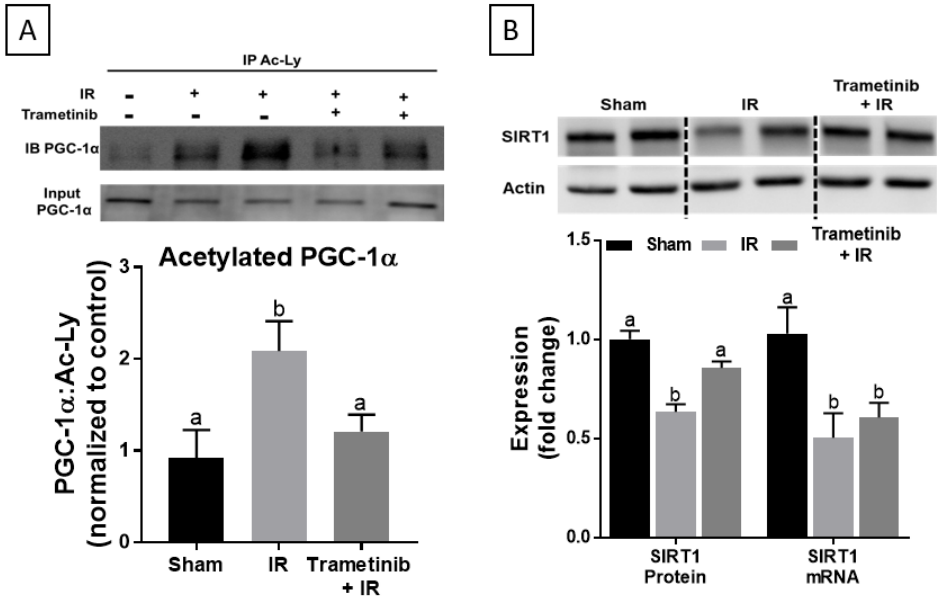

Figure 4.2: ERK1/2 Inhibition Attenuates PGC-1α Acetylation Increases Following 24 hr AKI. A) Representative immunoblot of PGC-1α following IP of acetylated lysine. B) Representative immunoblot of SIRT1, and analysis of SIRT1 protein and mRNA. Data are represented as mean ± S.E.M., n ≥ 4. Different superscripts indicate statistically significant differences ($P < 0.05$).

ERK1/2 Inhibition Attenuated NAD^+ Loss After 24 hr IR Injury but Not at 3 hr.

As SIRT1 enzymatic activity is dependent on the availability of cellular NAD^+, we examined the effect of ERK1/2 activation and inhibition on NAD^+ metabolism in the renal cortex following renal IR injury [45]. At 3 and 24 hr after renal IR injury trametinib pretreatment blocked ERK1/2 phosphorylation (Figure 4.1 A; Fig 4.3 A). NAD^+ and NADH did not change at 3 hr following IR injury in any group, however the ratio trended up in the trametinib + IR group (Figure 4.3 B-D). At 24 hr, NAD^+ and NADH decreased ~50% with no change in the NAD^+:NADH ratio in response to IR injury alone (Figure 4.3 E-G). Pretreatment with trametinib 1 hr before IR injury partially prevented the decrease of NAD^+ without a change in NADH loss, resulting in a marked increase in the NAD^+:NADH ratio (Figure 4.3 E-G). These results reveal that ERK1/2 plays a role in NAD+ metabolism during IR injury and inhibiting ERK1/2 attenuates the NAD^+ loss.

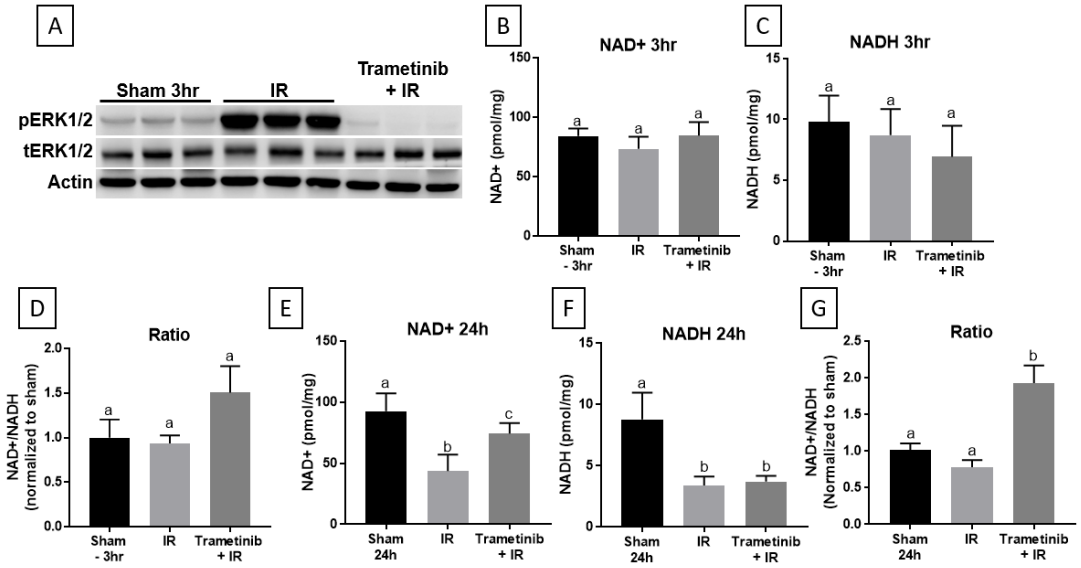

Figure 4.3: ERK1/2 Inhibition Attenuated NAD+ Loss After 24 hr IR Injury but Not at 3 hr. A) Representative immunoblot of pERK1/2 and tERK1/2 after IR AKI at 3 hr. B, C, E, F) NAD^+ and NADH Measurement after IR AKI at 3 and 24 hr in renal cortex. D, G) Ration of NAD^+/NADH analyzed after IR AKI at 3 and 24 hr. Data are represented as mean ± S.E.M., n ≥ 5. Different superscripts indicate statistically significant differences ($P < 0.05$).

ERK1/2 Activation Following IR Decreases NAMPT Protein and Trametinib Prevents IR-Induced NAMPT Loss.

To elucidate the mechanism of ERK1/2-mediated NAD+ and NADH loss in renal IR injury, protein and mRNA levels of the enzymes responsible for NAD^+ biosynthesis were measured (Fig 4.7 -Visual abstract). NAMPT protein was measured 3 and 24 hr after IR injury and no change was observed at 3 hr (Figure 4.4 A); however, at 24 hr NAMPT protein was decreased 50% compared to sham mice (Figure 4.4 B, C). Trametinib pretreatment increased NAMPT protein compared to the IR group at 3 hr (Figure 4.4 A), and at 24 hr prevented the NAMPT protein loss observed in the IR group (Figure 4.4 B, C).

Protein levels for the three enzymes responsible for conversion of NMN to NAD+ revealed that only NMNAT1 was decreased in the IR group and that trametinib prevented this decrease (Figure 4.4 B, C). NMNAT2 and NMNAT3 proteins were not changed in the IR group nor trametinib + IR group (Figure 4.4 B, C). The activity of NAMPT did not change in the IR and trametinib + IR group compared to sham activity (Figure 4.4 E). These results reveal that ERK1/2 inhibition increases NAMPT early after IR injury and prevents NAMPT and NMNAT1 protein loss 24 hr after IR injury. As both NAMPT and NMNAT1 contribute to NAD synthesis, and NAMPT is the rate-limiting enzyme in the salvage pathway (Figure 4.7 - Visual abstract) [46], and the salvage pathway is responsible for greater than 99% of the total NAD synthesis [30], ERK1/2 mediated NAD+ loss is the result of NAMPT and NMNAT1 protein loss.

To determine if the decrease in NAMPT and NMNAT1 proteins was the result of decreased transcription, mRNA of the respective proteins were measured. Both vehicle

and trametinib-treated IR groups exhibited ~60% reduction in NAMPT and NMNAT1 mRNA at 24 hr (Figure 4.4 D). Thus, ERK1/2 inhibition did not restore NAMPT and NMNAT1 mRNA but did restore protein (Figure 4.4 C), suggesting that ERK1/2 regulates these enzymes independent of transcription. Other NAD^+ salvage enzymes, NMNAT3 and NRK1, and the important NAD de novo enzyme, QPRT, also exhibited marked decreases in mRNA levels in the IR and trametinib + IR groups [47] (Figure 4.4 D). These results demonstrate that following IR injury the synthesis of key NAD^+ metabolizing enzyme mRNA are substantially decreased.

The microRNA, miR34a, can directly bind to the 3'-UTR of NAMPT mRNA and regulate NAMPT protein expression, and are inversely correlated [48]. Because NAMPT protein was increased at 3 hr and attenuated at 24 hr in the trametinib + IR group (Figure 4.4 A,B), miR34a was measured. At 3 hr miR34a levels decreased in the trametinib + IR group and were not altered in the 3 hr IR group (Figure 4.4 F). At 24 hr following IR injury, miR34a levels were still decreased in the trametinib + IR group compared to the sham and IR groups (Figure 4.4 G). These results correlate increased NAMPT protein when ERK1/2 is inhibited to decreased miR34a.

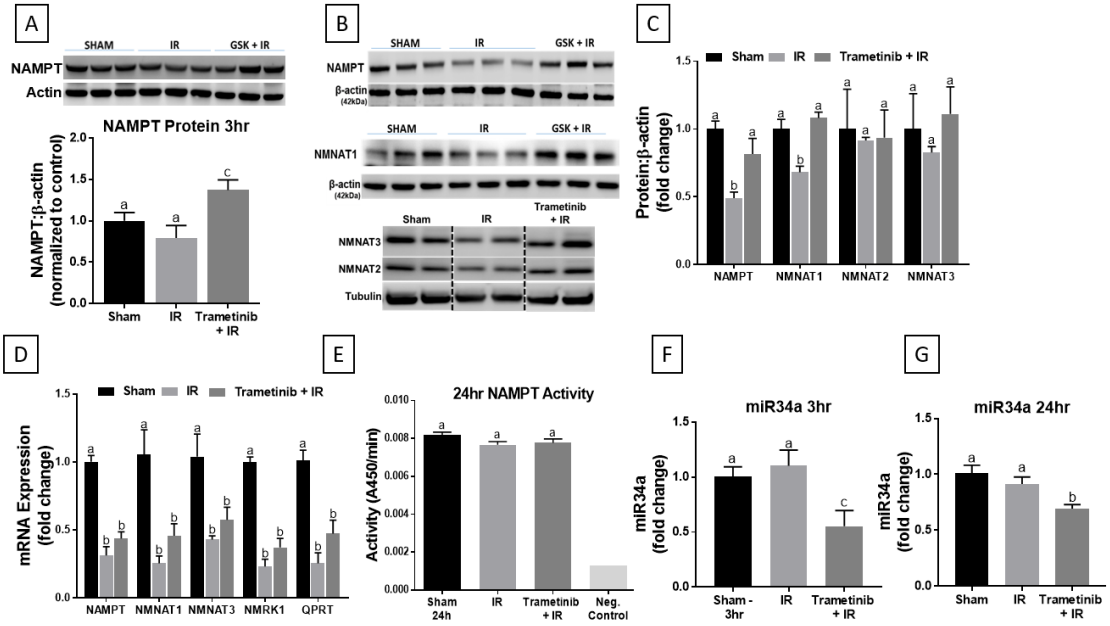

Figure 4.4: ERK1/2 Activation Following IR Decreases NAMPT Protein and Trametinib Prevents IR-Induced NAMPT Loss. A) Representative immunoblot and densitometry of NAMPT after IR AKI at 3 hr. B) Representative immunoblot of NAMPT, NMNAT1,2,3 after IR AKI at 24 hr. C) Densitometry analysis of NAMPT. D) mRNA expression measured for NAD biosynthetic pathway enzymes. E) Activity of NAMPT. F-G) miR34a expression measured after IR AKI at 3 and 24 hr. Data are represented as mean ± S.E.M., n ≥ 5. Different superscripts indicate statistically significant differences ($P < 0.05$).

ERK1/2 Physiologically Regulates miR34a. ERK1/2 Inhibition Decreases miR-34a, leading to increases in NAMPT Protein.

To examine if ERK1/2 also regulates miR34a and NAMPT protein at a physiological level we administered trametinib to naïve mice. Following a 4 hr trametinib treatment, ERK1/2 phosphorylation was completely inhibited in the renal cortex (Figure 4.5A). NAMPT protein increased 44% in the trametinib group compared to the control group, and NAMPT mRNA did not change (Figure 4.5A, B). Concurrently, miR34a expression decreased 40% in the trametinib treated group (Figure 4.5B). Interestingly, NAD^+ and NADH were not altered in response to the increased NAMPT protein (Figure 4.5C). These data reveal that ERK1/2 affects NAMPT and miR34a under physiological conditions and does so without changing NAD^+ and NADH content in mouse renal cortex.

To investigate whether ERK1/2 inhibition-induced increase in NAMPT protein is miR34a dependent, we utilized a miR34a mimic to prevent trametinib-induced decrease of miR34a. Naïve mice were treated with a mirVana miR34a mimic mixed with *in vivo*-jetPEI via retro-orbital injection to prevent trametinib treatment from decreasing miR34a [49]. The miR34a mimic increased miR34a levels in both the 34a mimic group and in the 34a mimic + trametinib group at least two-fold compared to vehicle (Figure 4.5D). Increasing miR34a levels in the cortex was not only able to prevent trametinib-induced NAMPT protein upregulation but also minimally decreased NAMPT protein in both the miR34a mimic group and the 34a + trametinib group (Figure 4.5E, F). In summary, ERK1/2 phosphorylation appears to regulate miR34a, and inhibition of ERK1/2 phosphorylation decreases miR34a, which leads to an increase in NAMPT

protein. This ERK1/2/miR34a/NAMPT pathway is prevented by increasing miR34a levels using a miR34a mimic, which prevented the trametinib-induced increase in NAMPT protein expression.

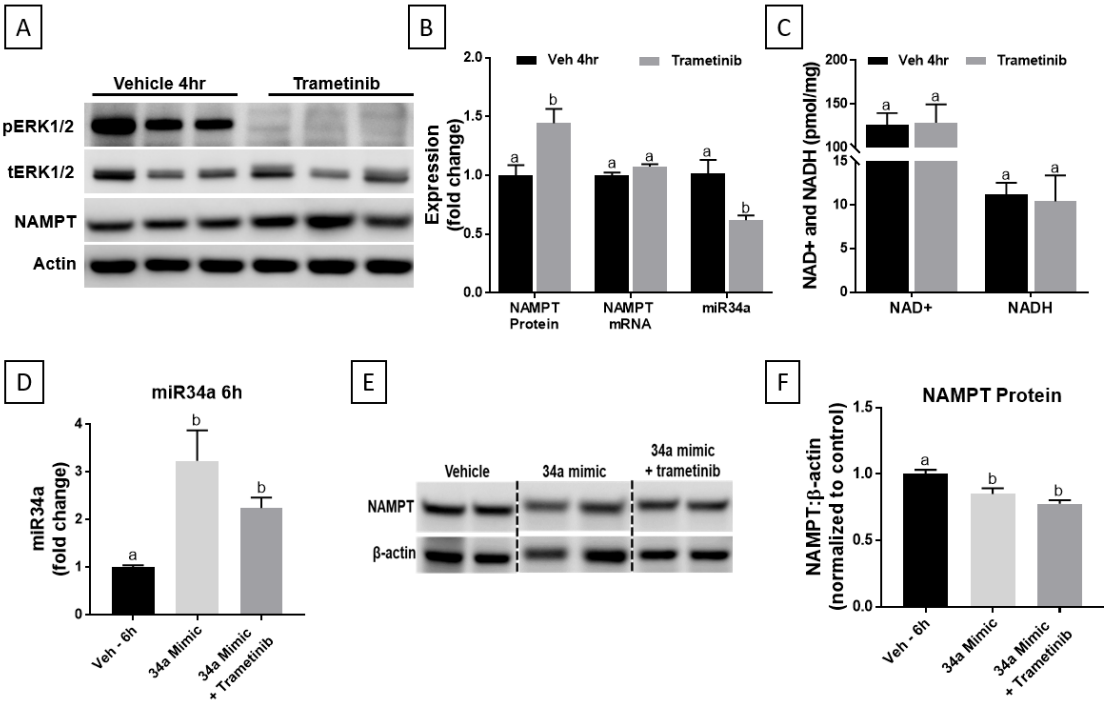

Figure 4.5: ERK1/2 Physiologically Regulates miR34a and ERK1/2 Inhibition Decreases miR-34a, leading to increases in NAMPT Protein. A) Representative immunoblot of pERK1/2, and NAMPT protein 4 hr after trametinib administration. B) Densitometry analysis of NAMPT protein, and mRNA and miRNA expression measurements of NAMPT and miR34a at 4 hr after trametinib treatment. C) NAD^+ and NADH content in renal cortex measured at 4 hr after trametinib treatment. D) miR34a expression after 34a mimic treatment in mice. E) Representative immunoblot of NAMPT protein after 34a mimic treatment in renal cortex. F) Densitometry analysis of NAMPT protein after 34a Mimic treatment. Data are represented as mean ± S.E.M., $n \geq 5$. Different superscripts indicate statistically significant differences ($P < 0.05$).

Trametinib-Induced Prevention of Serum Creatinine Elevation Following IR is Dependent on NAMPT Activity.

Because ERK1/2 inhibition increased NAMPT protein in a miR34a dependent pathway we sought to clarify the role that NAMPT protein contributes to trametinib-induced prevention of serum creatinine elevation in IR-induced AKI. We utilized the NAMPT inhibitor, FK866, [50, 51] and mice were pretreated before IR surgery with either vehicle or FK866 20 mg/kg [36]. Mice pretreated with trametinib were protected from IR-induced serum creatinine increases compared to the Veh + IR group (Figure 4.6 A). Mice pretreated with FK866 and subjected to IR exhibited did not have any effect on increased serum creatinine in the Veh + IR group. In contrast, mice pretreated with both FK866 and trametinib had the same increase in serum creatinine as the Veh + IR and FK866 + IR groups, and reversed the protective effect of trametinib (Figure 4.6 A). These results provide evidence that ERK1/2 inhibition by trametinib protects against IR-induced serum creatinine elevation after 24 hr by maintaining NAMPT and preventing NAD^+ decline following IR.

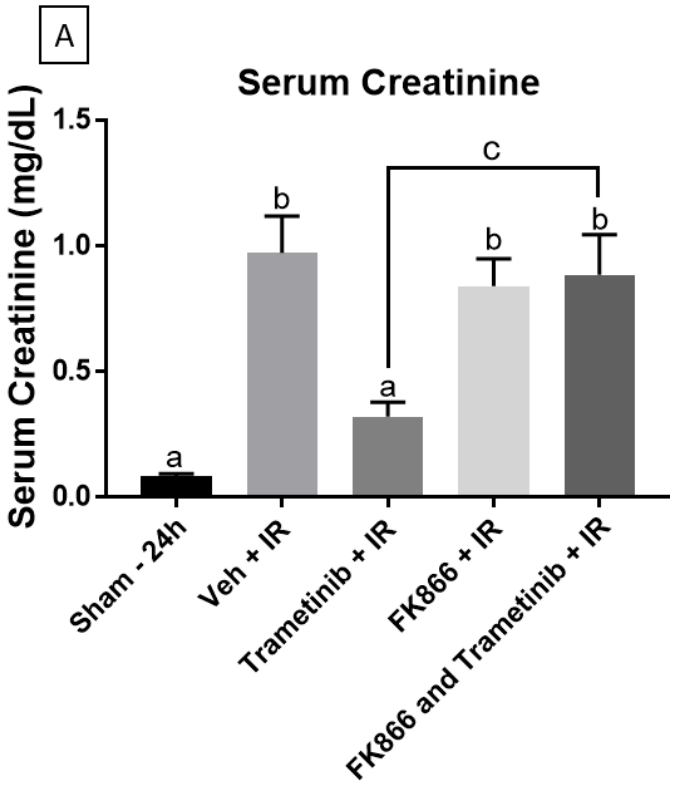

Figure 4.6: Trametinib-Induced Prevention of Serum Creatinine Elevation Following IR is Dependent on NAMPT Activity. A) Serum creatinine measurements following pretreatment with trametinib, FK866, and a combo of FK866 and trametinib after IR AKI at 24 hr. Data are represented as mean ± S.E.M., $n \geq 4$. Different superscripts indicate statistically significant differences ($P < 0.05$).

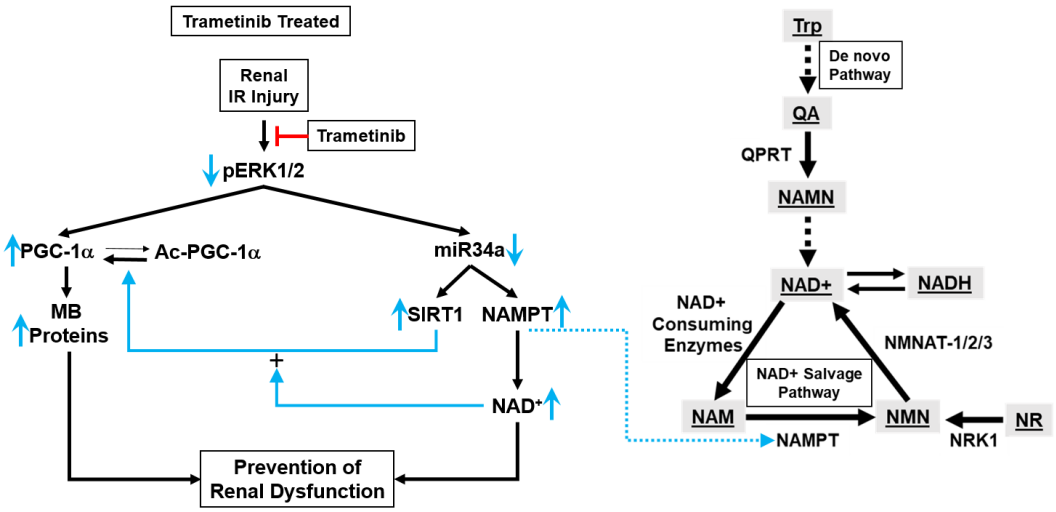

Figure 4.7: Visual Abstract. Proposed mechanism of trametinib-induced prevention of renal dysfunction following IR injury.

DISCUSSION

We have previously studied the role of ERK1/2 in PGC-1α signaling under physiological and pathological conditions and determined that early activation of ERK1/2 following renal IR injury was responsible for the initial decrease in PGC-1α mRNA expression, and correlated with kidney dysfunction [10]. Here, we have expanded our studies to understand the connection between ERK1/2 and NAD+ regulation under physiological and renal IR conditions, and in context with PGC-1α signaling. We determined that inhibition of ERK1/2 activation decreased miR34a, the microRNA regulator of both SIRT1 and NAMPT (Figure 4.7). The decrease in miR34a led to an increase in NAMPT protein under control conditions and attenuated the loss of NAMPT and SIRT1 after renal IR injury. Prevention of NAMPT loss attenuated decreases in NAD^+ following IR injury, and prevented PGC-1α acetylation through activation of SIRT1. Furthermore, this trametinib-induced miR34a/NAMPT regulation was prevented by pretreatment with a miR34a mimic, indicating increased NAMPT protein expression by ERK1/2 inhibition was dependent on miR34a.

Similar to our miR34a results, Choi SE et al., observed NAMPT protein regulation by miR34a in the liver of obese mice [48]. Hepatic NAMPT protein was lower in obese mice compared to controls, and was regulated by an increase in miR34a. SIRT1 was also shown to correspond with miR34a levels, as miR34a can bind to and repress NAMPT and SIRT1 mRNA translation [48, 52, 53]. ERK1/2 regulation of miR34a has not been well characterized; however, a few studies demonstrated that ERK1/2 phosphorylation is reduced as a result of a rise in miR34a expression [54, 55]. In liver

cancer, active ERK1/2 was shown to phosphorylate exportin-5, which led to a decrease in pre-miRNA export from the nucleus and a global reduction in miRNA [56]. However, a regulatory connection between a decrease in phosphorylated ERK1/2 and a decrease in miR34a expression, as reported in this study, has not been elucidated.

Because NAMPT protein increased at 4 hr after trametinib administration without any change in NAMPT mRNA, we conclude ERK1/2 inhibition rapidly decreases miR34a in the renal cortex and subsequently, induces an increase in NAMPT protein. Because NAMPT is the rate-limiting enzyme in the NAD^+ salvage pathway, and proximal tubules have been shown to have a high abundance of NAMPT [46, 57, 58], any prevention of the loss of this enzyme has the potential to directly impact the NAD^+ content and severity of the injury. As both Tran et al. and Guan et al. demonstrated within the kidney, NAD^+ levels can directly influence AKI susceptibility [31, 33]. However, this is not a kidney-specific phenomenon, as NAD^+ boosting or pathway upregulation has been shown to have positive health outcomes relating to multiple organs, including the liver, heart, pancreas, skeletal muscle, brain, and nervous system [59-66].

NAD^+ and NADH were not altered when NAMPT protein increased at 4 hr possibly demonstrating the salvage pathway maintains only a fixed NAD^+ level physiologically without the addition of NAD precursors. However, during an acute renal injury, we found that preventing the loss of NAMPT protein led to an attenuation of the NAD^+ decline at 24 hr following IR injury. In addition, using the NAMPT inhibitor, FK866,

we found trametinib treatment did not prevent an increase in serum creatinine if given in combination with FK866.

Trametinib administration prevented ERK1/2 phosphorylation in uninjured and IR injured renal cortical tissue. PGC-1α expression decreased following IR injury at 24 hr, which trametinib pretreatment attenuated. PGC-1α acetylation increased following IR injury in mice, which decreases PGC-1α transcriptional co-activator activity [43, 67]. Our group has previously demonstrated the SIRT1 activator SRT1720, in an AKI model, increased the deacetylation status of PGC-1α allowing for more effective recruitment of various transcription factors that stimulate the expression of downstream target genes [39, 43]. Here, we demonstrate the same concept using trametinib, and observed an increase in deacetylated PGC-1α in the trametinib mice following IR injury and an increase in MB associated proteins, including NDUFS1, NDUFB8, and COX1. Furthermore, trametinib pretreatment prevented the rise in serum creatinine at 24 hr post IR injury observed in the vehicle-treated group.

Because trametinib altered the acetylation status of PGC-1α and increased PGC-1α downstream targets of MB, SIRT1 and the necessary coenzyme for SIRT1 enzymatic activity, NAD^+, were further studied. The increase in deacetylated PGC-1α due to trametinib administration was discovered to likely stem from the attenuation of the decrease in SIRT1 protein and NAD^+ content following IR injury. The availability of NAD^+ is directly linked to the activity of SIRT1, therefore having more SIRT1 and NAD^+ available in the trametinib group prevented a decrease in SIRT1 activity following IR injury [44, 45, 68].

An increase of PGC-1α in a renal tubule inducible PGC-1α transgenic mouse model upregulated the enzymes of the de novo NAD biosynthetic pathway [31]. The opposite was found as a decrease in PGC-1α suppressed the enzymes of the NAD biosynthetic pathway, as observed in both $Pgc1\alpha^{-/-}$ uninjured kidneys and WT IR kidneys [31]. We observed similar results in our studies where PGC-1α is downregulated and NAD content is decreased after renal IR injury ([10] and present). Better renal functional outcomes were observed in the PGC-1α transgenic mice compared to controls, and worse outcomes were observed in the $Pgc1\alpha^{-/-}$ mice, linking PGC-1α and NAD to AKI severity. Here, a decrease in PGC-1α protein and PGC-1α acetylation, prevented renal dysfunction as measured by serum creatinine.

These experimental results have identified three important findings: 1) Confirmation of ERK1/2 inhibition before IR AKI attenuates the downregulation of PGC-1α and certain MB targets, 2) ERK1/2 inhibition is able to decrease miR34a levels acutely leading to SIRT1 and NAMPT increases, 3) NAMPT protein is vital for ERK1/2 inhibition-induced reduction in IR AKI severity (Figure 1A). In addition, trametinib pretreatment prevented ERK1/2 phosphorylation and attenuated kidney dysfunction as measured by serum creatinine at 24 hrs following IR AKI. ERK1/2 inhibition attenuated decreases in PGC-1α protein, PGC-1α acetylation, and specific downstream MB targets, SIRT1 and NAMPT protein, and NAD^+ after IR injury.

REFERENCES

1. Forrester, S.J., et al., *Epidermal Growth Factor Receptor Transactivation: Mechanisms, Pathophysiology, and Potential Therapies in the Cardiovascular System.* Annu Rev Pharmacol Toxicol, 2016. **56**: p. 627-53.
2. Eblen, S.T., *Extracellular-Regulated Kinases: Signaling From Ras to ERK Substrates to Control Biological Outcomes.* Adv Cancer Res, 2018. **138**: p. 99-142.
3. Daub, H., et al., *Role of transactivation of the EGF receptor in signalling by G-protein-coupled receptors.* Nature, 1996. **379**(6565): p. 557-60.
4. Luttrell, L.M., et al., *Gbetagamma subunits mediate Src-dependent phosphorylation of the epidermal growth factor receptor. A scaffold for G protein-coupled receptor-mediated Ras activation.* J Biol Chem, 1997. **272**(7): p. 4637-44.
5. Wainstein, E. and R. Seger, *The dynamic subcellular localization of ERK: mechanisms of translocation and role in various organelles.* Curr Opin Cell Biol, 2016. **39**: p. 15-20.
6. Roskoski, R., Jr., *ERK1/2 MAP kinases: structure, function, and regulation.* Pharmacol Res, 2012. **66**(2): p. 105-43.
7. Cagnol, S. and J.C. Chambard, *ERK and cell death: mechanisms of ERK-induced cell death--apoptosis, autophagy and senescence.* FEBS J, 2010. **277**(1): p. 2-21.
8. Keshet, Y. and R. Seger, *The MAP kinase signaling cascades: a system of hundreds of components regulates a diverse array of physiological functions.* Methods Mol Biol, 2010. **661**: p. 3-38.
9. Jain, R., et al., *ERK Activation Pathways Downstream of GPCRs.* Int Rev Cell Mol Biol, 2018. **338**: p. 79-109.
10. Collier, J.B., et al., *Rapid Renal Regulation of Peroxisome Proliferator-activated Receptor gamma Coactivator-1alpha by Extracellular Signal-Regulated Kinase 1/2 in Physiological and Pathological Conditions.* J Biol Chem, 2016. **291**(52): p. 26850-26859.
11. Berger, E., et al., *Mitochondrial function controls intestinal epithelial stemness and proliferation.* Nat Commun, 2016. **7**: p. 13171.
12. Patel, A.S., et al., *Epithelial cell mitochondrial dysfunction and PINK1 are induced by transforming growth factor-beta1 in pulmonary fibrosis.* PLoS One, 2015. **10**(3): p. e0121246.
13. Lottes, R.G., et al., *Lactate as substrate for mitochondrial respiration in alveolar epithelial type II cells.* Am J Physiol Lung Cell Mol Physiol, 2015. **308**(9): p. L953-61.
14. Rui, L., *Energy metabolism in the liver.* Compr Physiol, 2014. **4**(1): p. 177-97.
15. Zuk, A. and J.V. Bonventre, *Acute Kidney Injury.* Annu Rev Med, 2016. **67**: p. 293-307.
16. Hall, A.M., et al., *Multiphoton imaging reveals differences in mitochondrial function between nephron segments.* J Am Soc Nephrol, 2009. **20**(6): p. 1293-302.
17. Vainshtein, A., et al., *Role of PGC-1alpha during acute exercise-induced autophagy and mitophagy in skeletal muscle.* Am J Physiol Cell Physiol, 2015. **308**(9): p. C710-9.
18. Wu, Z., et al., *Mechanisms controlling mitochondrial biogenesis and respiration through the thermogenic coactivator PGC-1.* Cell, 1999. **98**(1): p. 115-24.
19. Lynch, M.R., M.T. Tran, and S.M. Parikh, *PGC1alpha in the kidney.* Am J Physiol Renal Physiol, 2018. **314**(1): p. F1-F8.
20. Scarpulla, R.C., *Transcriptional paradigms in mammalian mitochondrial biogenesis and function.* Physiol Rev, 2008. **88**(2): p. 611-38.

21. Puigserver, P. and B.M. Spiegelman, *Peroxisome proliferator-activated receptor-gamma coactivator 1 alpha (PGC-1 alpha): transcriptional coactivator and metabolic regulator.* Endocr Rev, 2003. **24**(1): p. 78-90.
22. Puigserver, P., et al., *A cold-inducible coactivator of nuclear receptors linked to adaptive thermogenesis.* Cell, 1998. **92**(6): p. 829-39.
23. Smith, J.A., et al., *Suppression of mitochondrial biogenesis through toll-like receptor 4-dependent mitogen-activated protein kinase kinase/extracellular signal-regulated kinase signaling in endotoxin-induced acute kidney injury.* J Pharmacol Exp Ther, 2015. **352**(2): p. 346-57.
24. Rasbach, K.A. and R.G. Schnellmann, *PGC-1alpha over-expression promotes recovery from mitochondrial dysfunction and cell injury.* Biochem Biophys Res Commun, 2007. **355**(3): p. 734-9.
25. Jesinkey, S.R., et al., *Formoterol restores mitochondrial and renal function after ischemia-reperfusion injury.* J Am Soc Nephrol, 2014. **25**(6): p. 1157-62.
26. Cameron, R.B., C.C. Beeson, and R.G. Schnellmann, *Structural and pharmacological basis for the induction of mitochondrial biogenesis by formoterol but not clenbuterol.* Sci Rep, 2017. **7**(1): p. 10578.
27. Katsyuba, E. and J. Auwerx, *Modulating NAD(+) metabolism, from bench to bedside.* EMBO J, 2017. **36**(18): p. 2670-2683.
28. Preyat, N. and O. Leo, *Complex role of nicotinamide adenine dinucleotide in the regulation of programmed cell death pathways.* Biochem Pharmacol, 2016. **101**: p. 13-26.
29. Hershberger, K.A., A.S. Martin, and M.D. Hirschey, *Role of NAD(+) and mitochondrial sirtuins in cardiac and renal diseases.* Nat Rev Nephrol, 2017. **13**(4): p. 213-225.
30. Mori, V., et al., *Metabolic profiling of alternative NAD biosynthetic routes in mouse tissues.* PLoS One, 2014. **9**(11): p. e113939.
31. Tran, M.T., et al., *PGC1alpha drives NAD biosynthesis linking oxidative metabolism to renal protection.* Nature, 2016. **531**(7595): p. 528-32.
32. Allison, S.J., *Acute kidney injury: Improved fuel metabolism protects against AKI.* Nat Rev Nephrol, 2016. **12**(5): p. 255.
33. Guan, Y., et al., *Nicotinamide Mononucleotide, an NAD(+) Precursor, Rescues Age-Associated Susceptibility to AKI in a Sirtuin 1-Dependent Manner.* J Am Soc Nephrol, 2017. **28**(8): p. 2337-2352.
34. Nowak, G. and R.G. Schnellmann, *L-ascorbic acid regulates growth and metabolism of renal cells: improvements in cell culture.* Am J Physiol, 1996. **271**(6 Pt 1): p. C2072-80.
35. Gilmartin, A.G., et al., *GSK1120212 (JTP-74057) is an inhibitor of MEK activity and activation with favorable pharmacokinetic properties for sustained in vivo pathway inhibition.* Clin Cancer Res, 2011. **17**(5): p. 989-1000.
36. Yoshino, J., et al., *Nicotinamide mononucleotide, a key NAD(+) intermediate, treats the pathophysiology of diet- and age-induced diabetes in mice.* Cell Metab, 2011. **14**(4): p. 528-36.
37. Funk, J.A. and R.G. Schnellmann, *Persistent disruption of mitochondrial homeostasis after acute kidney injury.* Am J Physiol Renal Physiol, 2012. **302**(7): p. F853-64.
38. Tran, M., et al., *PGC-1alpha promotes recovery after acute kidney injury during systemic inflammation in mice.* J Clin Invest, 2011. **121**(10): p. 4003-14.

39. Funk, J.A. and R.G. Schnellmann, *Accelerated recovery of renal mitochondrial and tubule homeostasis with SIRT1/PGC-1alpha activation following ischemia-reperfusion injury.* Toxicol Appl Pharmacol, 2013. **273**(2): p. 345-54.
40. Funk, J.A., S. Odejinmi, and R.G. Schnellmann, *SRT1720 induces mitochondrial biogenesis and rescues mitochondrial function after oxidant injury in renal proximal tubule cells.* J Pharmacol Exp Ther, 2010. **333**(2): p. 593-601.
41. Kim, S.B., et al., *Acetylation of PGC1alpha by histone deacetylase 1 downregulation is implicated in radiation-induced senescence of brain endothelial cells.* J Gerontol A Biol Sci Med Sci, 2018.
42. Jeninga, E.H., K. Schoonjans, and J. Auwerx, *Reversible acetylation of PGC-1: connecting energy sensors and effectors to guarantee metabolic flexibility.* Oncogene, 2010. **29**(33): p. 4617-24.
43. Gerhart-Hines, Z., et al., *Metabolic control of muscle mitochondrial function and fatty acid oxidation through SIRT1/PGC-1alpha.* EMBO J, 2007. **26**(7): p. 1913-23.
44. Morigi, M., L. Perico, and A. Benigni, *Sirtuins in Renal Health and Disease.* J Am Soc Nephrol, 2018. **29**(7): p. 1799-1809.
45. Canto, C. and J. Auwerx, *Targeting sirtuin 1 to improve metabolism: all you need is NAD(+)?* Pharmacol Rev, 2012. **64**(1): p. 166-87.
46. Revollo, J.R., A.A. Grimm, and S. Imai, *The NAD biosynthesis pathway mediated by nicotinamide phosphoribosyltransferase regulates Sir2 activity in mammalian cells.* J Biol Chem, 2004. **279**(49): p. 50754-63.
47. Ishidoh, K., et al., *Quinolinate phosphoribosyl transferase, a key enzyme in de novo NAD(+) synthesis, suppresses spontaneous cell death by inhibiting overproduction of active-caspase-3.* Biochim Biophys Acta, 2010. **1803**(5): p. 527-33.
48. Choi, S.E., et al., *Elevated microRNA-34a in obesity reduces NAD+ levels and SIRT1 activity by directly targeting NAMPT.* Aging Cell, 2013. **12**(6): p. 1062-72.
49. Bonnet, M.E., et al., *Systemic delivery of sticky siRNAs targeting the cell cycle for lung tumor metastasis inhibition.* J Control Release, 2013. **170**(2): p. 183-90.
50. Hasmann, M. and I. Schemainda, *FK866, a highly specific noncompetitive inhibitor of nicotinamide phosphoribosyltransferase, represents a novel mechanism for induction of tumor cell apoptosis.* Cancer Res, 2003. **63**(21): p. 7436-42.
51. Yoshino, J., J.A. Baur, and S.I. Imai, *NAD(+) Intermediates: The Biology and Therapeutic Potential of NMN and NR.* Cell Metab, 2018. **27**(3): p. 513-528.
52. Yamakuchi, M., M. Ferlito, and C.J. Lowenstein, *miR-34a repression of SIRT1 regulates apoptosis.* Proc Natl Acad Sci U S A, 2008. **105**(36): p. 13421-6.
53. Lee, J. and J.K. Kemper, *Controlling SIRT1 expression by microRNAs in health and metabolic disease.* Aging (Albany NY), 2010. **2**(8): p. 527-34.
54. Yang, Y., et al., *The epigenetically-regulated miR-34a targeting c-SRC suppresses RAF/MEK/ERK signaling pathway in K-562 cells.* Leuk Res, 2017. **55**: p. 91-96.
55. Zarone, M.R., et al., *Evidence of novel miR-34a-based therapeutic approaches for multiple myeloma treatment.* Sci Rep, 2017. **7**(1): p. 17949.
56. Sun, H.L., et al., *ERK Activation Globally Downregulates miRNAs through Phosphorylating Exportin-5.* Cancer Cell, 2016. **30**(5): p. 723-736.
57. Wakino, S., K. Hasegawa, and H. Itoh, *Sirtuin and metabolic kidney disease.* Kidney Int, 2015. **88**(4): p. 691-8.

58. Hasegawa, K., et al., *Renal tubular Sirt1 attenuates diabetic albuminuria by epigenetically suppressing Claudin-1 overexpression in podocytes.* Nat Med, 2013. **19**(11): p. 1496-504.
59. Mouchiroud, L., et al., *The NAD(+)/Sirtuin Pathway Modulates Longevity through Activation of Mitochondrial UPR and FOXO Signaling.* Cell, 2013. **154**(2): p. 430-41.
60. Yamamoto, T., et al., *Nicotinamide mononucleotide, an intermediate of NAD+ synthesis, protects the heart from ischemia and reperfusion.* PLoS One, 2014. **9**(6): p. e98972.
61. Horton, J.L., et al., *Mitochondrial protein hyperacetylation in the failing heart.* JCI Insight, 2016. **2**(1).
62. Revollo, J.R., et al., *Nampt/PBEF/Visfatin regulates insulin secretion in beta cells as a systemic NAD biosynthetic enzyme.* Cell Metab, 2007. **6**(5): p. 363-75.
63. Zhang, H., et al., *NAD(+) repletion improves mitochondrial and stem cell function and enhances life span in mice.* Science, 2016. **352**(6292): p. 1436-43.
64. Hou, Y., et al., *NAD(+) supplementation normalizes key Alzheimer's features and DNA damage responses in a new AD mouse model with introduced DNA repair deficiency.* Proc Natl Acad Sci U S A, 2018. **115**(8): p. E1876-E1885.
65. Di Stefano, M., et al., *NMN Deamidase Delays Wallerian Degeneration and Rescues Axonal Defects Caused by NMNAT2 Deficiency In Vivo.* Curr Biol, 2017. **27**(6): p. 784-794.
66. Rajman, L., K. Chwalek, and D.A. Sinclair, *Therapeutic Potential of NAD-Boosting Molecules: The In Vivo Evidence.* Cell Metab, 2018. **27**(3): p. 529-547.
67. Rohas, L.M., et al., *A fundamental system of cellular energy homeostasis regulated by PGC-1alpha.* Proc Natl Acad Sci U S A, 2007. **104**(19): p. 7933-8.
68. Kong, L., et al., *Sirtuin 1: A Target for Kidney Diseases.* Mol Med, 2015. **21**: p. 87-97.

CHAPTER FIVE:

Future Directions for ERK1/2-Mediated Mitochondrial Biogenesis Signaling

Elucidating the EGFR Ligand Responsible for ERK1/2-Mediated MB Signaling

While ERK1/2-mediated MB was elucidated in the scope of this project, there are additional questions that remain unanswered. We used the MEK1/2 inhibitor, trametinib, to prevent ERK1/2 activation as a consequence of IR injury. By doing so we observed a prevention in the downregulation of PGC-1α and PGC-1α downstream gene targets. Not only did trametinib pretreatment prevent the negative regulation of PGC-1α, it prevented a rise in serum creatinine. In chapter two, we made the observation that the EGFR inhibitor, erlotinib, also inhibited ERK1/2 phosphorylation. The inhibition of ERK1/2 phosphorylation using erlotinib was not as strong as the treatment with trametinib, yet, we observed very similar downstream effects. By blocking ERK1/2 phosphorylation thru inhibiting the EGFR, we increased PGC-1α and NRF1 mRNA in our cultured primary rabbit renal proximal tubule cells (RPTC), again, very similar to our observation with trametinib. Erlotinib administration to naïve mice decreased ERK1/2 activation and increased PGC-1α mRNA, even at a physiological level.

Interestingly, pretreatment with erlotinib blunted the increase in ERK1/2 phosphorylation typically seen following IR injury in the renal cortex. We observed a prevention of PGC-1α mRNA downregulation, as well as an increase in PGC-1α protein. Most importantly, this prevention of negative PGC-1α regulation after IR injury, prevented a rise in serum creatinine similar to trametinib. It should be noted the prevention of the rise of serum creatinine was not as great in the erlotinib groups compared to the trametinib groups, but was significant from vehicle + IR group. These findings are in contrast to some studies which has suggested EGFR inhibition or the use

of waved-2 mice (mice with reduced EGFR tyrosine kinase activity), actually causes worsening kidney damage and dysfunction following injury [1-3]. The observation is that EGFR inhibition prevents tubule dedifferentiation and proliferation. Our studies were not setup to examine those biological functions, however, a one-time dose of erlotinib prior to IR injury leading to AKI, seems to be beneficial in the acute phase. With only a single dose, however, the drug would be out of the circulatory system in ~ 24 hr, possibly preventing any dedifferentiation and proliferation effects observed in other studies. This contrast in studies brings up an interesting concept, in that global inhibition of EGFR signaling may not be the best tactic for preventing AKI.

Because we observed similar downstream prevention of PGC-1α and PGC-1α related genes in both our trametinib and erlotinib groups, yet erlotinib did not block ERK1/2 phosphorylation to the extent trametinib did, there may be a specific ligand that is causing the negative regulation of PGC-1α and related MB targets following IR injury. In other words, there may be a specific ligand that binds to EGFR and causes ERK1/2 phosphorylation that is the driving force to negatively regulate PGC-1α and downstream MB targets. Therefore, my first future project experiments would focus on finding the EGFR ligand responsible for ERK1/2 activation at the initiation of IR injury.

These projects would potentially help identify a pharmacological target more specific for pre-treatment before surgeries known to cause renal dysfunction (ex. cardiac surgeries). Inhibiting one specific ligand versus inhibiting MEK1/2 or the EGFR would be more specific, possibly have less side effects, and contribute to less organ system

alterations in patients with other disease states. Another possible benefit of identifying one specific ligand that prevents the same downregulation of PGC-1a as ERK1/2 inhibition is that the ligand inhibitor may be druggable beyond a one-time pretreatment dose.

Studies have shown consistent ERK1/2 inhibition following AKI is detrimental and worsens kidney function [4-7]. There are only seven known EGFR ligands [8] : 1) epidermal growth factor (EGF), 2) transforming growth factor-alpha (TGFA), 3) heparin-binding EGF-like growth factor (HB-EGF), 4) betacellulin (BTC), 5) amphiregulin (AREG), 6) epiregulin (EREG), 7) epigen (EPGN). Most EGFR ligands are upregulated rapidly following renal insult and activate the EGFR through membrane bound or cleaved interactions [3, 9, 10]. EGFR ligands are cleaved by proteases and a disintegrin and metalloproteinase (ADAMs) [11, 12]. Some preliminary experiments using our RPTC cultures has shown that broadly inhibiting matrix metalloproteinase (MMPs) using the compounds, marimistat and TAPI-2, we get partial inhibition of ERK1/2 phosphorylation [13, 14], as seen in the figures below (Figure 5.1 and Figure 5.2).

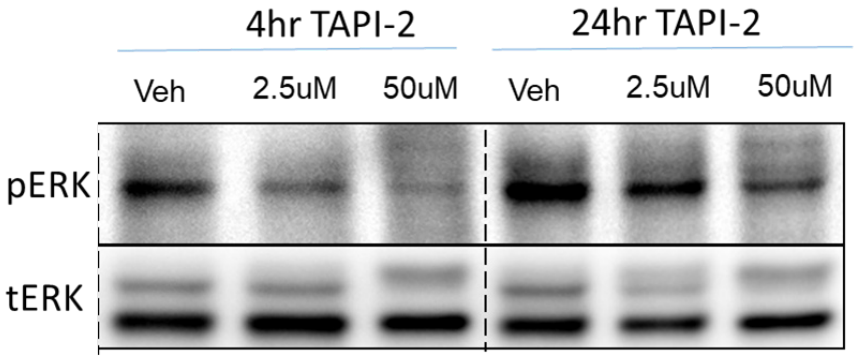

Figure 5.1: Broad MMP inhibition, using TAPI-2, decreases ERK1/2 phosphorylation at 4 and 24 hr after dosing in RPTC culture.

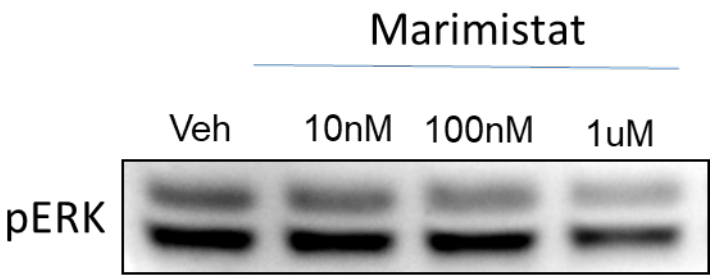

Figure 5.2: Marimistat decreases ERK1/2 phosphorylation at 4 hr after dosing in RPTC culture.

Mitochondrial Supercomplexes in Relation to Pharmacological Activation of MB

Our lab has previously demonstrated that pharmacological activation of MB in our RPTC cultures increases PGC-1α and downstream MB targets at a mRNA and protein level. A phenotypic marker of our MB pharmacological agents is an increase in oxygen consumption after the addition of a proton uncoupling agent (FCCP) as measured by the Seahorse XF96 Analyzer [15]. By measuring oxygen consumption rate following FCCP, we are mimicking how well the mitochondria can handle an injury or outside stressor. The higher the oxygen consumption rate the more new mitochondria generated following pharmacological treatment, or the more efficient the current mitochondria are due to increased electron transport proteins [15-17].

Recently, the electron transport chain (ETC) assembly has been investigated to observe the various complexes of the ETC and how they interact with each other. The ETC assembly can be static or dynamic, and these complex interactions following injury are altered. The term mitochondrial supercomplexes is used to denote ETC complex I, II, III, IV, and cytochrome c assembling together as one complex assembly instead of multiple individual complexes [18]. As seen below, ETC complexes can be assembled into one supercomplexes [19] (Figure 5.3). Mitochondrial supercomplexes with various configurations and stoichiometries occur in mitochondria from different sources [20-24]. However, alterations in mitochondrial supercomplex formation following treatment with pharmacological agents that induce renal MB at a physiological and pathological level, has not been elucidated.

MB and mitochondrial supercomplex assembly enhances many of the same biological pathways. Mitochondrial supercomplex formation has been shown to enhance mitochondrial efficiency, increase respiratory reserve capacity, increase ATP production, lower ROS formation, is altered after ischemic injury, and declines with age [25-28]. The above-mentioned phenomena are all similar to observations made with increased PGC-1α and MB, along with a decline following injury and with age [29-32]. Mitochondrial supercomplex assembly was observed following 24 hr IR injury with a 1 hr pretreatment with vehicle or trametinib (1mg/kg). Figure 5.4 depicts the gel, PVDF membrane, and immunoblot for mitochondrial complexes following a modified blue-native PAGE (BN-PAGE) experiment. Figure 5.5 shows side-by-side a mitochondrial supercomplex BN-PAGE from a review article next our experimental BN-PAGE following 24 hr IR. No quantifications were performed, however, two supercomplexes, complex V assembled with complex III_2 + IV_1 and complex III_2 + IV_2, look to be increased in the 24 hr IR group, whereas the trametinib treated animals have those supercomplexes levels similar to sham. This increase in supercomplex formation in the IR group may be a compensatory mechanism in which the damaged cortex needs to be as efficient as possible. The trametinib treated animal are not as injured, as previously shown in chapter 2 and chapter 4. Therefore, supercomplex formation may not be required at 24 hr following IR injury because the scope of the injury does not dictate the increased formation of supercomplexes.

Timing may play a crucial role in mitochondrial supercomplex formation following injury. As we have only performed a 24 hr time point, much more work following IR

injury would need to done to outline a timing pathway in response to IR injury. Various supercomplexes may be favored during different time points after IR injury and depending on the severity of the injury [33, 34]. Alterations in these supercomplexes following administration of a pharmacological agent that induces MB would be of interest to further enhance the identification of a pharmacological agent that has the potential for therapeutic use for treatment of AKI.

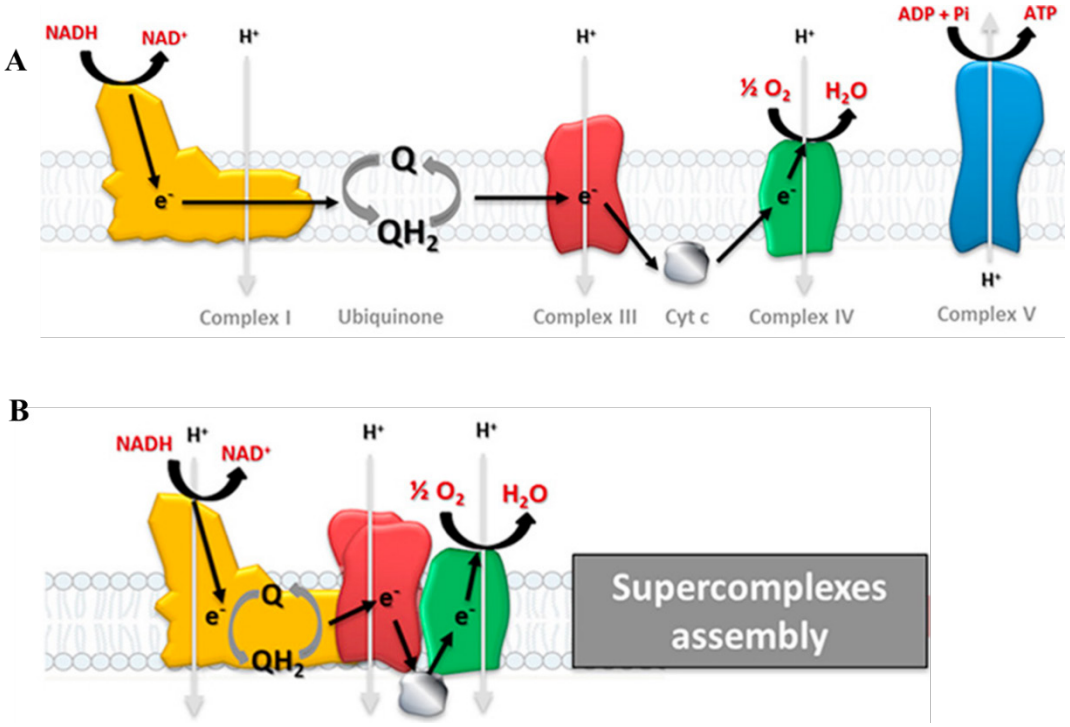

Figure 5.3: A) Mitochondrial electron transport chain complexes depicted in a non-supercomplexes state. B) Mitochondrial supercomplexes assembly.

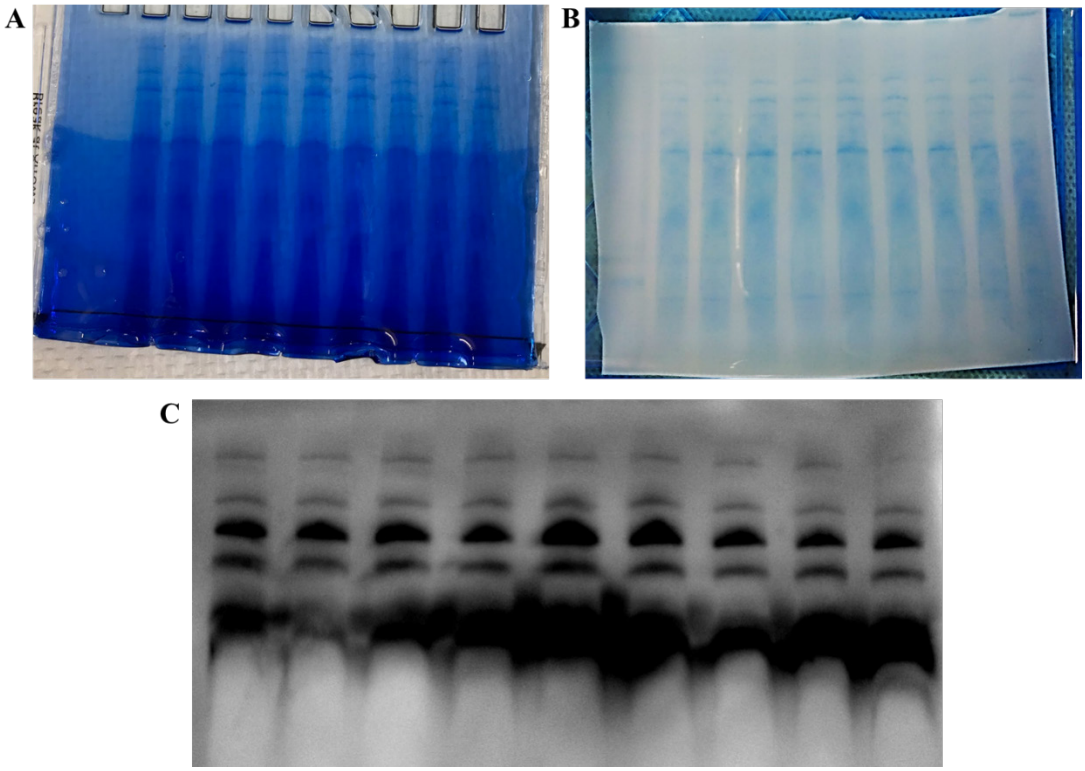

Figure 5.4: A) Tris-glycine gel following BN-PAGE using isolated mitochondria from the renal cortex of mouse kidneys. B) PVDF membrane following BN-PAGE modified protocol. C) Immunoblot of PVDF membrane after incubation with mitochondrial complex antibodies. Further clarification can be found in figure 5.5.

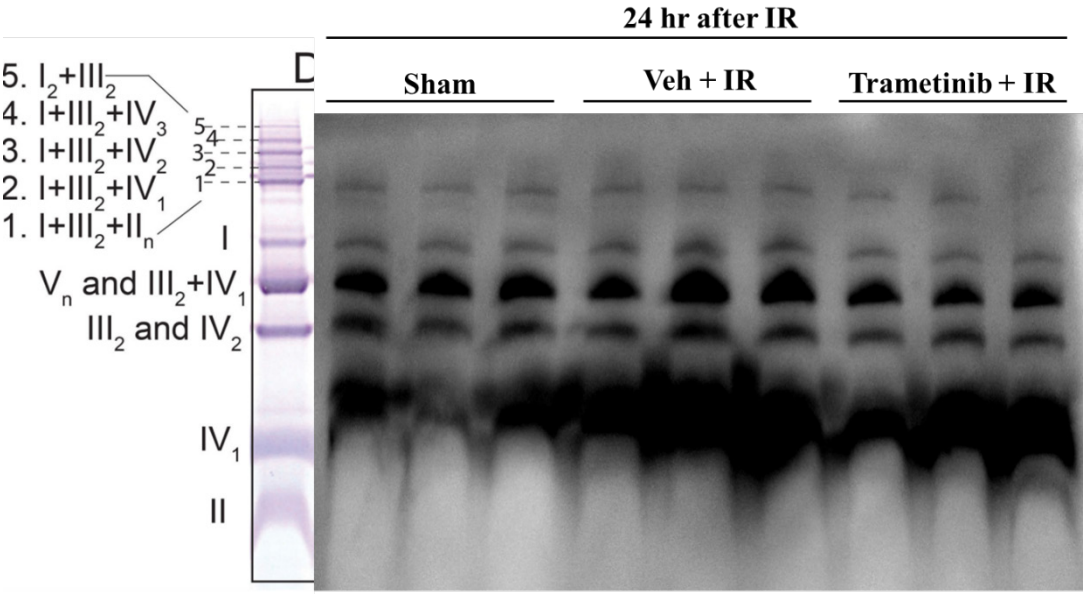

Figure 5.5: Immunoblot of PVDF membrane after modified BN-PAGE and incubation with mitochondrial complex antibodies. Next to our image is a representative mitochondrial supercomplex image pulled from an instructional review by Auwerx, et al. Adapted from (26928661)

REFERENCES

1. He, S., et al., *EGFR activity is required for renal tubular cell dedifferentiation and proliferation in a murine model of folic acid-induced acute kidney injury.* Am J Physiol Renal Physiol, 2013. **304**(4): p. F356-66.
2. Zeng, F., A.B. Singh, and R.C. Harris, *The role of the EGF family of ligands and receptors in renal development, physiology and pathophysiology.* Exp Cell Res, 2009. **315**(4): p. 602-10.
3. Sakai, M., et al., *Production of heparin binding epidermal growth factor-like growth factor in the early phase of regeneration after acute renal injury. Isolation and localization of bioactive molecules.* J Clin Invest, 1997. **99**(9): p. 2128-38.
4. Chen, H.H., et al., *Heme oxygenase-1 ameliorates kidney ischemia-reperfusion injury in mice through extracellular signal-regulated kinase 1/2-enhanced tubular epithelium proliferation.* Biochim Biophys Acta, 2015. **1852**(10 Pt A): p. 2195-201.
5. Jang, H.S., et al., *Activation of ERK accelerates repair of renal tubular epithelial cells, whereas it inhibits progression of fibrosis following ischemia/reperfusion injury.* Biochim Biophys Acta, 2013. **1832**(12): p. 1998-2008.
6. Bonventre, J.V., *Maladaptive proximal tubule repair: cell cycle arrest.* Nephron Clin Pract, 2014. **127**(1-4): p. 61-4.
7. Kwon, D.S., et al., *Signal transduction of MEK/ERK and PI3K/Akt activation by hypoxia/reoxygenation in renal epithelial cells.* Eur J Cell Biol, 2006. **85**(11): p. 1189-99.
8. Singh, B., G. Carpenter, and R.J. Coffey, *EGF receptor ligands: recent advances.* F1000Res, 2016. **5**.
9. Hise, M.K., et al., *Control of the epidermal growth factor receptor and its ligands during renal injury.* Nephron, 2001. **88**(1): p. 71-9.(ad
10. Takemura, T., et al., *Role of membrane-bound heparin-binding epidermal growth factor-like growth factor (HB-EGF) in renal epithelial cell branching.* Kidney Int, 2002. **61**(6): p. 1968-79.
11. Huovila, A.P., et al., *Shedding light on ADAM metalloproteinases.* Trends Biochem Sci, 2005. **30**(7): p. 413-22.
12. Asakura, M., et al., *Cardiac hypertrophy is inhibited by antagonism of ADAM12 processing of HB-EGF: metalloproteinase inhibitors as a new therapy.* Nat Med, 2002. **8**(1): p. 35-40.
13. Knapinska, A.M., et al., *SAR Studies of Exosite-Binding Substrate-Selective Inhibitors of A Disintegrin And Metalloprotease 17 (ADAM17) and Application as Selective in Vitro Probes.* J Med Chem, 2015. **58**(15): p. 5808-24.
14. Raissi, A.J., et al., *Enhanced potency of the metalloprotease inhibitor TAPI-2 by multivalent display.* Bioorg Med Chem Lett, 2014. **24**(8): p. 2002-7.
15. Peterson, Y.K., et al., *beta2-Adrenoceptor agonists in the regulation of mitochondrial biogenesis.* Bioorg Med Chem Lett, 2013. **23**(19): p. 5376-81.
16. Cameron, R.B., C.C. Beeson, and R.G. Schnellmann, *Development of Therapeutics That Induce Mitochondrial Biogenesis for the Treatment of Acute and Chronic Degenerative Diseases.* J Med Chem, 2016. **59**(23): p. 10411-10434.
17. Wills, L.P., et al., *Assessment of ToxCast Phase II for Mitochondrial Liabilities Using a High-Throughput Respirometric Assay.* Toxicol Sci, 2015. **146**(2): p. 226-34.
18. Genova, M.L. and G. Lenaz, *Functional role of mitochondrial respiratory supercomplexes.* Biochim Biophys Acta, 2014. **1837**(4): p. 427-43.

19. Huertas, J.R., et al., *Antioxidant effect of exercise: Exploring the role of the mitochondrial complex I superassembly.* Redox Biol, 2017. **13**: p. 477-481.
20. Schagger, H. and K. Pfeiffer, *Supercomplexes in the respiratory chains of yeast and mammalian mitochondria.* EMBO J, 2000. **19**(8): p. 1777-83.
21. Eubel, H., et al., *Respiratory chain supercomplexes in plant mitochondria.* Plant Physiol Biochem, 2004. **42**(12): p. 937-42.
22. Wittig, I., et al., *Supercomplexes and subcomplexes of mitochondrial oxidative phosphorylation.* Biochim Biophys Acta, 2006. **1757**(9-10): p. 1066-72.
23. Vonck, J. and E. Schafer, *Supramolecular organization of protein complexes in the mitochondrial inner membrane.* Biochim Biophys Acta, 2009. **1793**(1): p. 117-24.
24. Genova, M.L. and G. Lenaz, *A critical appraisal of the role of respiratory supercomplexes in mitochondria.* Biol Chem, 2013. **394**(5): p. 631-9.
25. Greggio, C., et al., *Enhanced Respiratory Chain Supercomplex Formation in Response to Exercise in Human Skeletal Muscle.* Cell Metab, 2017. **25**(2): p. 301-311.
26. Gomez, L.A. and T.M. Hagen, *Age-related decline in mitochondrial bioenergetics: does supercomplex destabilization determine lower oxidative capacity and higher superoxide production?* Semin Cell Dev Biol, 2012. **23**(7): p. 758-67.
27. Paradies, G., et al., *Mitochondrial bioenergetics decay in aging: beneficial effect of melatonin.* Cell Mol Life Sci, 2017. **74**(21): p. 3897-3911.
28. Itoh, K., et al., *Mitochondrial dynamics in neurodegeneration.* Trends Cell Biol, 2013. **23**(2): p. 64-71.
29. Tran, M.T., et al., *PGC1alpha drives NAD biosynthesis linking oxidative metabolism to renal protection.* Nature, 2016. **531**(7595): p. 528-32.
30. Fernandez-Marcos, P.J. and J. Auwerx, *Regulation of PGC-1alpha, a nodal regulator of mitochondrial biogenesis.* Am J Clin Nutr, 2011. **93**(4): p. 884S-90.
31. Tan, Z., et al., *The Role of PGC1alpha in Cancer Metabolism and its Therapeutic Implications.* Mol Cancer Ther, 2016. **15**(5): p. 774-82.
32. Lynch, M.R., M.T. Tran, and S.M. Parikh, *PGC1alpha in the kidney.* Am J Physiol Renal Physiol, 2018. **314**(1): p. F1-F8.
33. Camara, A.K., M. Bienengraeber, and D.F. Stowe, *Mitochondrial approaches to protect against cardiac ischemia and reperfusion injury.* Front Physiol, 2011. **2**: p. 13.
34. Kuter, K., et al., *Adaptation within mitochondrial oxidative phosphorylation supercomplexes and membrane viscosity during degeneration of dopaminergic neurons in an animal model of early Parkinson's disease.* Biochim Biophys Acta, 2016. **1862**(4): p. 741-753.